# Deep Brain Stimulation nelle distonie e nella Malattia di Parkinson

Dott. Michele Cavallo

Direttore UO Neurochirurgia

16 Aprile 20115

# Talamo e gangli della base

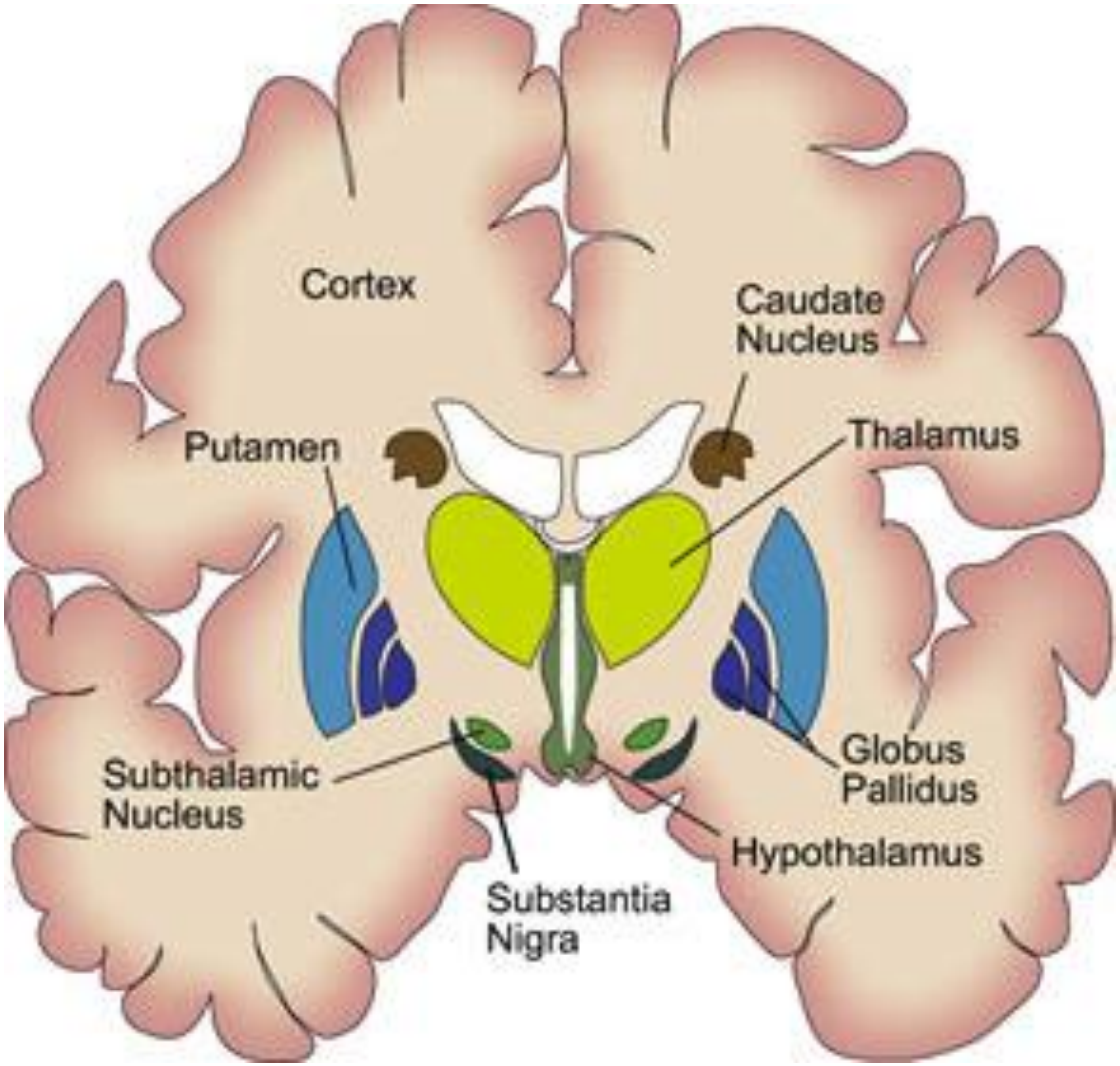

# Nuclei talamici

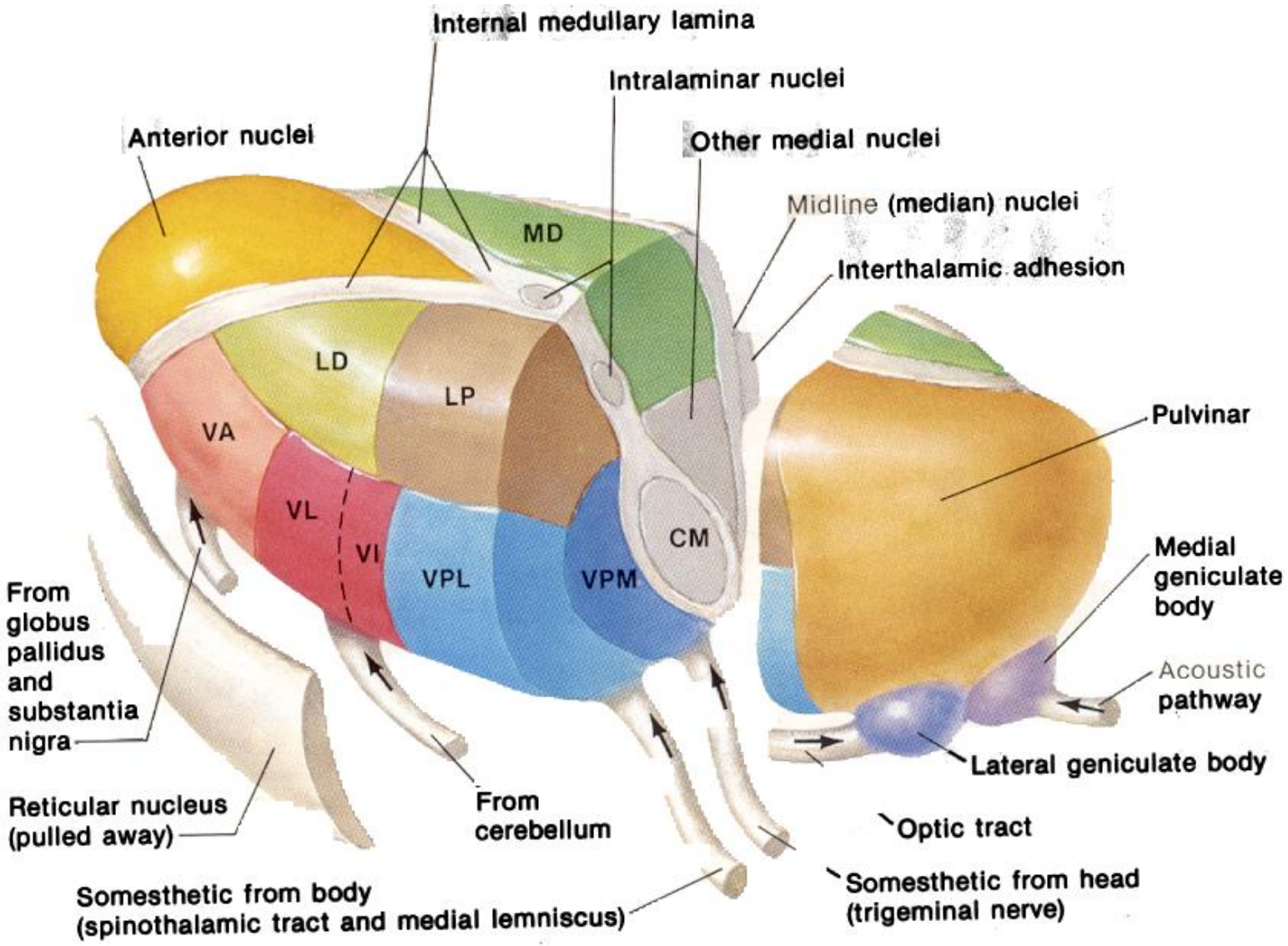

- DBS: nata oltre 25 anni fa, si è dimostrata sicura ed efficace per tremore Essenziale, M. di Parkinson, Distonia
- Successiva estensione delle indicazioni per la DBS a diverse malattie del SNC
- Tratta i sintomi, non la malattia
- Variabilità dei risultati interindividuali
- Variazione nel tempo dell'efficacia/effetti indesiderati

- Progressi nell'identificazione neuroradiologica del target
- Progressi nei sistemi di applicazione degli elettrodi

- Nuove acquisizioni neurofisiologiche sull'attività dei nuclei della base
- Nuovi tipi di stimolazione
- Nuovi sistemi di stimolazione/registrazione
- Nuovi elettrodi

# Indicazioni alla terapia chirurgica

- Malattia di Parkinson idiopatica avanzata
- Grave disabilità
- Perdita di efficacia della terapia farmacologica
- Effetti collaterali da prolungato trattamento con L-dopa

- Scale di valutazione della M. di Parkinson:
  - Unified Parkinson Disease Rating Scale (UPDRS)
  - Hoehn-Yahr

# Valutazione funzionale del paziente (UPDRS score)

Paziente _____ Data dell'osservazione _____

## SCALA UNIFICATA DI VALUTAZIONE DEL MALATO PARKINSONIANO (UPDRS)

### I CAPACITÀ MENTALI, COMPORTAMENTO E UMORE

| | | | | | |
|---|---|---|---|---|---|
| 1. Disturbi intellettivi | 0 | 1 | 2 | 3 | 4 |
| 2. Disturbi percettivi o del pensiero | 0 | 1 | 2 | 3 | 4 |
| 3. Depressione | 0 | 1 | 2 | 3 | 4 |
| 4. Motivazioni/Iniziativa | 0 | 1 | 2 | 3 | 4 |

### II ATTIVITÀ DELLA VITA QUOTIDIANA

| | | | | | |
|---|---|---|---|---|---|
| 5. Parola | 0 | 1 | 2 | 3 | 4 |
| 6. Salivazione | 0 | 1 | 2 | 3 | 4 |
| 7. Deglutizione | 0 | 1 | 2 | 3 | 4 |
| 8. Scrittura | 0 | 1 | 2 | 3 | 4 |
| 9. Tagliare i cibi | 0 | 1 | 2 | 3 | 4 |
| 10. Abbigliamento | 0 | 1 | 2 | 3 | 4 |
| 11. Igiene personale | 0 | 1 | 2 | 3 | 4 |
| 12. Girarsi nel letto | 0 | 1 | 2 | 3 | 4 |
| 13. Cadute | 0 | 1 | 2 | 3 | 4 |
| 14. "Freezing" | 0 | 1 | 2 | 3 | 4 |
| 15. Marcia | 0 | 1 | 2 | 3 | 4 |
| 16. Tremore | 0 | 1 | 2 | 3 | 4 |
| 17. Disturbi sensitivi | 0 | 1 | 2 | 3 | 4 |

### III ESAME MOTORIO

| | | | | | |
|---|---|---|---|---|---|
| 18. Parola | 0 | 1 | 2 | 3 | 4 |
| 19. Espressione del volto | 0 | 1 | 2 | 3 | 4 |
| 20. Tremore a riposo | 0 | 1 | 2 | 3 | 4 |
| 21. Tremore d'azione | 0 | 1 | 2 | 3 | 4 |
| 22. Rigidità | 0 | 1 | 2 | 3 | 4 |
| 23. "Finger taps" | 0 | 1 | 2 | 3 | 4 |
| 24. Movimenti delle mani | 0 | 1 | 2 | 3 | 4 |
| 25. Movimenti rapidi delle mani | 0 | 1 | 2 | 3 | 4 |
| 26. Agilità delle gambe | 0 | 1 | 2 | 3 | 4 |
| 27. Alzarsi da una sedia | 0 | 1 | 2 | 3 | 4 |
| 28. Postura | 0 | 1 | 2 | 3 | 4 |
| 29. Deambulazione | 0 | 1 | 2 | 3 | 4 |
| 30. Stabilità posturale | 0 | 1 | 2 | 3 | 4 |
| 31. Bradicinesia e ipocinesia | 0 | 1 | 2 | 3 | 4 |

# Valutazione funzionale del paziente (UPDRS score)

## IV COMPLICAZIONI DOVUTE ALLA TERAPIA
(NELLA SETTIMANA PRECEDENTE L'OSSERVAZIONE)

### A. DISCINESIE

| | | | | | |
|---|---|---|---|---|---|
| 32. Durata | 0 | 1 | 2 | 3 | 4 |
| 33. Disabilità | 0 | 1 | 2 | 3 | 4 |
| 34. Discinesie dolorose | 0 | 1 | 2 | 3 | 4 |
| 35. "Early morning dystonia" | 0 | 1 | 2 | 3 | 4 |

### B. FLUTTUAZIONI CLINICHE

| | | |
|---|---|---|
| 36. Periodi "off" prevedibili | sì - 1 | no - 0 |
| 37. Periodi "off" non prevedibili | sì - 1 | no - 0 |
| 38. Periodi "off" improvvisi | sì - 1 | no - 0 |

| | | | | | |
|---|---|---|---|---|---|
| 39. Parte del giorno in "off" | 0 | 1 | 2 | 3 | 4 |

### C. ALTRE COMPLICAZIONI

| | | |
|---|---|---|
| 40. Anoressia, nausea, vomito | sì - 1 | no - 0 |
| 41. Disturbi del sonno | sì - 1 | no - 0 |
| 42. Ipotensione ortostatica | sì - 1 | no - 0 |

### UPDRS

| | | |
|---|---|---|
| Sezione I | Subtotale (max 16) | |
| Sezione II | Subtotale (max 52) | |
| Sezione III | Subtotale (max 56) | |
| Sezione IV | Subtotale (max 26) | |
| Punteggio totale | | |

### ALTRO

### TRATTAMENTO PRESCRITTO

# Deep Brain Stimulation

# IMPIANTO BILATERALE

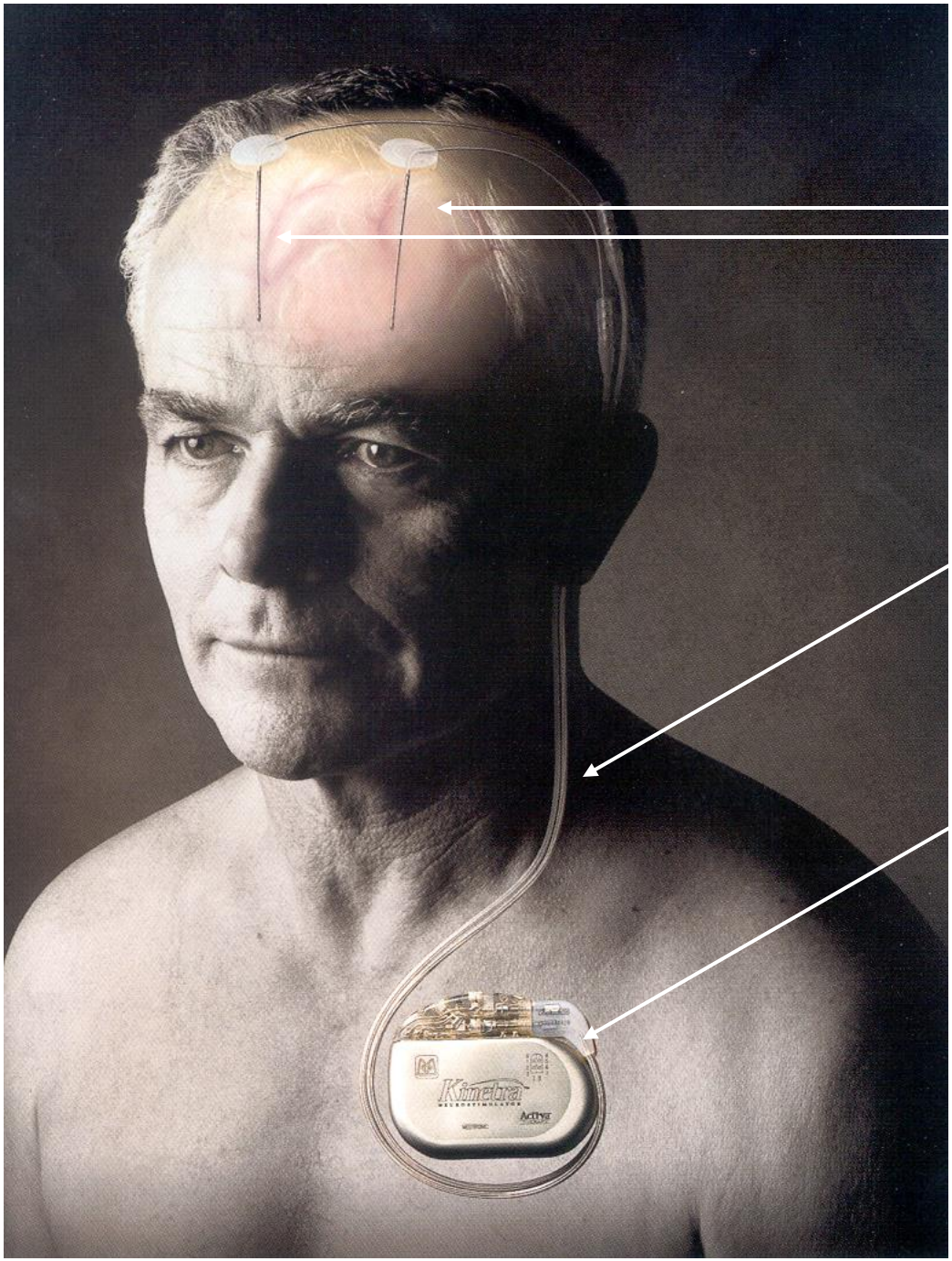


Elettrocateteri per DBS

Estensione tunnellizzata sottocute

Generatore di impulsi bicanale Mod. Kinetra

# M. di Parkinson

# M. di Parkinson

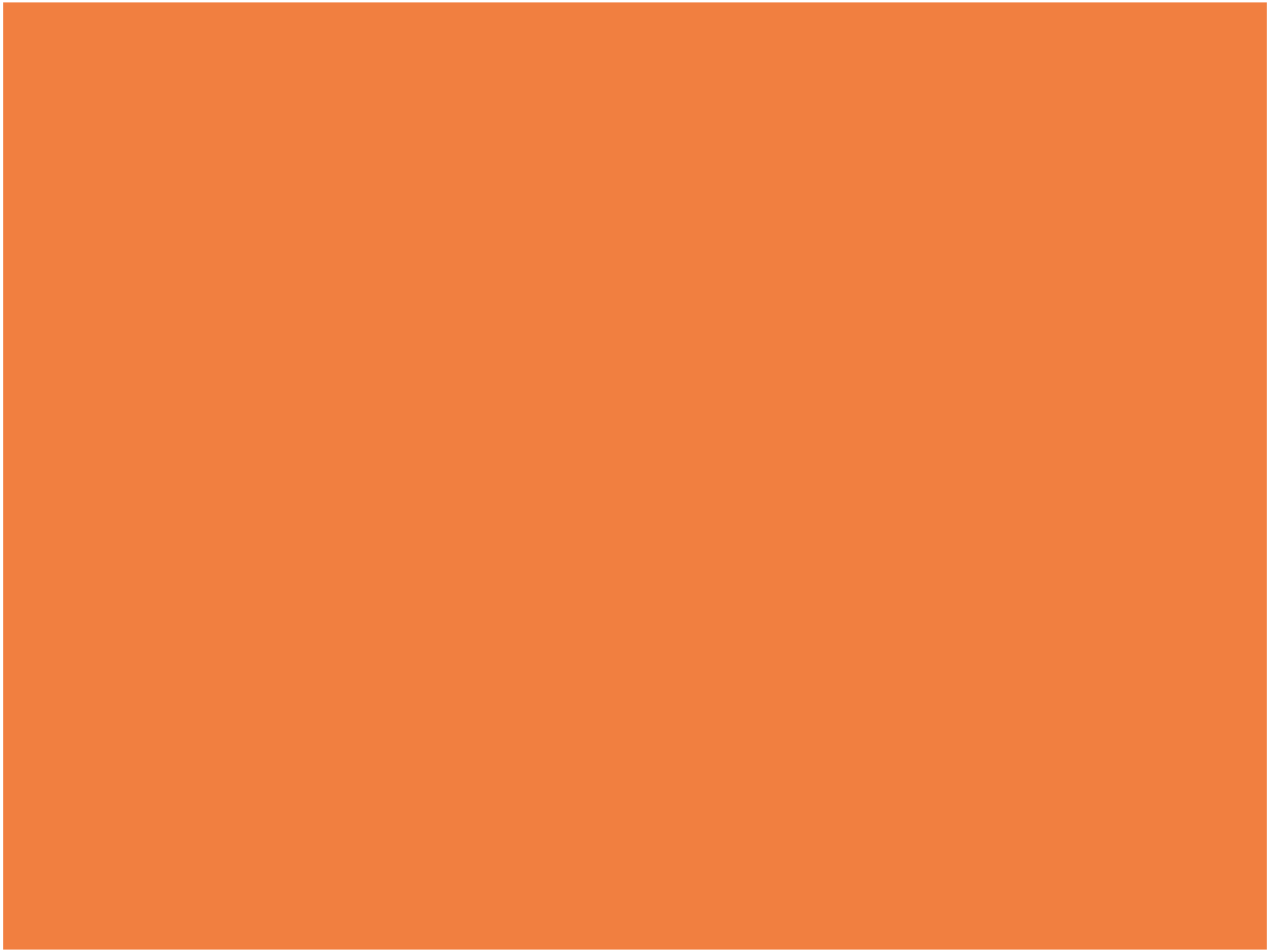

# Distonia

- Sindrome caratterizzata da contrazioni muscolari involontarie e sostenute di più muscoli antagonisti, in genere stereotipate, che parassitano in movimento volontario e possono provocare movimenti di torsione e posture abnormi
  - Classificazione in base alla distribuzione
    - Focali
    - Segmentarie
    - Multifocali
    - Generalizzate
    - Emidistonia
  - Classificazione in base all'etiologia
    - Primarie
    - Distonia plus (associata a Parkinson, mioclono)
    - Secondarie
    - Eredodegenerative
    - Psicogene

# Distonia generalizzata primaria DYT1 +

# Distonia generalizzata primaria con genetica negativa

# Distonia generalizzata primaria tardiva con genetica negativa

# Distonia multifocale primaria con genetica negativa

# Distonia generalizzata secondaria

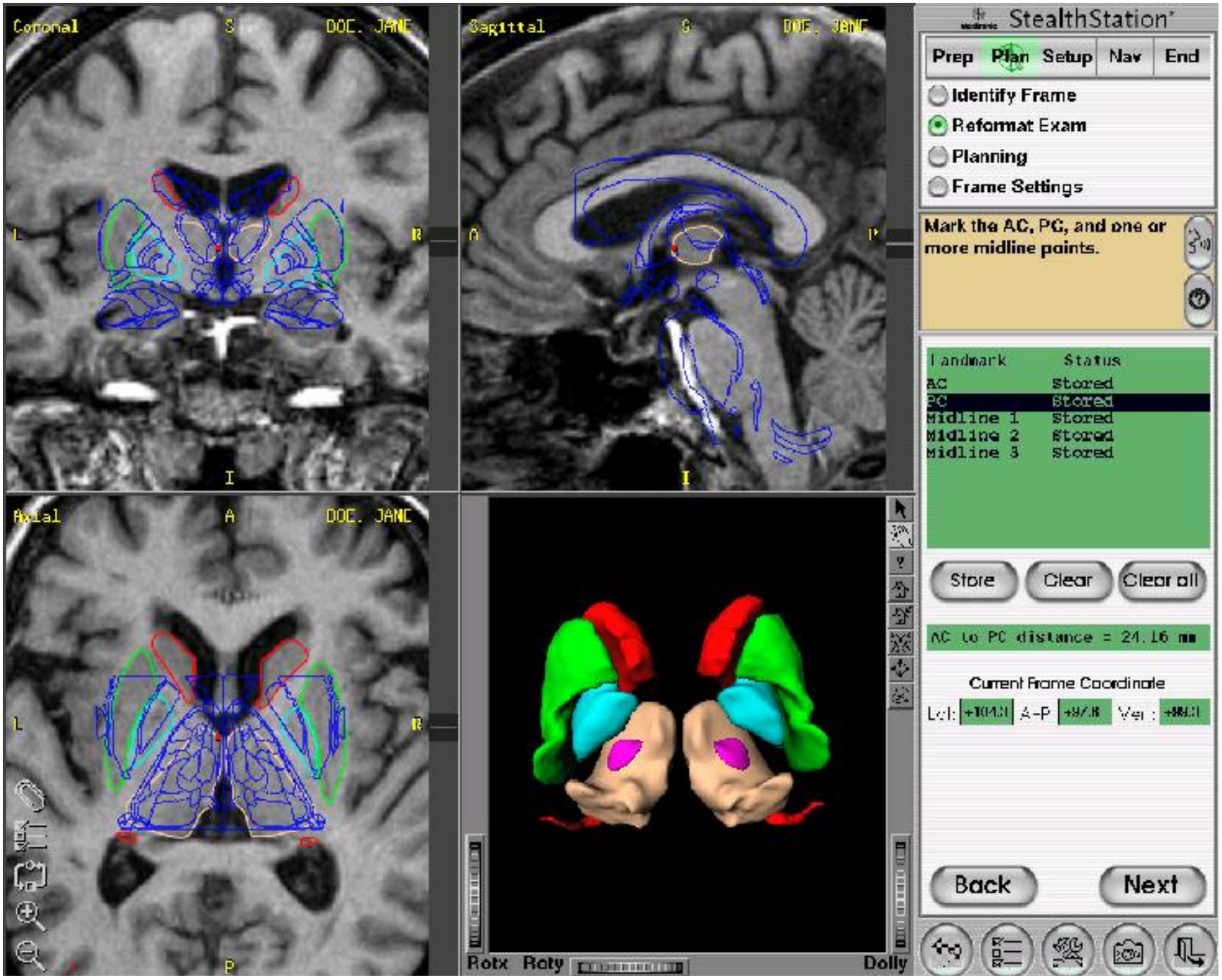
Coronal
S
DOE, JANE
L
R
I
Sagittal
S
DOE, JANE
A
P
I
Axial
A
DOE, JANE
L
R
P
Rotx
Roty
Dolly
StealthStation
Prep
Plan
Setup
Nav
End
Identify Frame
Reformat Exam
Planning
Frame Settings
Mark the AC, PC, and one or more midline points.
Landmark
Status
AC
Stored
PC
Stored
Midline 1
Stored
Midline 2
Stored
Midline 3
Stored
Store
Clear
Clear all
AC to PC distance = 24.16 mm
Current Frame Coordinate
Lat:
A-P
Ver :
Back
Next

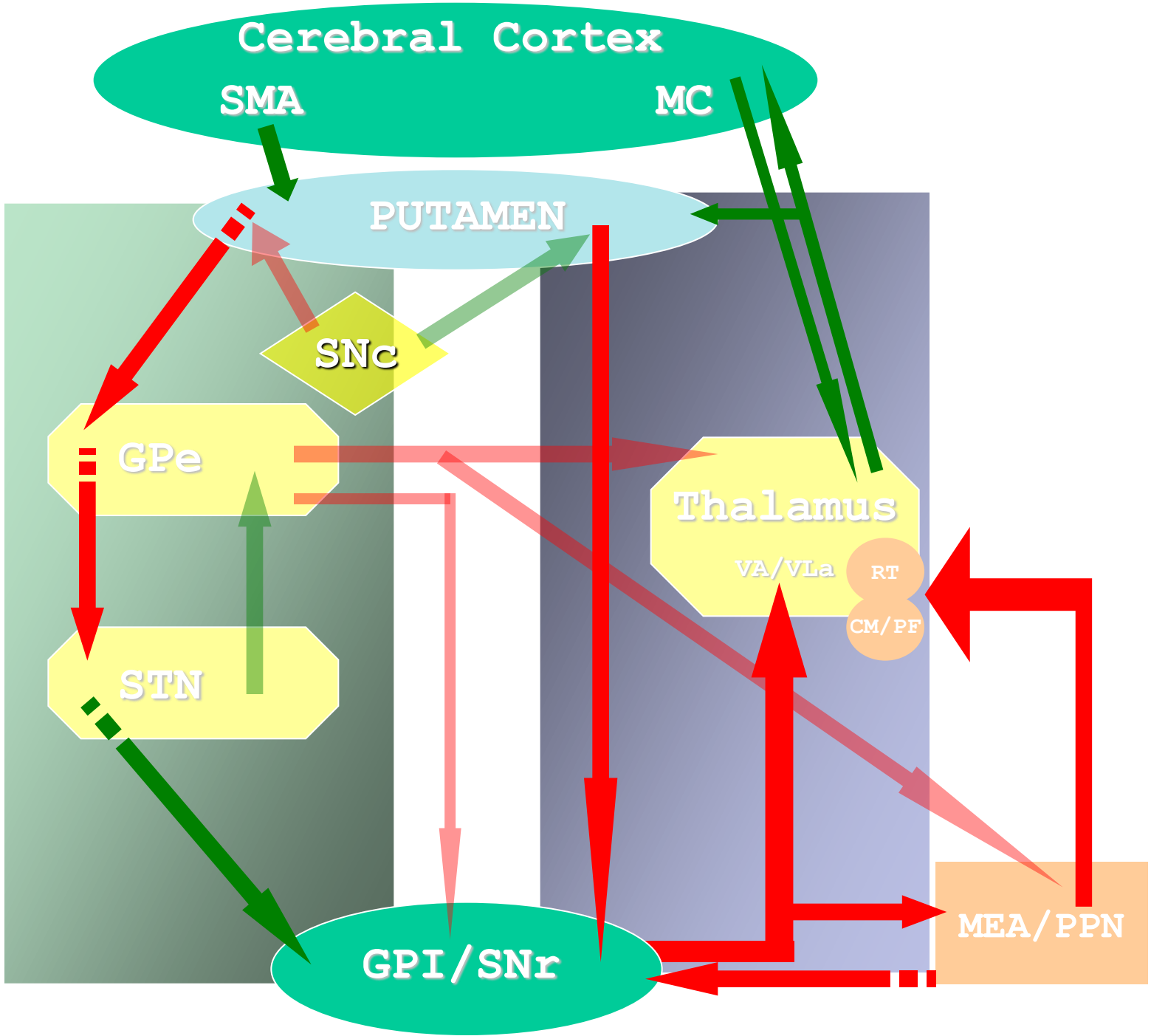
Cerebral Cortex
SMA
MC
PUTAMEN
SNc
GPe
STN
Thalamus
VA/VLa
RT
CM/PF
MEA/PPN
GPI/SNr

**Corteccia Cerebrale – GPe – STN + GPi/SNr – Thalamus Vl**

**Via indiretta** – circuito di soppressione parallelo alla via diretta - iperattività del circuito per perdita dell'inibizione SNr-mediata

***Sintomi negativi***: difficoltà a passare ad un nuovo schema motorio: *acinesia*

# Sinergia via diretta ed indiretta

*Attivate da uno specifico* atto motorio*, iniziato al livello corticale*

**Via indiretta***: interviene temperando il pattern motorio corticale ed evitando interferenze*

**Via diretta***: lo rinforza*

# Indicazione alla DBS

CAPSIT-PD (Core Asessment Program for Surgical Interventional Therapies in PD)

1) Parkinson idiopatico (70-30%)
2) Assenza di lesioni cerebrali significative
3) Età < 70 aa (*)
4) Malattia avanzata e/o SDR da trattamento farmacologico di lungo periodo
5) Grado di disabilità: UPDRS dopo 12 h off-terapia
6) Buona risposta al test L-Dopa (miglioramento del 50% nella scala UPDRS)
7) Assenza di malattie psichiatriche (Valutazione psichiatrica preoperatoria)
8) Motivazioni personali/familiari all'intervento
9) Assenza di demenze e deficit congitivi
10) Valutazione neuroradiologica preoperatoria
11) Valutazione neurochirurgica ed internistica

# DBS per M. di Parkinson

| *SINTOMI* | *VIM* | *STN* | *GPi* |
|---|---|---|---|
| Tremore | +++ | +++ | ++ |
| Rigidità | +(+) | +++ | ++ |
| Acinesia | +/- | +++ | ++ |
| Distonie Fase OFF | +/- | +++ | +++ |
| Discinesie | +/- | +++ | +++ |
| Instabilità posturale | - | +++ | ? |

# Targets funzionali per le sindromi distoniche

- **Globo Pallido**
  - **GPi**
- **Talamo**
  - **Ventrale orale anteriore**
  - **Ventrale orale posteriore**
  - **Ventrale orale interno**
  - **Centro mediano - parafascicolare**
  - **Ventrale posteromediale e posterolaterale**
  - **Ventrale intermedio**
  - **Pulvinar**
- **Zona incerta**
- **STN e Campi di Forel H1 e H2**
- **Nucleo rosso**
- **Nucleo interstiziale di Cajal**

# Target funzionale per la DBS della distonia

## GPi

### porzione ventro-postero-laterale (Laitinen)

- **Posizione anatomica variabile rispetto alla linea bicommissurale**

# IPOTESI SUL MECCANISMO D'AZIONE DELLA DBS

***Blocco depolarizzante:*** i neuroni verrebbero depolarizzati massivamente e non sarebbero più in grado di condurre un potenziale per tempi prolungati;

***Neural Jamming:*** la stimolazione cronica disturberebbe la rete neurale, interferendo con i circuiti sinaptici e modificando gli assetti recettoriali dei neurotrasmettitori

***Stimolazione di circuiti assonali e dendritici locali:*** l'impulso fornito sarebbe in grado di attivare preferenzialmente circuiti inibitori

# DBS del nucleo Subtalamico

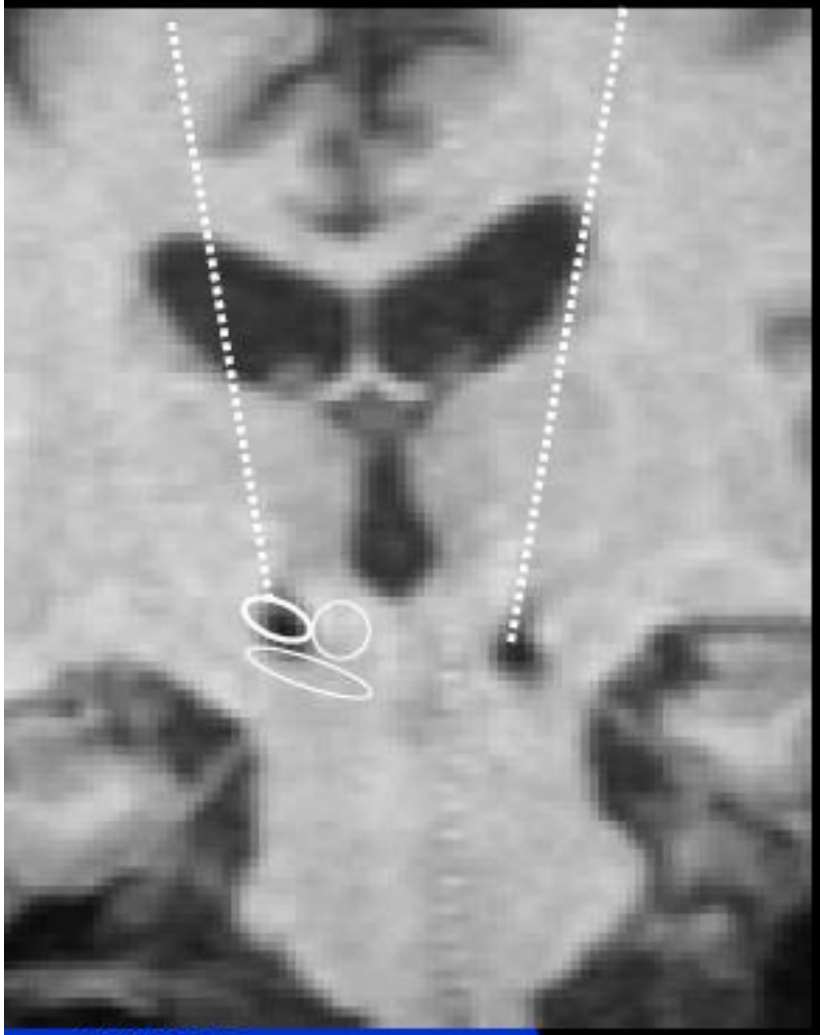

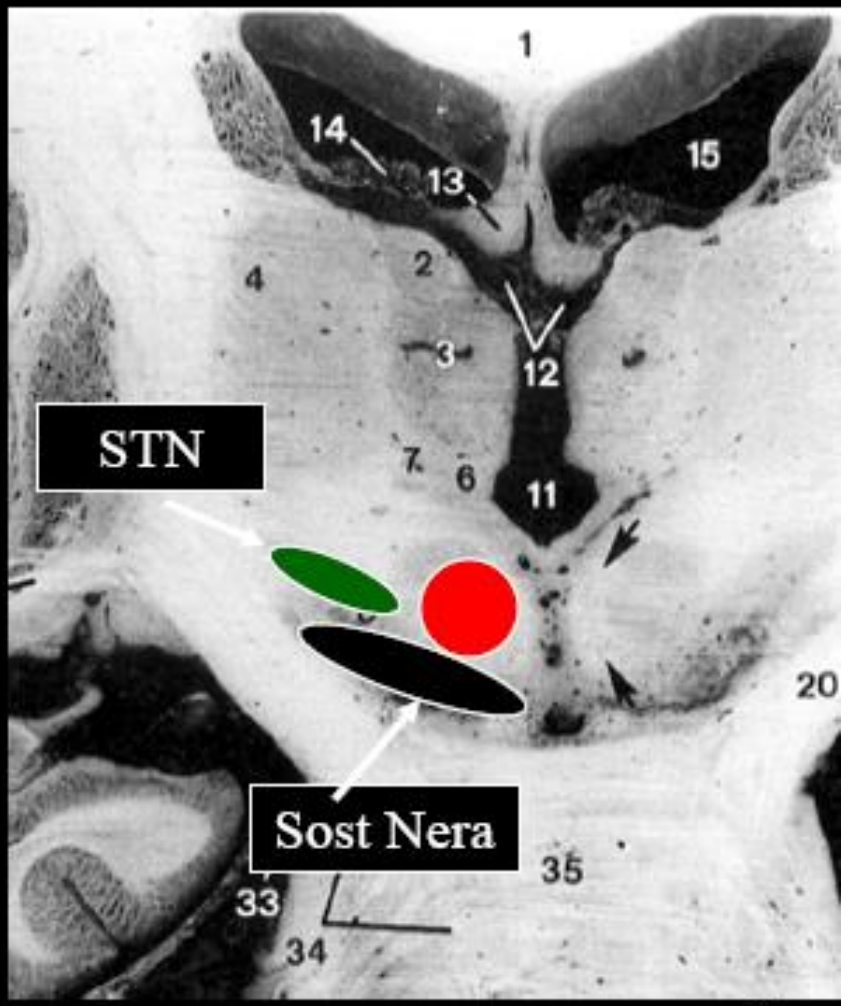

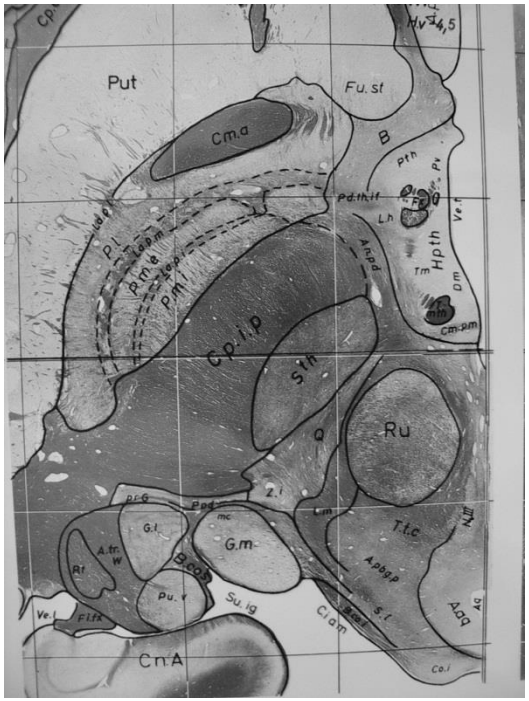


STN assiale

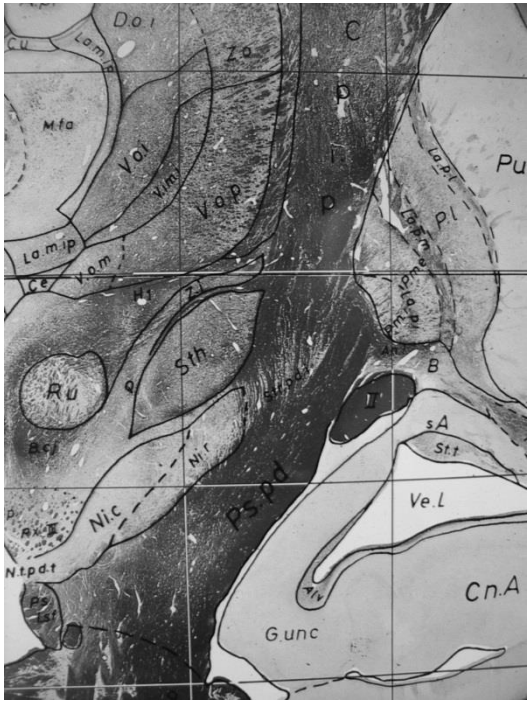


STN coronale

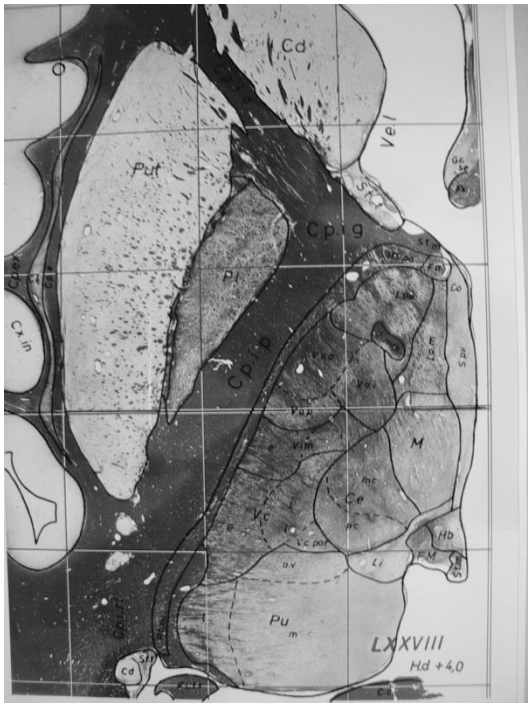


VIM assiale

**Atlante stereotassico di Schaltenbrand**


STN sagittale

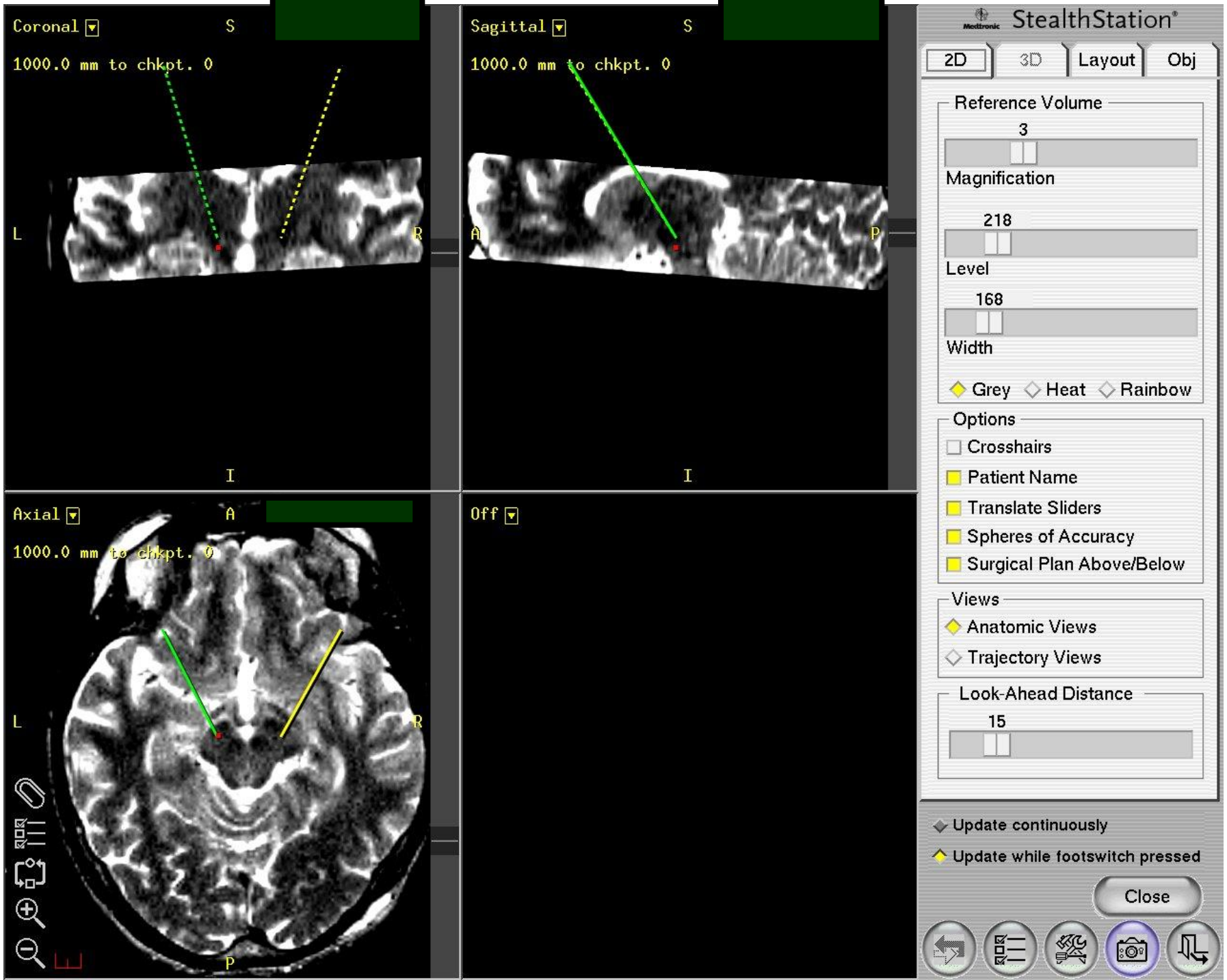
Coronal
S
1000.0 mm to chkpt. 0
L
R
I
Sagittal
S
1000.0 mm to chkpt. 0
A
P
I
Axial
A
1000.0 mm to chkpt. 0
L
R
P
Off
Medtronic
StealthStation®
2D
3D
Layout
Obj
Reference Volume
3
Magnification
218
Level
168
Width
Grey
Heat
Rainbow
Options
Crosshairs
Patient Name
Translate Sliders
Spheres of Accuracy
Surgical Plan Above/Below
Views
Anatomic Views
Trajectory Views
Look-Ahead Distance
15
Update continuously
Update while footswitch pressed
Close

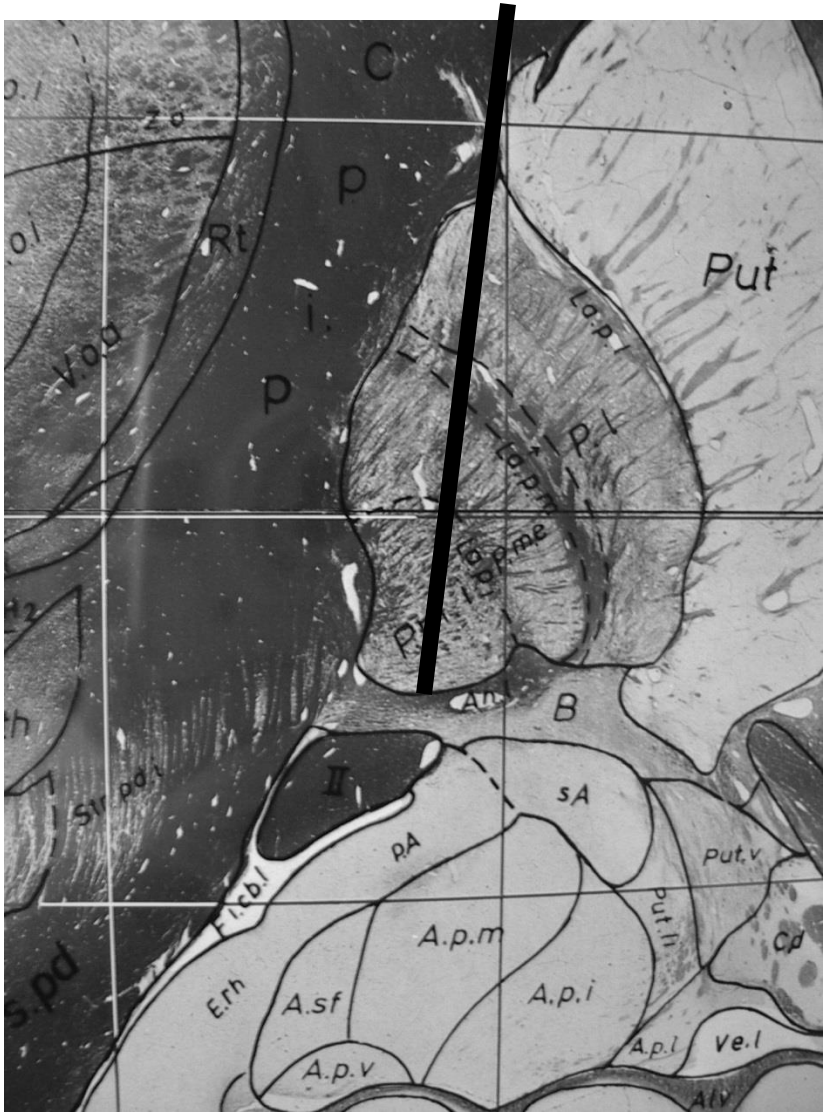


GPi coronale

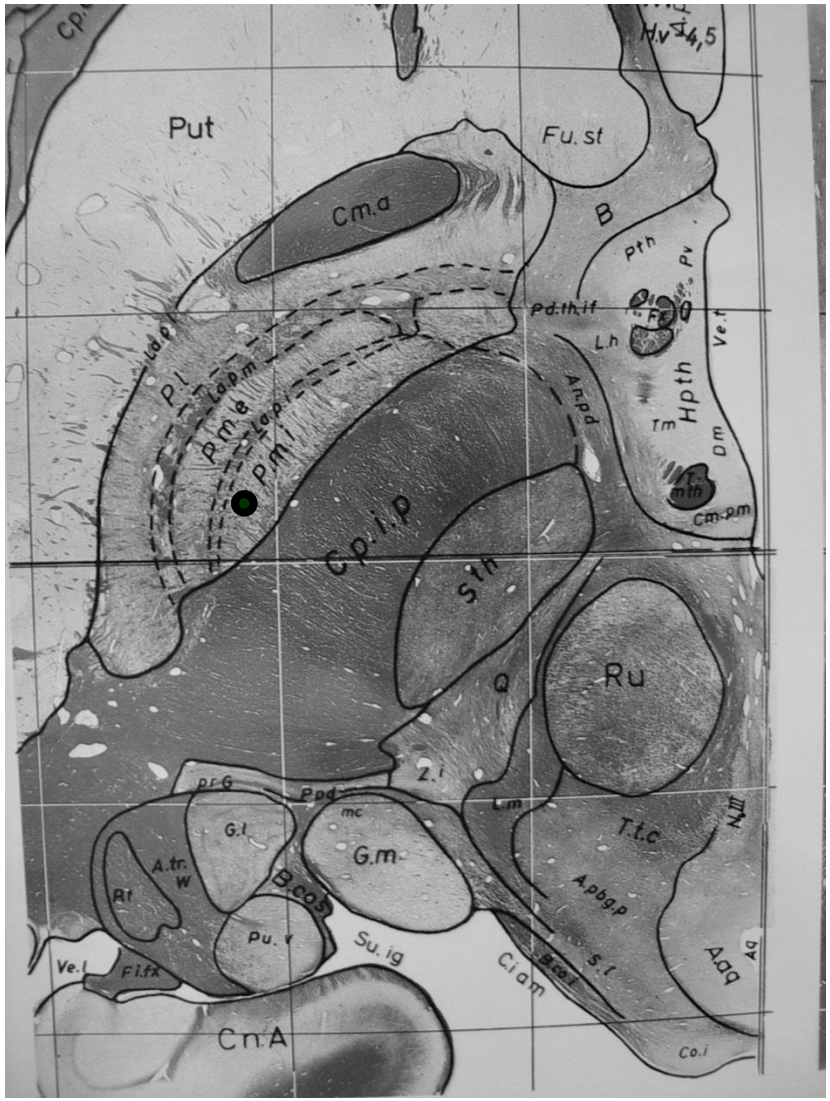


GPi assiale

# Localizzazione stereotassica del GPi con software dedicato “Framelink®”

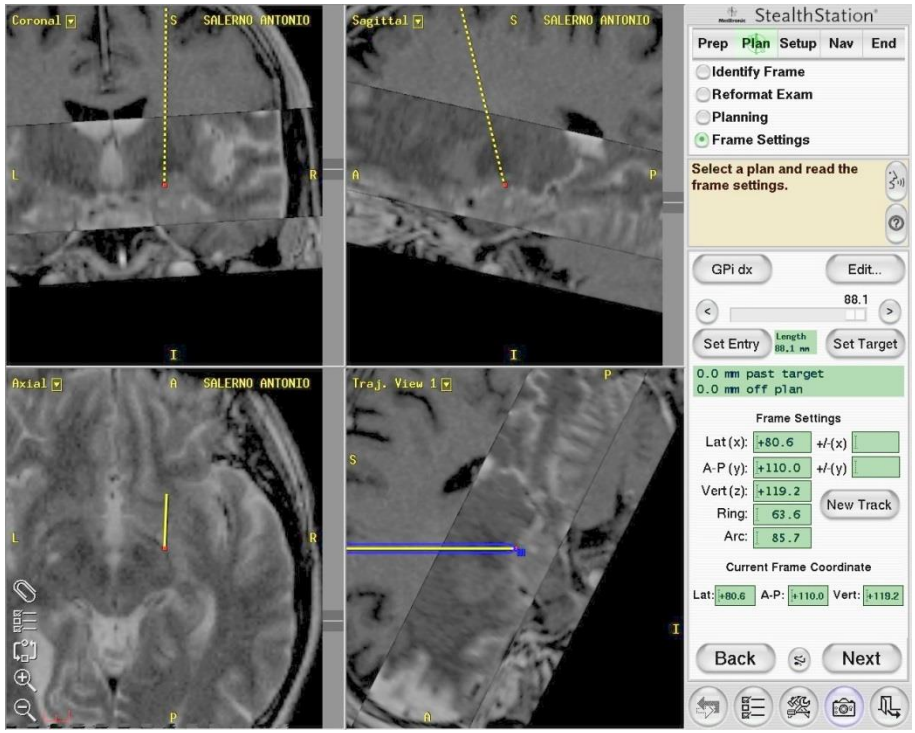


Proiezione tracce su RM

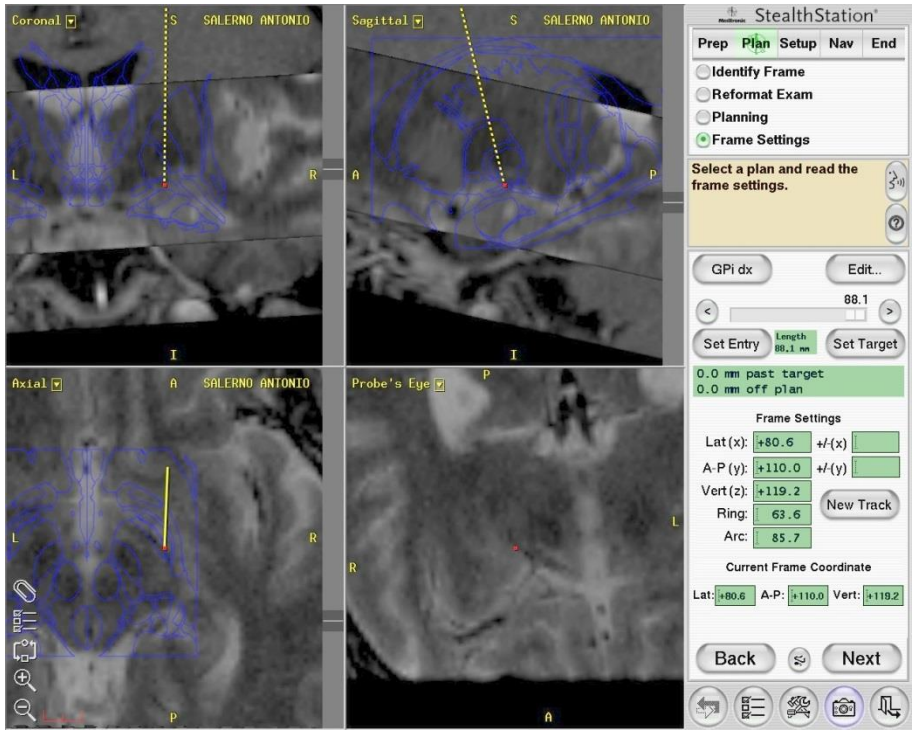


Proiezione tracce su RM con atlante

# Scelta della traiettoria

## STN

0 10 20

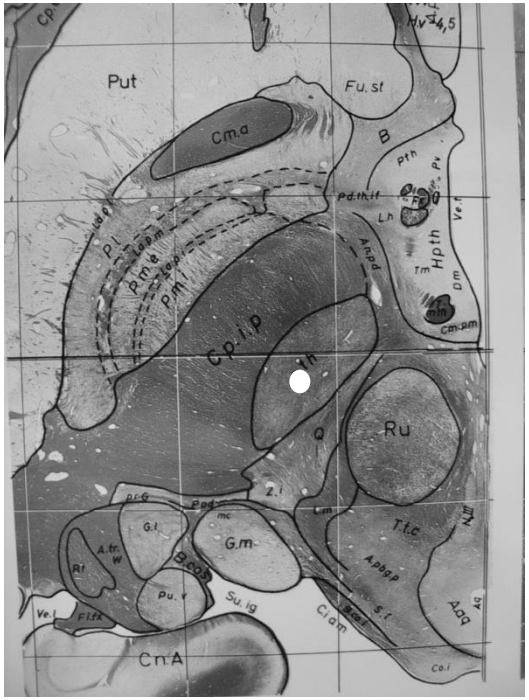


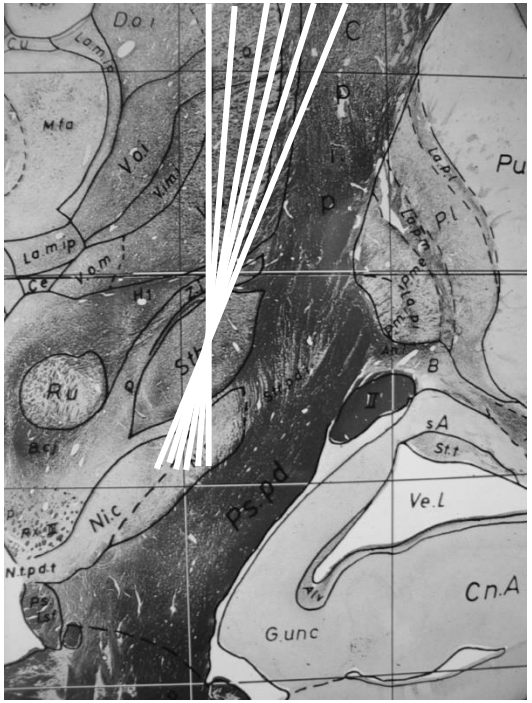


70 60 50

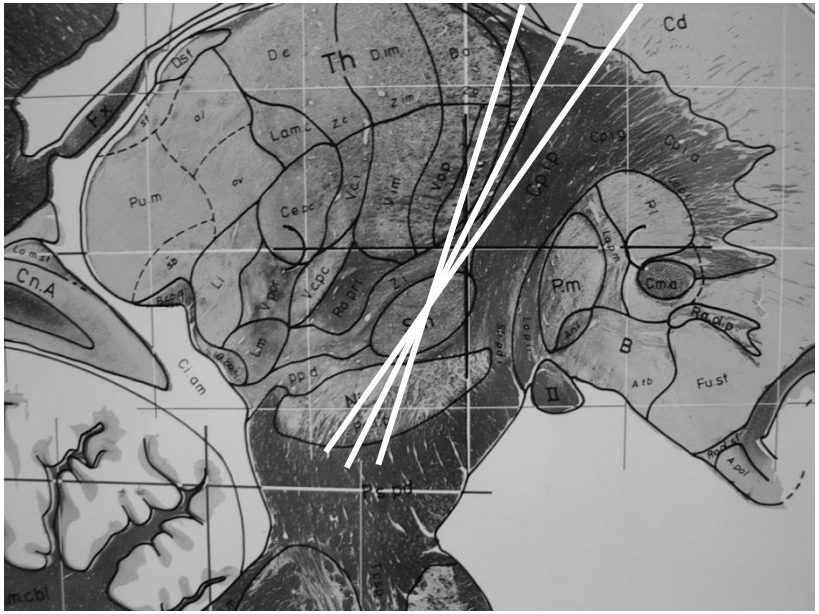


Ass

Coro

Sagi

# Software FrameLink®

## Medtronic, Minneapolis USA

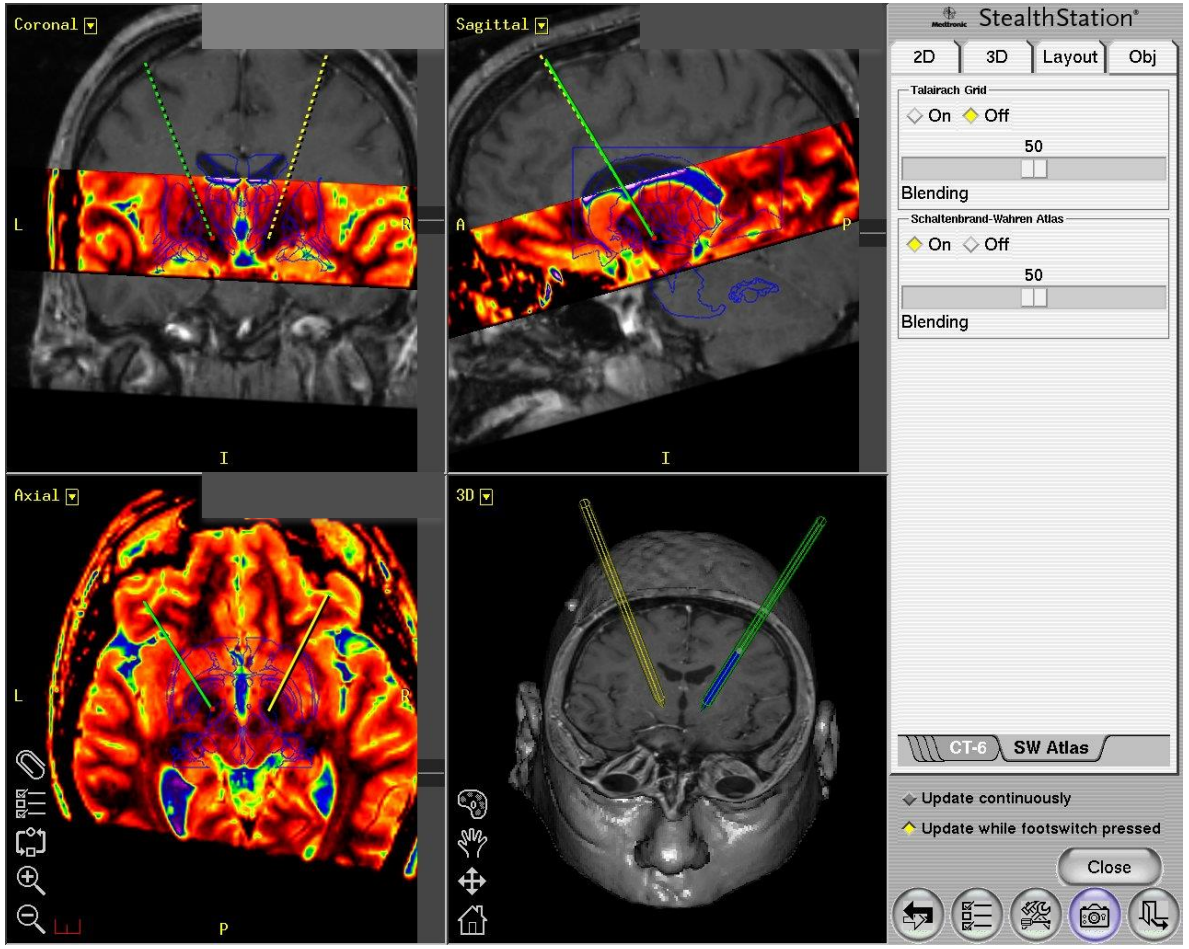


Azienda Ospedaliero-Universitaria S. Anna Ferrara
Dipartimento di Neuroscienze e Riabilitazione
Unità Operativa di Neurochirurgia

Curr Neurol Neurosci Rep. 2013 August ; 13(8): 371. doi:10.1007/s11910-013-0371-2.

# Technological Advances In The Surgical Treatment Of Movement Disorders

**Robert E. Gross, MD, PhD**[1,2,3] and **Margaret E. McDougal, BS**[1]
[1]Department of Neurosurgery, Emory University School of Medicine, Atlanta, GA
[2]Department of Neurology, Emory University School of Medicine, Atlanta, GA
[3]Coulter Department of Biomedical Engineering, Georgia Institute of Technology, Atlanta, GA

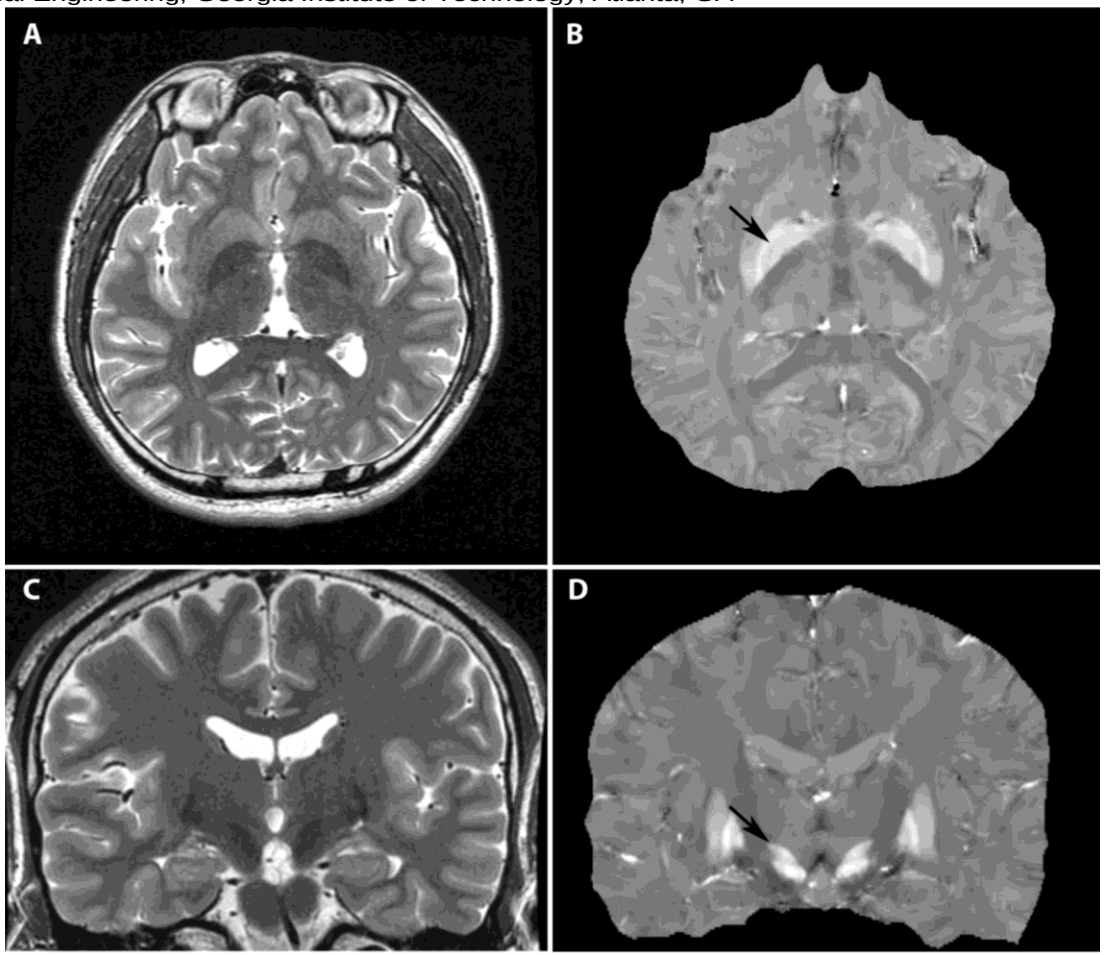


**Fig. 1.**
Quantitative Susceptibility Mapping clearly demonstrating the globus pallidus internus (GPi) on axial images (B, arrow) and the subthalamic nucleus (STN) on coronal images (D, arrow), as compared to traditional T2-weighted imaging (A, C). (Images courtesy of Brian Kopell, Mt. Sinai School of Medicine, and Tian Liu, Cornell University)

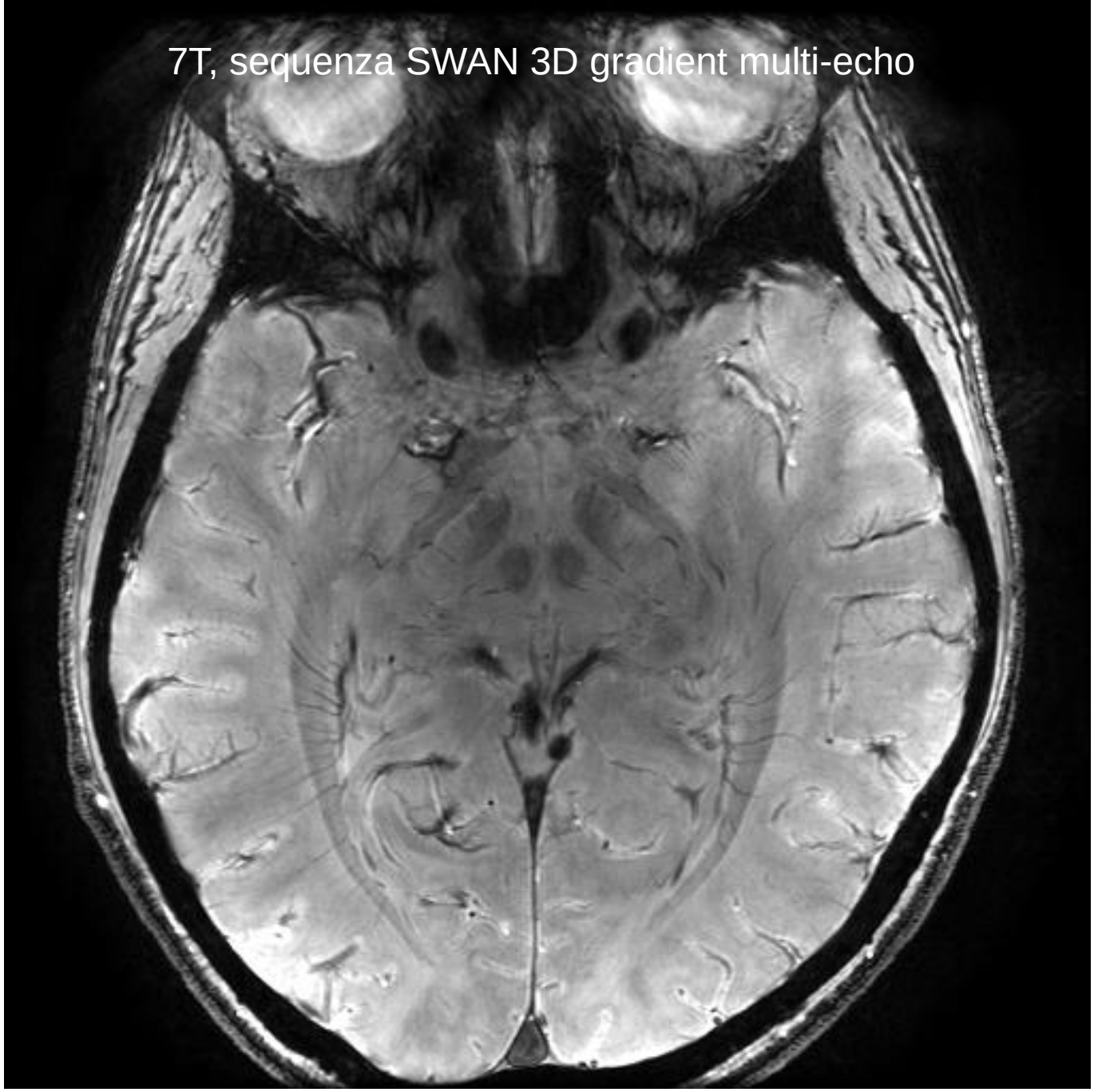
7T, sequenza SWAN 3D gradient multi-echo

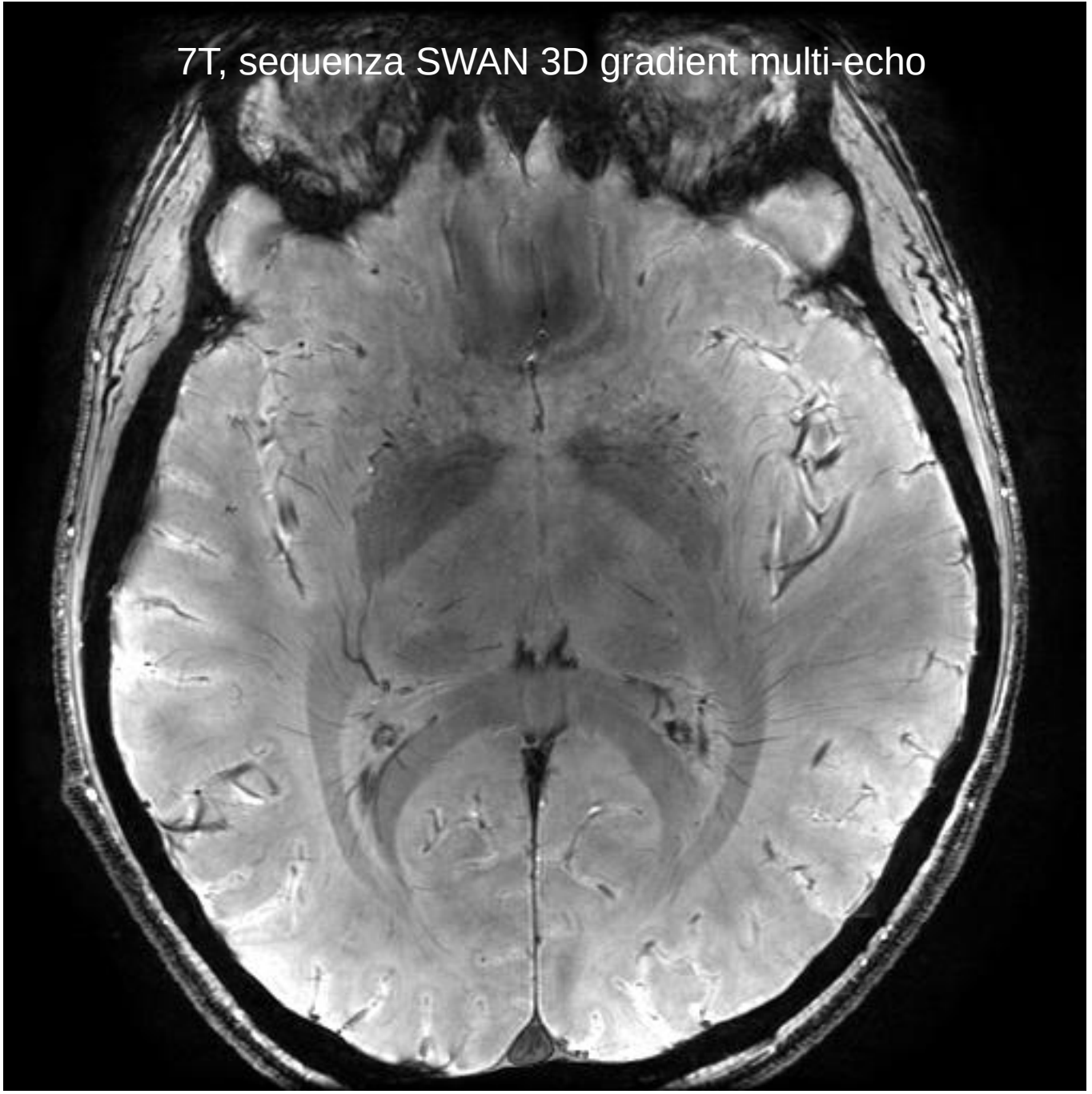
7T, sequenza SWAN 3D gradient multi-echo

Neuroimage. 2012 Feb 1;59(3):2035-44. doi: 10.1016/j.neuroimage.2011.10.016. Epub 2011 Oct 21.

# High resolution MR anatomy of the subthalamic nucleus: imaging at 9.4 T with histological validation.

Massey LA1, Miranda MA, Zrinzo L, Al-Helli O, Parkes HG, Thornton JS, So PW, White MJ, Mancini L, Strand C, Holton JL, Hariz MI, Lees AJ, Revesz T, Yousry TA.

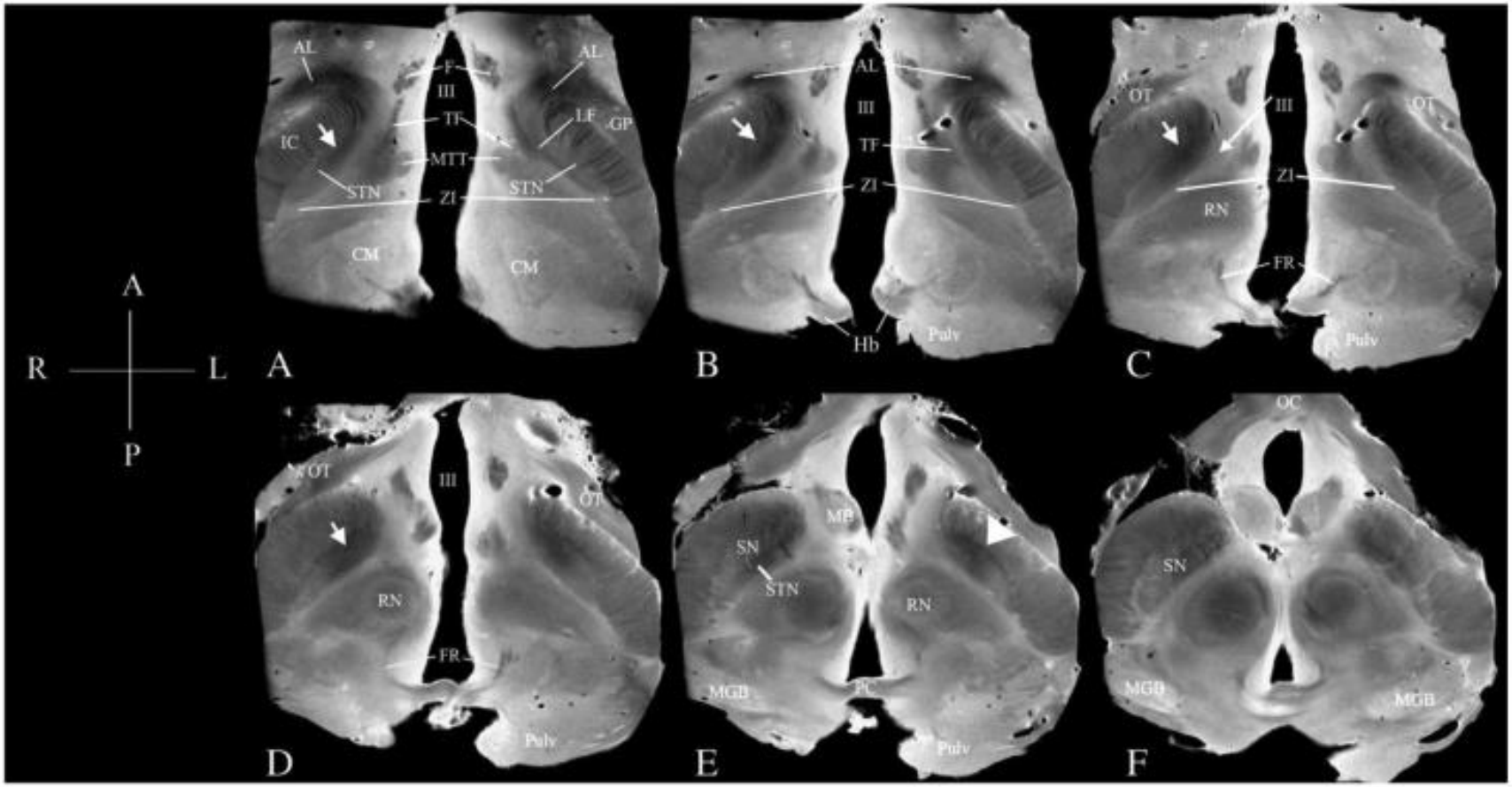


**Fig. 2.** Axial Plane. The anatomy of the STN on SE MRI at 9.4 T showing both halves of the midbrain in serial axial sections from superior to inferior levels [A-F]. Long white arrow: anteromedial border of the STN defined by the confluence of the ZI and posterior border of the hypothalamus. Short white arrow: medial hypointensity of the STN (seen in 6/9 subthalamic nuclei studied). Arrow head in 2E identifying the hypointense band forming the anterior border of the STN and enabling discrimination from the SN at more inferior levels—see 2E on the right side the most inferior portion of the STN can distinguished medial to the SN. Acquired with an in-plane resolution of 88 μm. Orientation: A—anterior, P—posterior, M—medial, L—lateral.

Neuroimage. 2012 Feb 1;59(3):2035-44. doi: 10.1016/j.neuroimage.2011.10.016. Epub 2011 Oct 21.

# High resolution MR anatomy of the subthalamic nucleus: imaging at 9.4 T with histological validation.

Massey LA1, Miranda MA, Zrinzo L, Al-Helli O, Parkes HG, Thornton JS, So PW, White MJ, Mancini L, Strand C, Holton JL, Hariz MI, Lees AJ, Revesz T, Yousry TA.

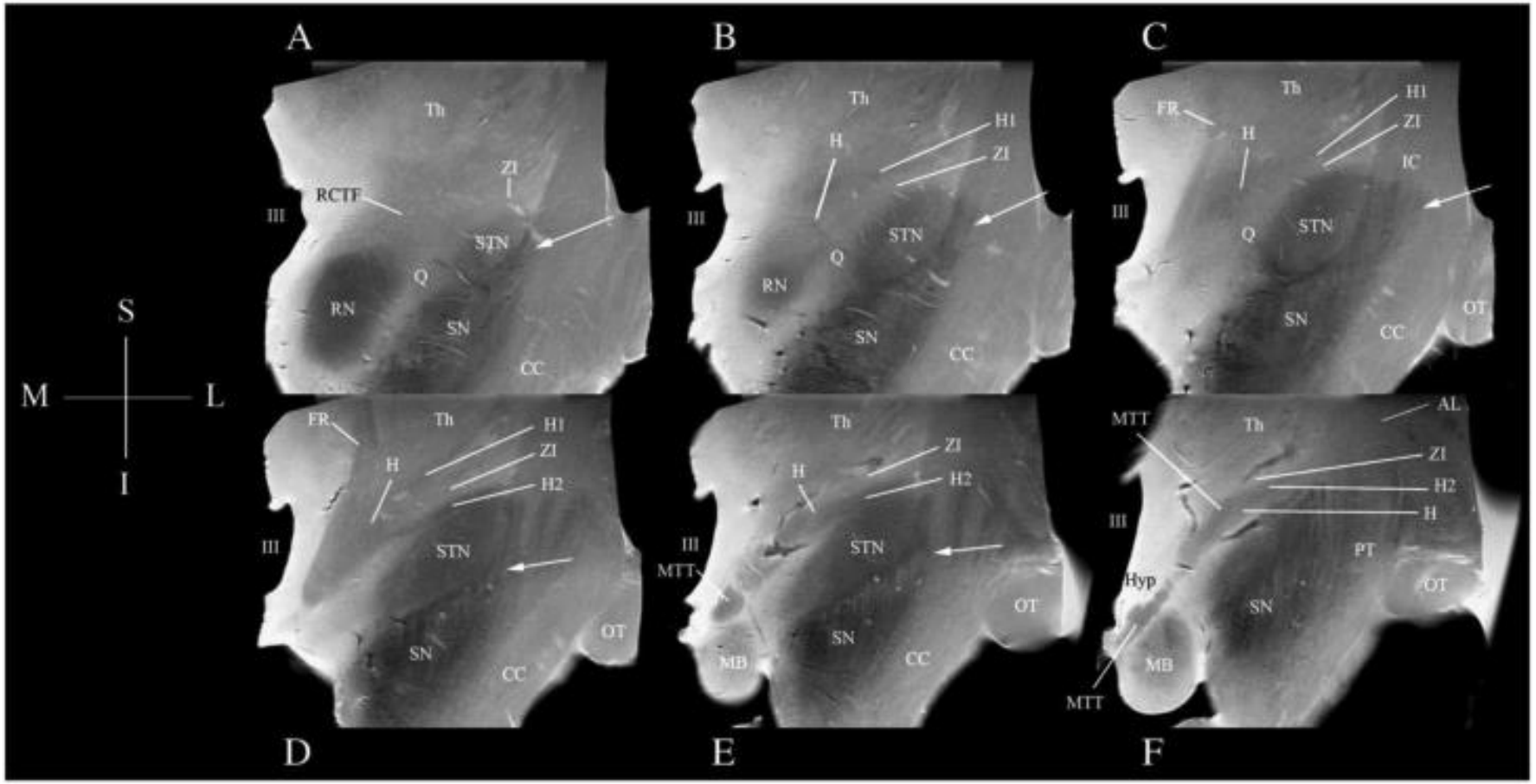


**Fig. 4.** Coronal plane: The STN in serial 1 mm coronal sections in a control case from posterior to anterior [A–F]. The SN can be seen enveloping the inferolateral border of the STN (white arrow). Acquired with an in-plane resolution of 88 μm. Orientation: S—superior, I—inferior, M—medial, L—lateral.

Neuroimage. 2012 Feb 1;59(3):2035-44. doi: 10.1016/j.neuroimage.2011.10.016. Epub 2011 Oct 21.

# High resolution MR anatomy of the subthalamic nucleus: imaging at 9.4 T with histological validation.

Massey LA1, Miranda MA, Zrinzo L, Al-Helli O, Parkes HG, Thornton JS, So PW, White MJ, Mancini L, Strand C, Holton JL, Hariz MI, Lees AJ, Revesz T, Yousry TA.

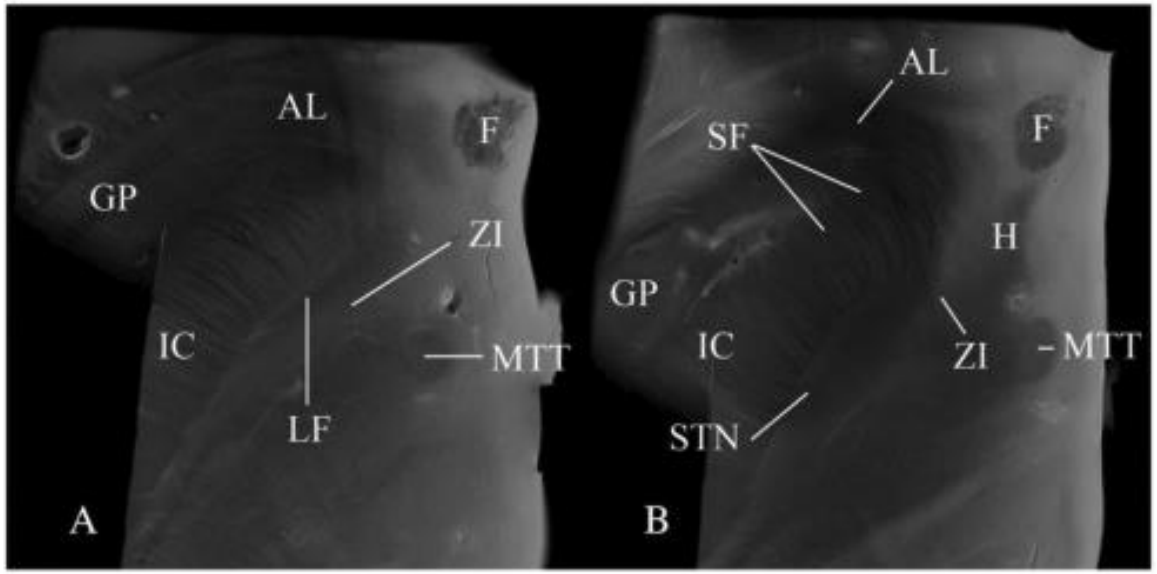


**Fig. 5.** The STN in the axial plane using SE MRI with image resolution acquired at 44 μm in plane. Panel A just above the level of the STN, Panel B at a superior level of the STN above the RN. The resolution of these images allows clear identification the fibres of the subthalamic fasciculus radiating through the internal capsule.

Neuroimage. 2012 Feb 1;59(3):2035-44. doi: 10.1016/j.neuroimage.2011.10.016. Epub 2011 Oct 21.

**High resolution MR anatomy of the subthalamic nucleus: imaging at 9.4 T with histological validation.**

Massey LA1, Miranda MA, Zrinzo L, Al-Helli O, Parkes HG, Thornton JS, So PW, White MJ, Mancini L, Strand C, Holton JL, Hariz MI, Lees AJ, Revesz T, Yousry TA.

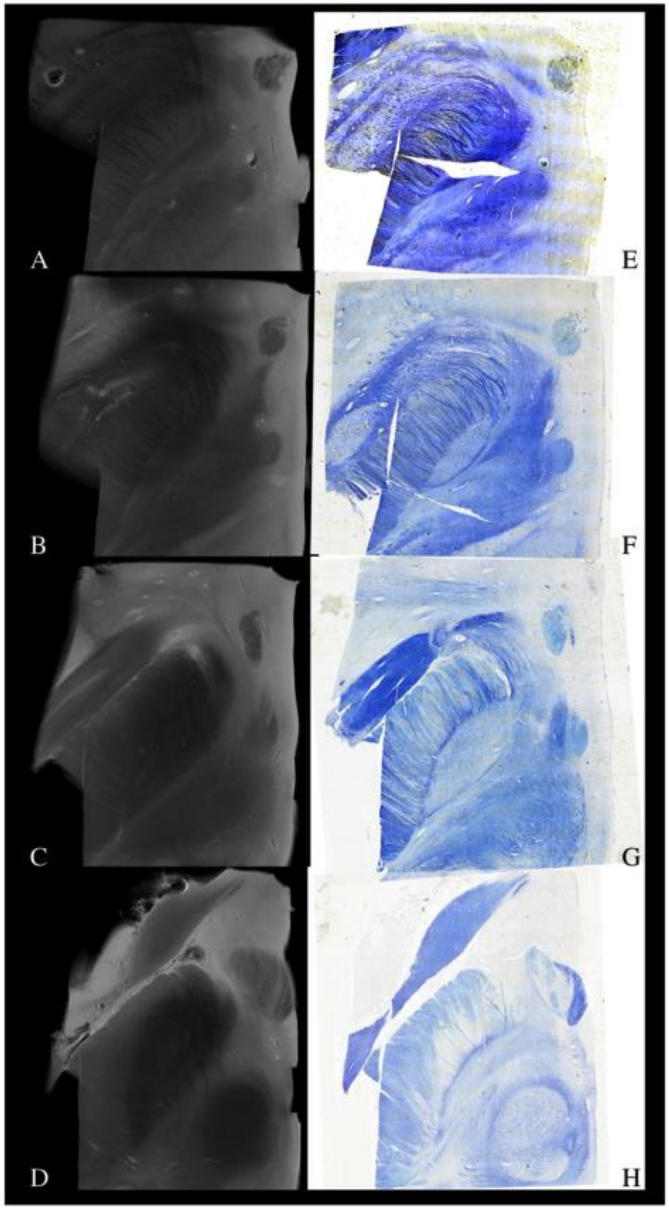


**Fig. 6.** Comparison of 9.4 T SE MRI images [A–D] and histological sections stained using the LFB/CV method [EG]. MRI in plane resolution 88 μm. Images are unlabelled to make comparison easier. For anatomical labels see Fig. 3. The STN is identified clearly as an almond shaped structure surrounded by white matter tracts (blue stain on LFB/CV images). LFB/CV staining within the STN was uniform in 4/4 cases with no particular anteromedial/posterolateral gradient evident. Structures corresponding to the borders of the STN can be clearly identified: at superior levels the LF can be seen as a dark blue myelinated structure corresponding to a region of hypointensity on T2w images [A and E]. One step inferiorly [B and F] the STN is clearly demarcated by a rim of dark blue staining and the fibres of the subthalamic fasciculus are seen radiating through the internal capsule—corresponding to the hypointensity seen on the anterolateral border of the STN on T2w/PDw images. The posteromedial border is clearly defined on the LFB/CV images as white matter tracts but on the MR images there is a relatively hyperintense signal arising from the region of the zona incerta [B and F]. A region densely staining for myelin is seen separating the STN anteromedially from the superior SN posterolaterally on the LFB/CV image—this corresponds to a relatively hypointense region on the MR image [D and H]. It can be seen that the medial border of the STN is less clearly defined on the LFB/CV image at this level near the posterior aspect of the anteromedial tip on the LFB/CV image but this remains well defined on the 9.4 T SE MR image [H].

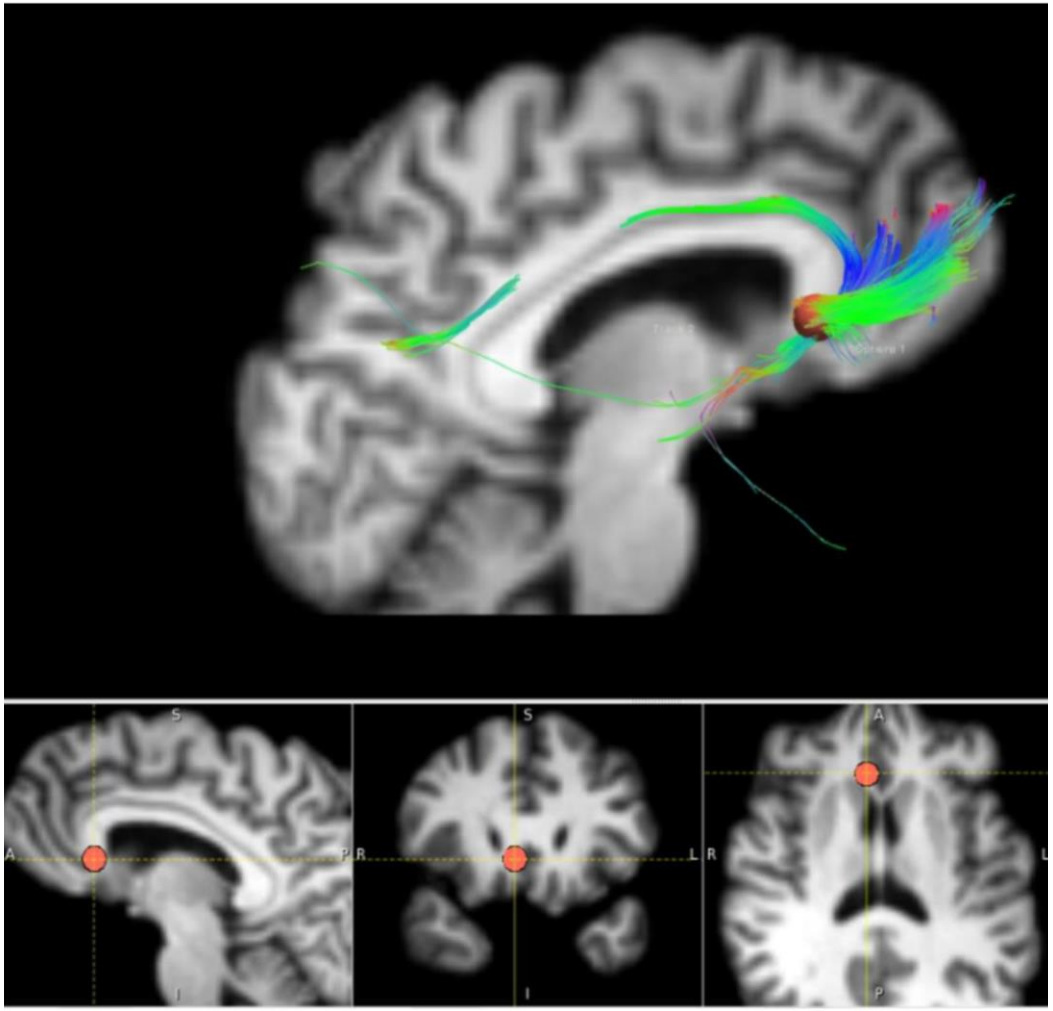


**Fig. 2.**
Deterministic diffusion tensor imaging (DTI) used in an individual patient undergoing deep brain stimulation of the subgenual cingulate cortex (SCC) for treatment-resistant major depressive disorder. The DBS site chosen is depicted by the red dot (bottom images), at the nexus of fibers projecting to the ventromedial orbitofrontal cortex, the cingulate bundle, and the nucleus accumbens. (Images courtesy of Helen Mayberg and Patrico Riva Posse, Emory University).

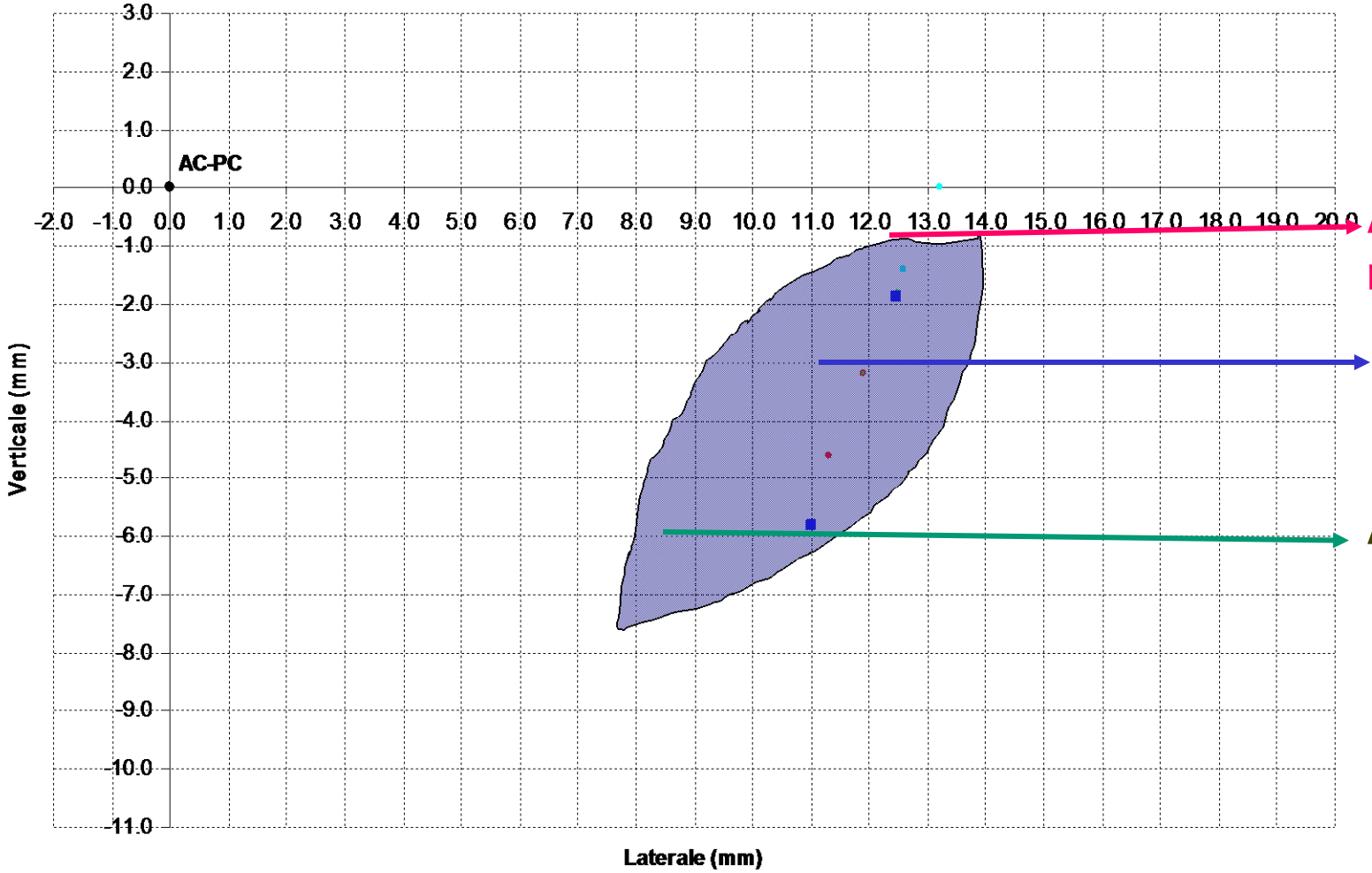


Area sensori-motoria

Area associativa

Area limbica

# Confirmation of functional zones within the human subthalamic nucleus: Patterns of connectivity and sub-parcellation using diffusion weighted imaging

Christian Lambert [a,*], Ludvic Zrinzo [b], Zoltan Nagy [a], Antoine Lutti [a], Marwan Hariz [b], Thomas Foltynie [b], Bogdan Draganski [c], John Ashburner [a], Richard Frackowiak [c]



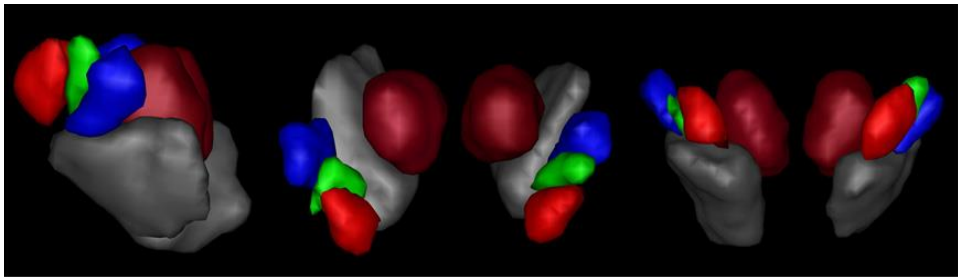

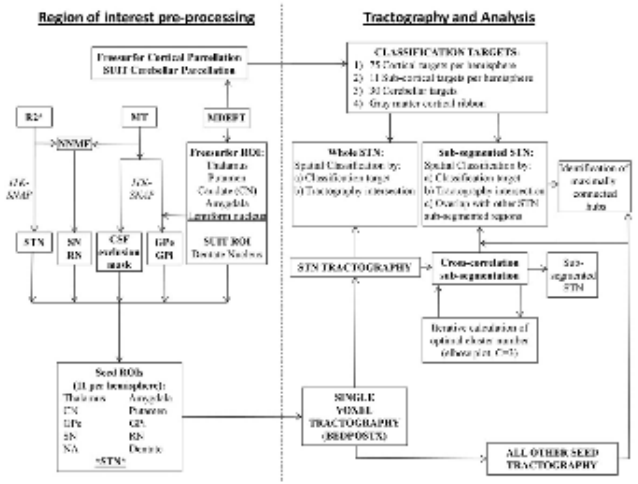


**Fig. 1.** Methodological pipeline, refer to text for details. Abbreviations: CSF = Cerbrospinal fluid, CN = Caudate nucleus, GPe = External segment of the globus pallidus, GPi = Internal segment of the globus pallidus, MT = Magnetic transfer, NA = Nucleus accumbens, NNMF = Non-negative matrix factorisation, RN = Red nucleus, SN = Substantia nigra, STN = Subthalamic nucleus.

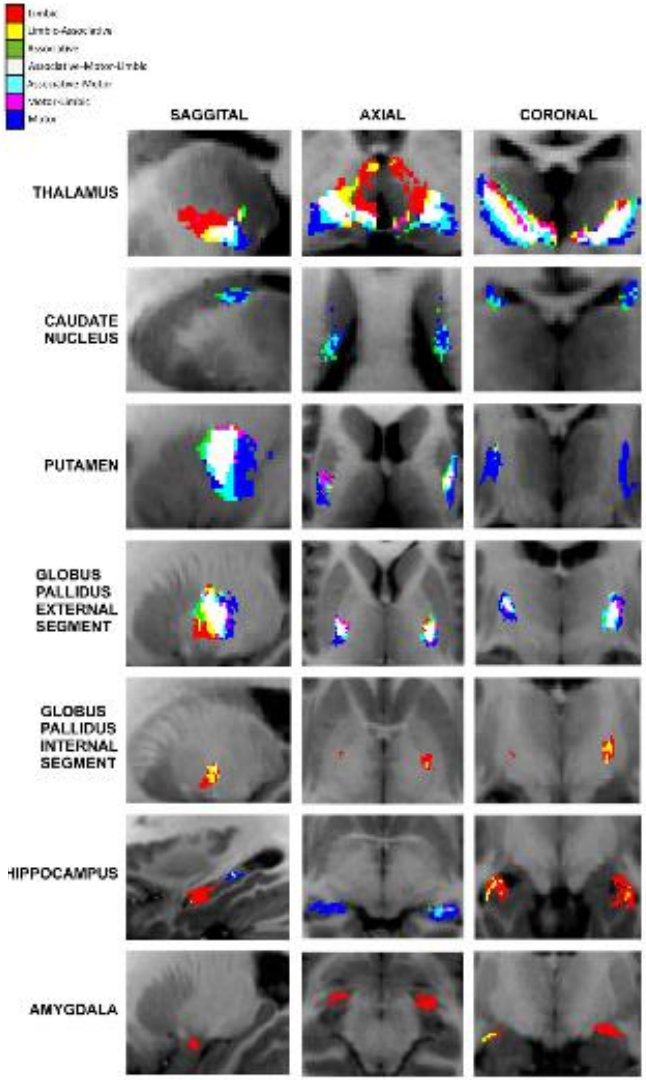


**Fig. 6.** Overlap of group averaged projections from sub-segmented STN regions. Overlap regions are defined by group averaged tractography distributions in standard space for each STN subregion, and then classifying each ROI brain voxel according to the combination of these average distributions that is connected with it. This is summarised in the top left legend. These demonstrate that the associative regions previously shown (Supplementary Material 2) represent an overlapping network between distinctive motor and limbic networks, sharing regions common to both.

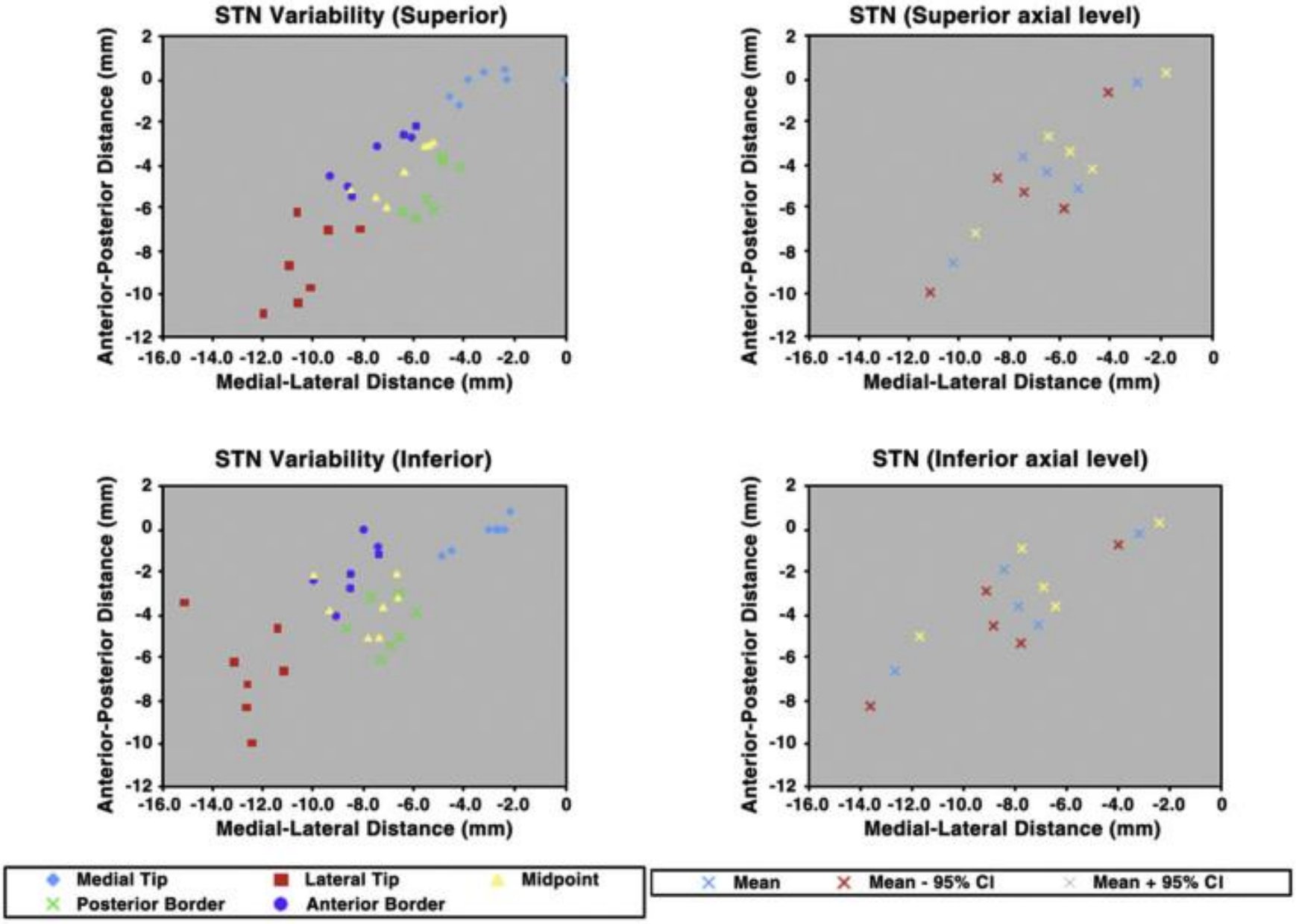


**Fig. 9.** Variability of the position of the STN. Scatter plots on the left include the measured locations of points for all available cases for superior and inferior levels examined. Scatter plots on the right show the mean position relative to the midpoint between the fornix and mamillothalamic tract in the axial plane. The upper and lower 95% confidence intervals are also plotted using coordinates in the *x*- and *y*-axis. Points plotted to give the profile of the STN are the medial and lateral tip, the anterior and posterior midpoints and the midpoint of the STN. See Fig. 11. All samples were reoriented such that the midpoint between the MTT and fornix is at position 0 in the *x*- and *y*-axis. See Table 3 for mean values and standard deviation.

# Sistemi di localizzazione del target

**SISTEMI STEREOTASSICI**
**SISTEMI STEREOTASSICI FRAMELESS**
**RM INTRAOPERATORIA**

- Allo stato attuale non vi sono dati che dimostrino la superiorità di un sistema stereotassico rispetto ad un altro;
- Il sistema stereotassico usato deve essere sottoposto a verifiche periodiche di precisione spaziale;
- I sistemi frameless utilizzano la neuronavigazione, che permette un'ottima precisione spaziale
- I sistemi di localizzazione diretta in Risonanza Magnetica non sono ancora applicabili per la complessità e i costi elevati

# Sistema stereotassico di Leksell

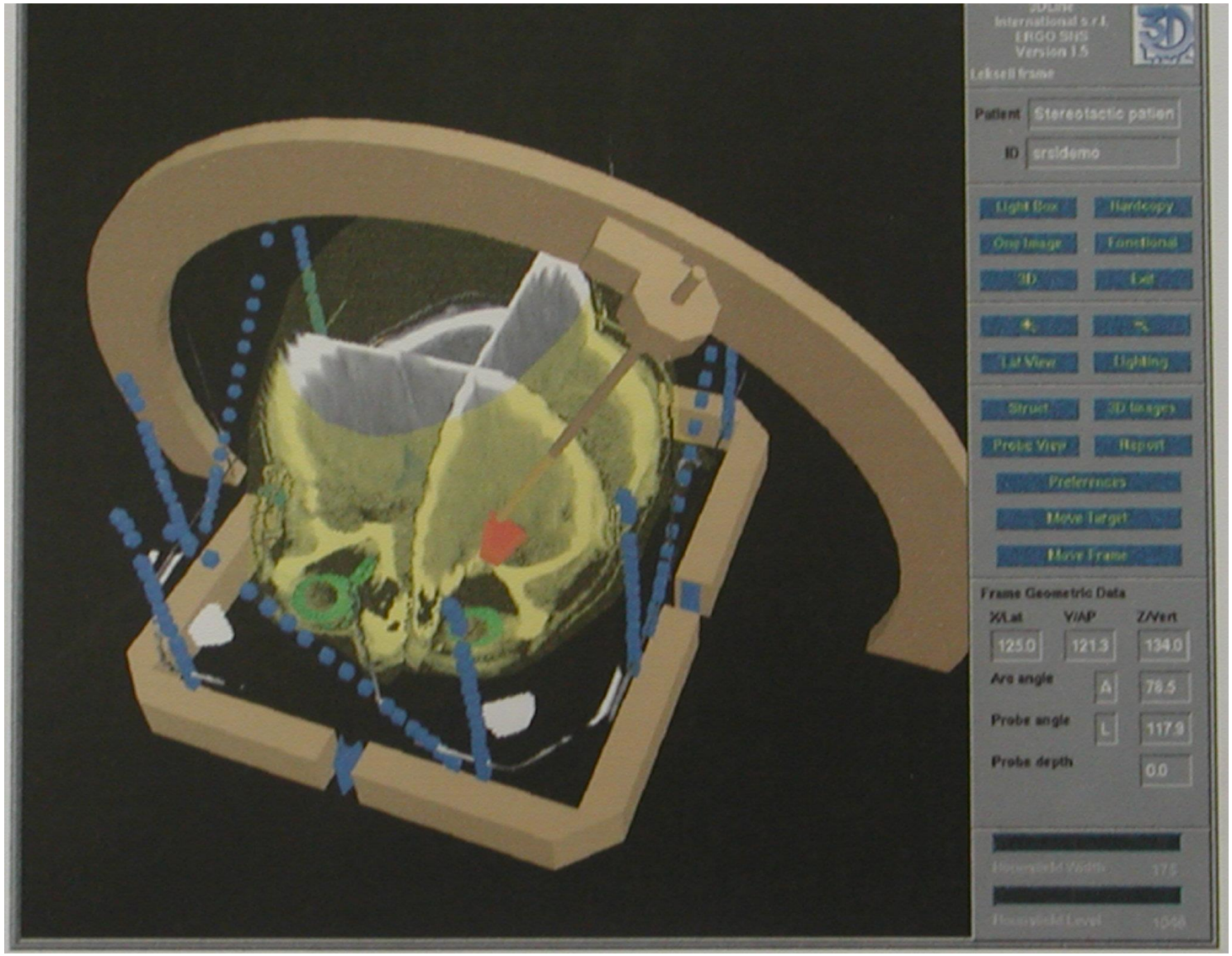

# NexFrame

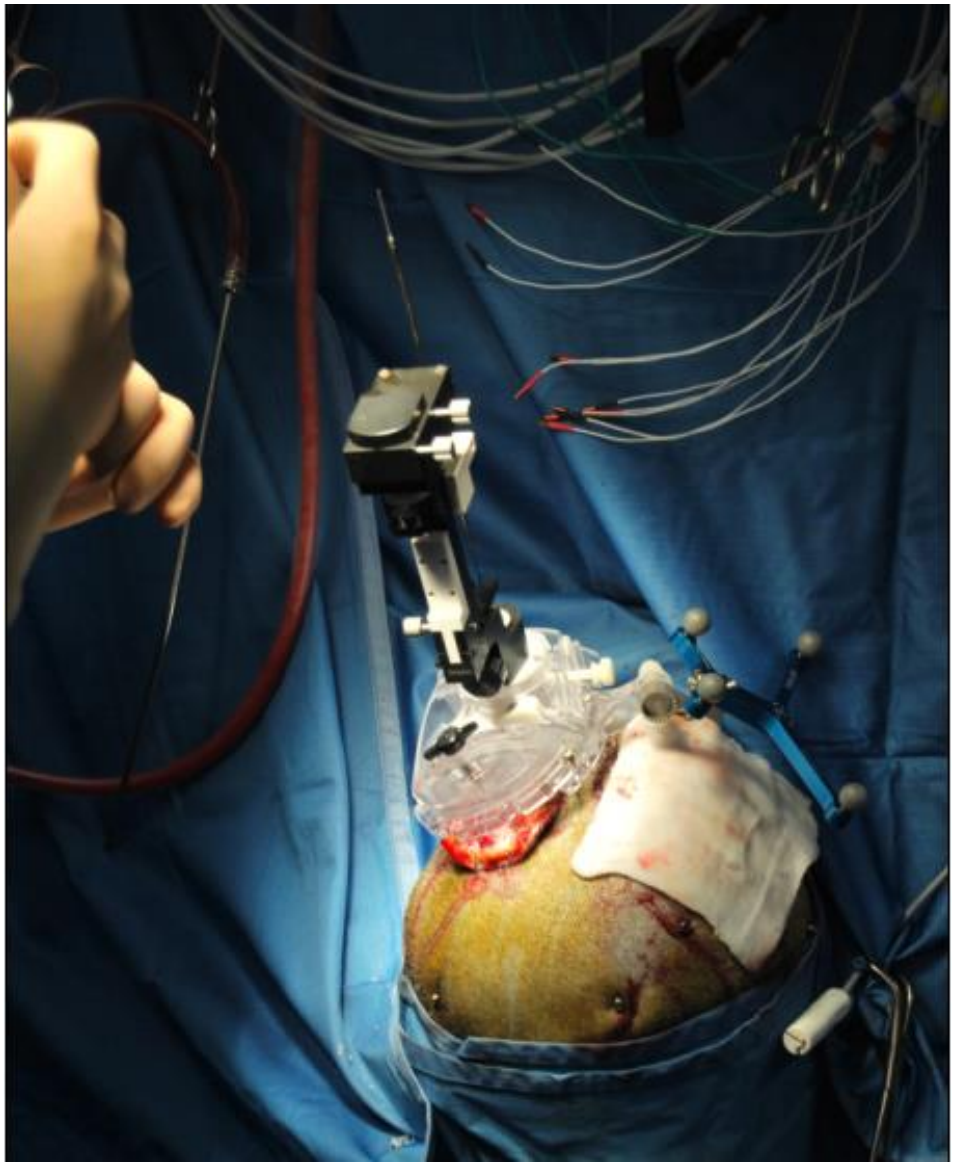

Cortesia dott. M

# Intraoperative MRI DBS

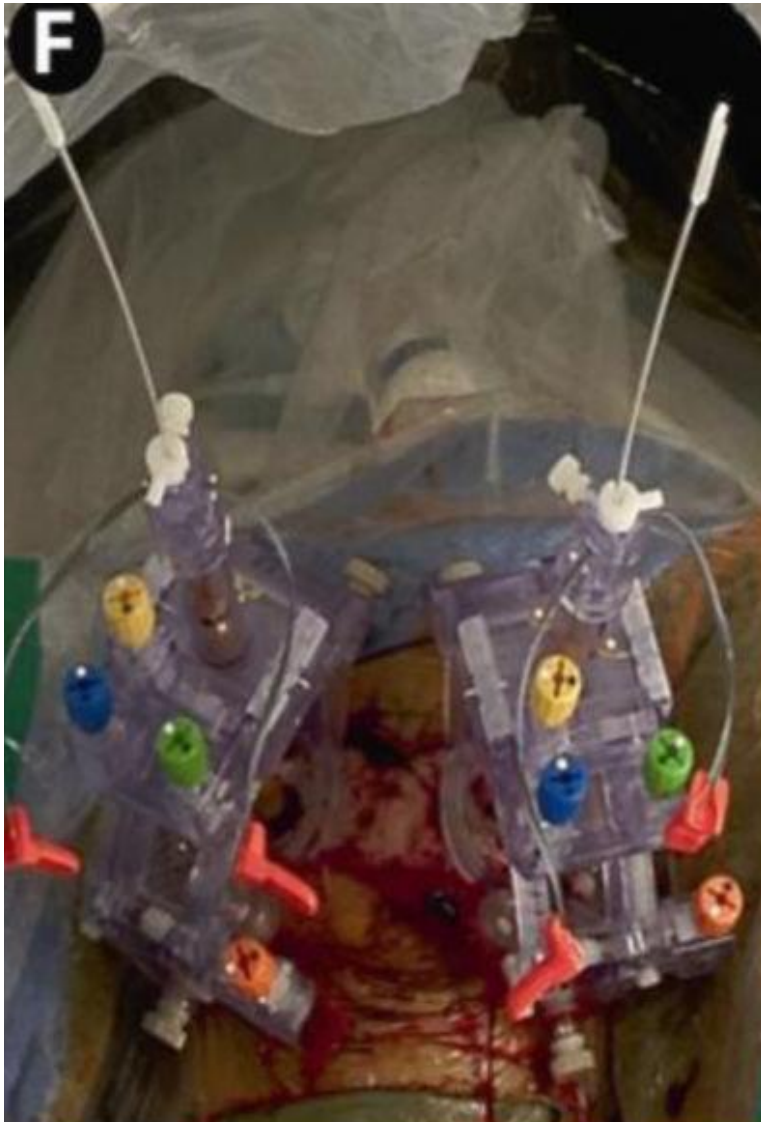

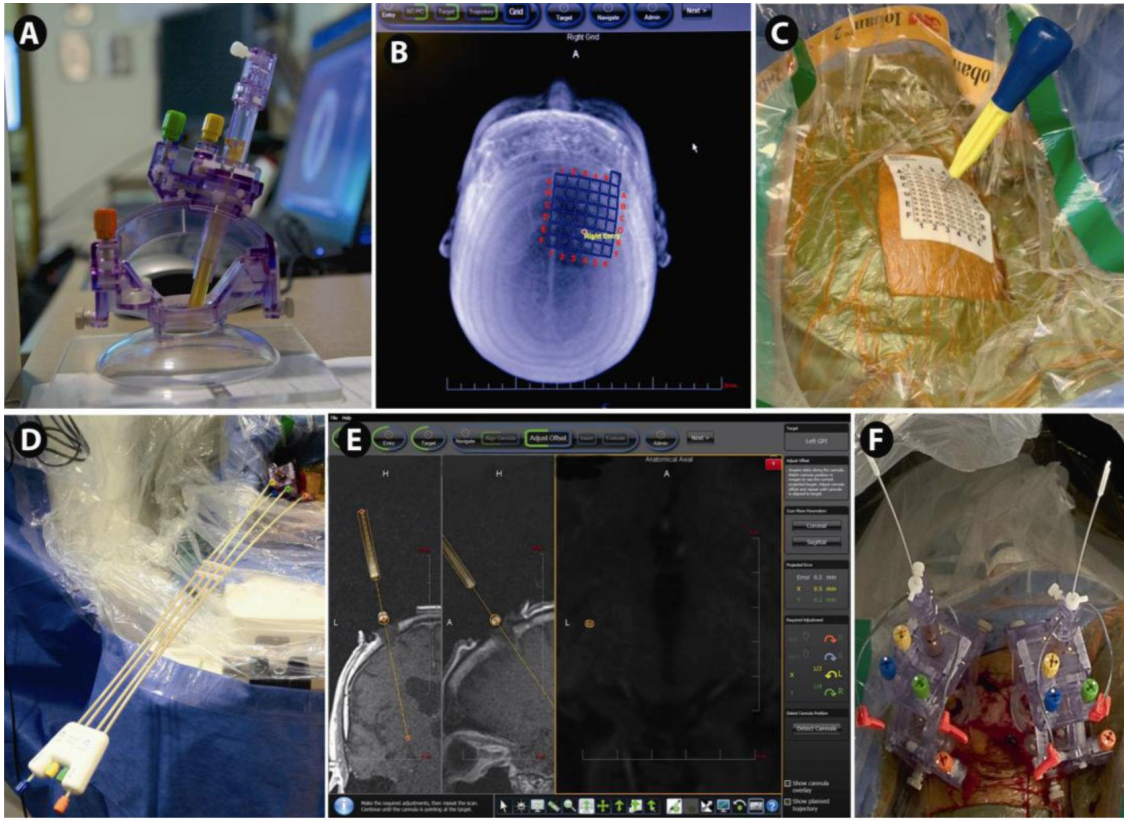


**Fig. 3.**
DBS implantation by direct targeting technique in the intraoperative or interventional MRI scanner: Implantation of globus pallidus internus (GPi) DBS lead(s) using the ClearPoint® SMARTframe (MRI Interventions, Irvine, CA). The skull-mounted targeting cannula is shown in A. Adjustments of pitch/roll and X/Y movements are driven by gears (colored knobs). The entry is determined with respect to a fiducial grid (B, C), and the software determines the point on the grid through which to mark the bone (C). Iterative adjustments are made to the pitch/roll and X/Y using the controller (D) attached to the SMARTFrame, as determined by the software, to align the cannula with the target (E). After final alignment to submillimeter accuracy, an MRI-compatible (i.e. minimal artifact and approved for use in MRI) ceramic stylet is inserted to target through a peel-away catheter. After MR-confirmation of accurate targeting, the stylet is replaced with the DBS lead(s) (F), followed in some centers by a final MRI demonstrating accurate DBS lead position, and finally removal of the peel-away catheter.

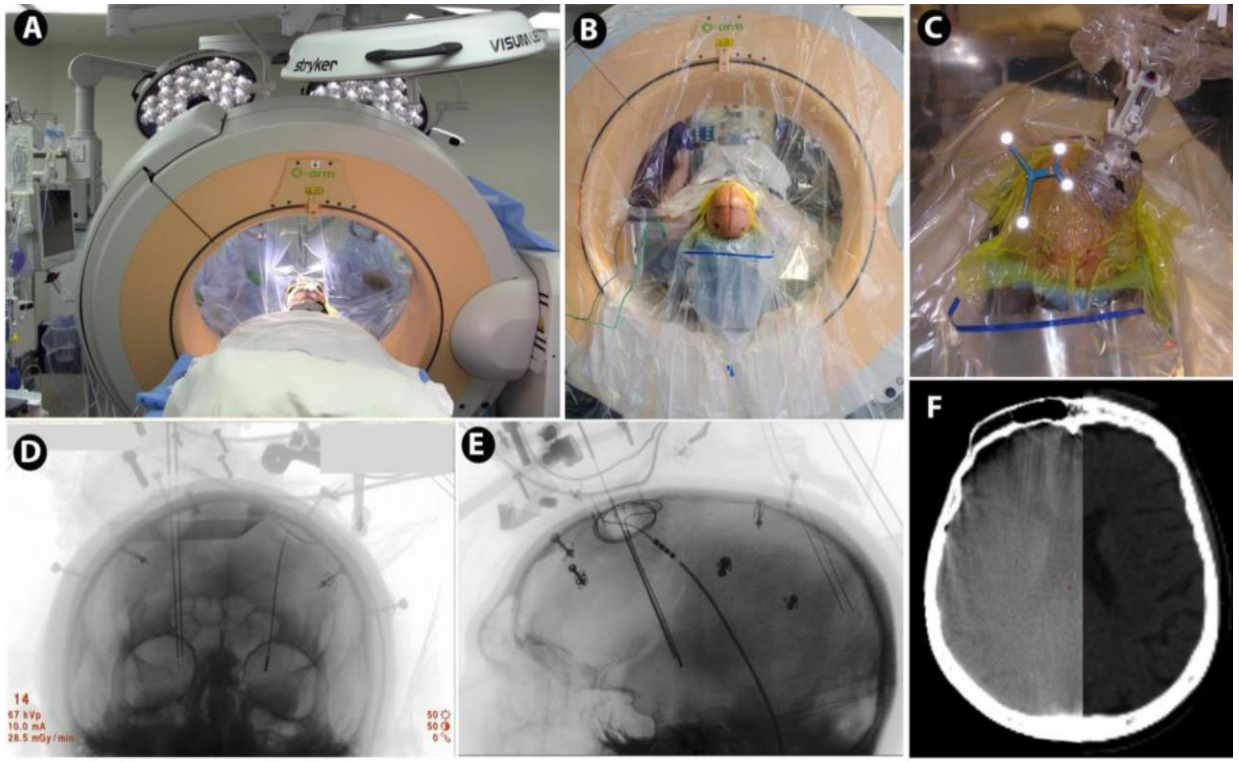


**Fig. 4.**
Stereotactic intraoperative CT scanning for 3D radiological control of DBS implantation. Patient positioned within the O-arm® (Medtronic) (A, B). The reference frame for 'frameless' navigation is shown (light reflecting off fiducials) to the left of the NexFrame®, a skull-mounted targeting frame with microelectrode inserted (C). The O-arm allows both anterior-posterior (D) and lateral (E) radiography that can be co-registered to the preoperative MRI or CT, using the Stealth® Framelink® navigation workstation (Medtronic). This may be used to track the accuracy of microelectrode insertions, as shown, contributing to the interpretation of neurophysiological recordings. The O-arm also allows 3D CT imaging (F, left), which can be co-registered to the pre-operative imaging (F, right), that can be used for both post-implantation DBS location verification, as well as for bone fiducial registration, allowing the entire procedure (beyond the preoperative MRI scan) to be completed in the operating room. (Images courtesy of Kathryn Holloway, Medical College of Virginia).

assiale

coronale

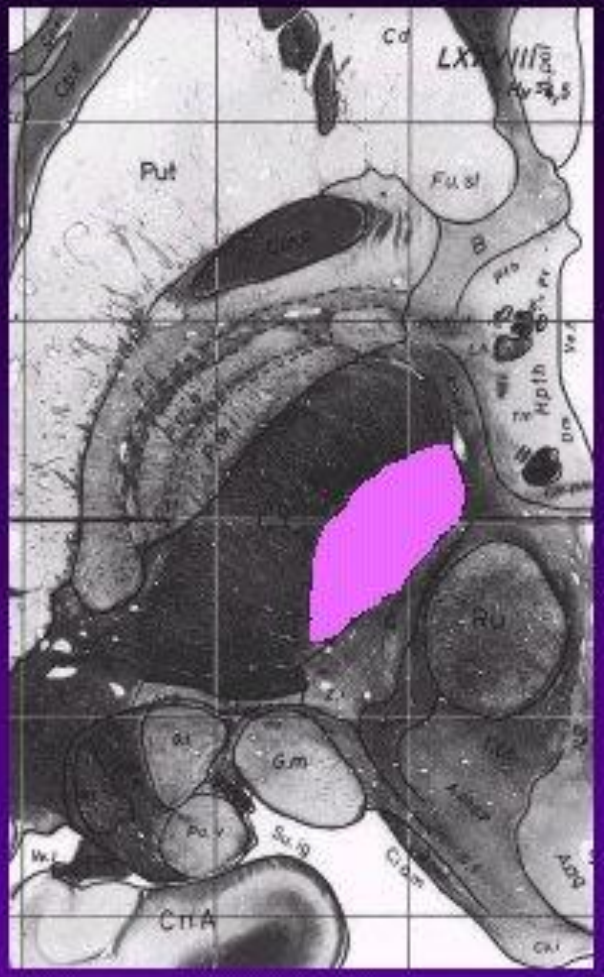


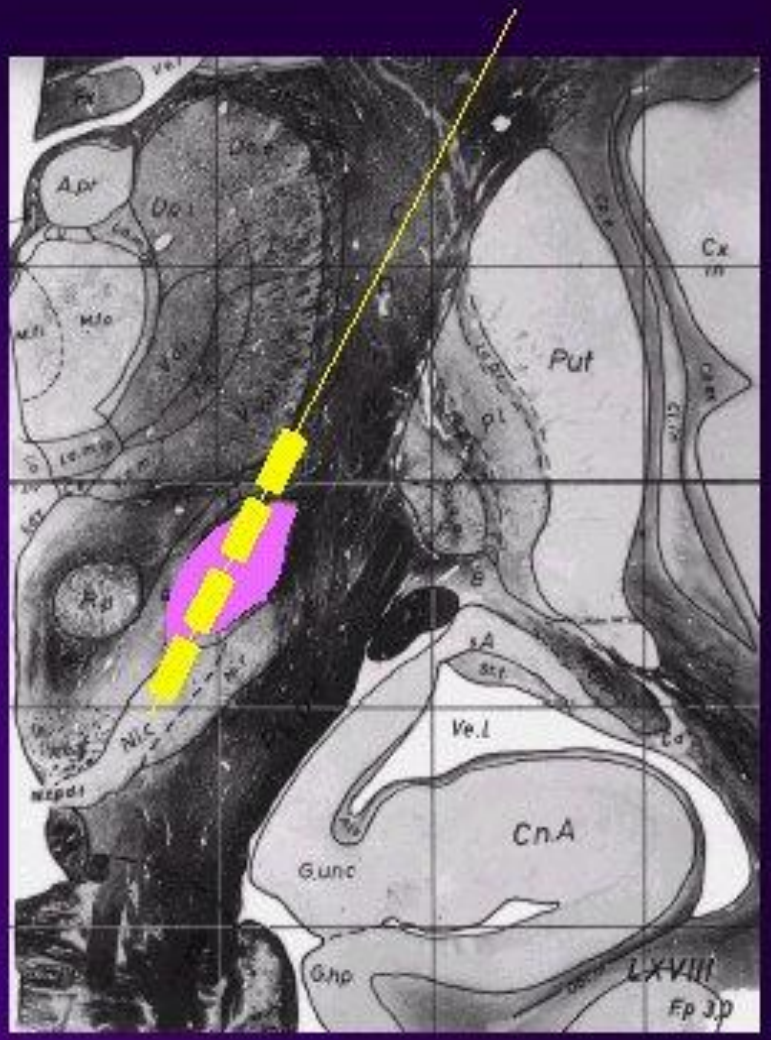


# ANGOLO DI APPROCCIO

# Scelta della traiettoria - GPi

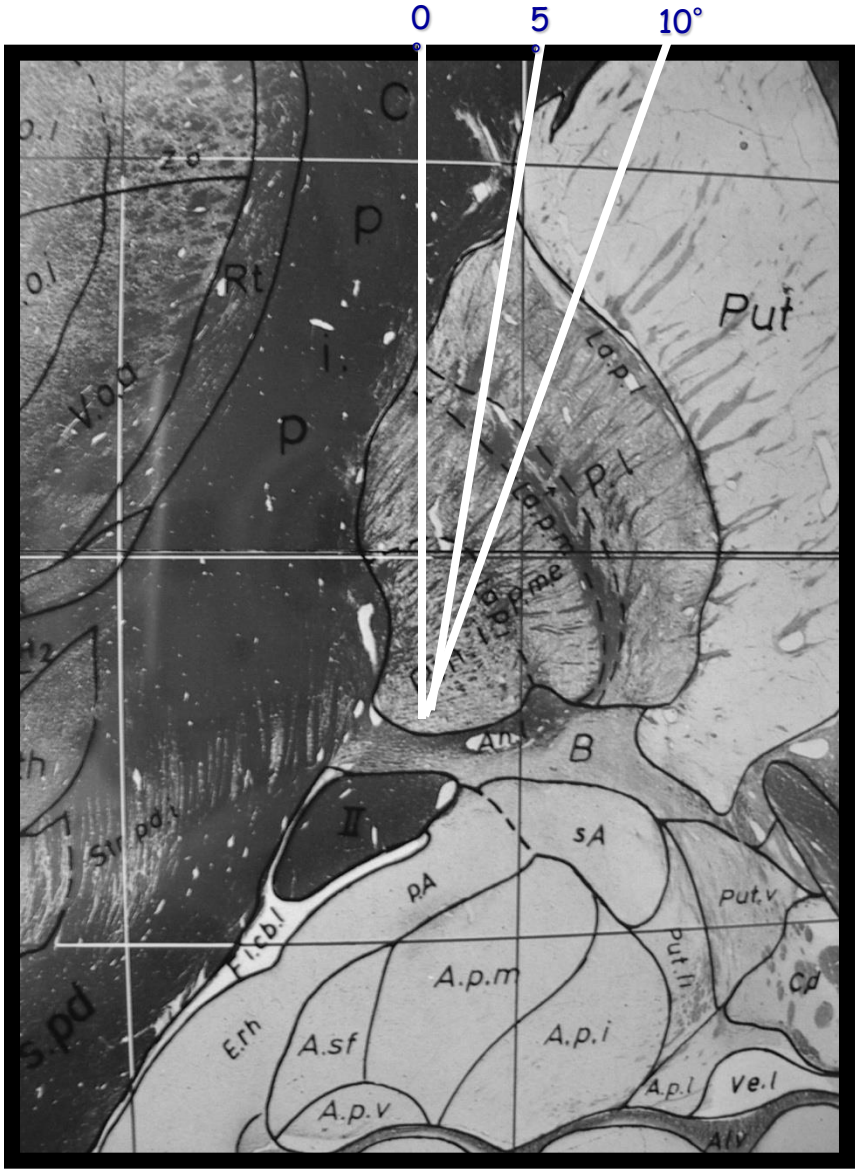


GPi sulla sezione coronale, 2 mm
davanti al midpoint bicommissurale

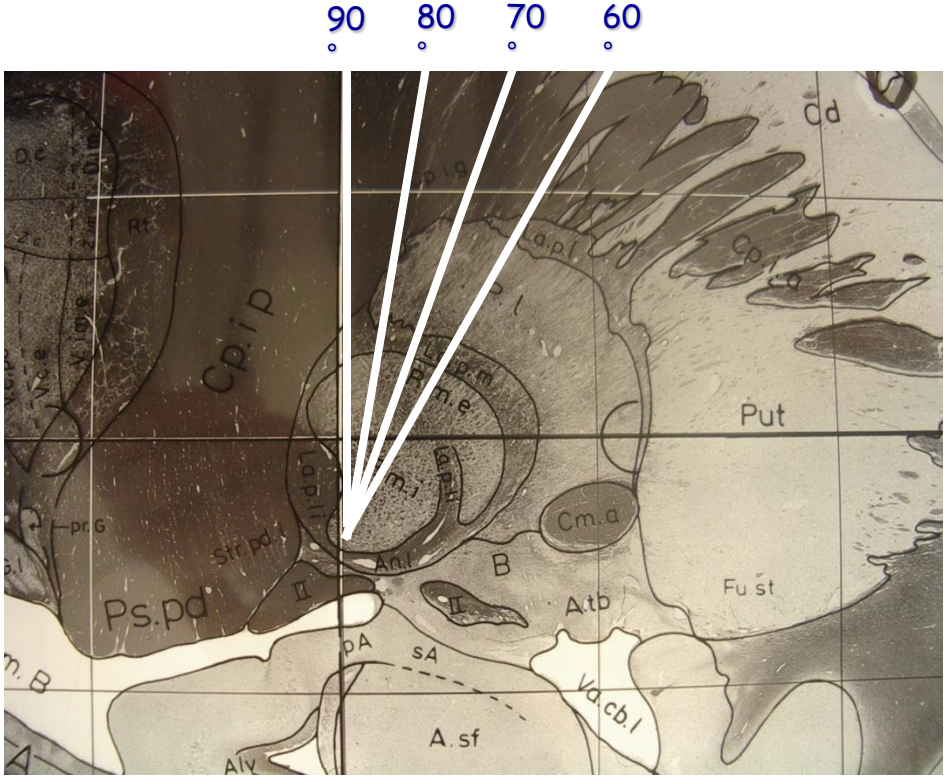


GPi sulla sezione sagittale, 20 mm
dalla linea mediana

Schaltenbrand Wahren, 1977

# Progressi nell'identificazione del target

## Target "parzialmente" visibile

**Metodi di identificazione radiologica diretta**

**Metodi neurofisiologici**

- **Microregistazione**
- **Microstimolazione**
- **Macrostimolazione**

# Localizzazione stereotassica del Target

## Sistema stereotassico di Leksell

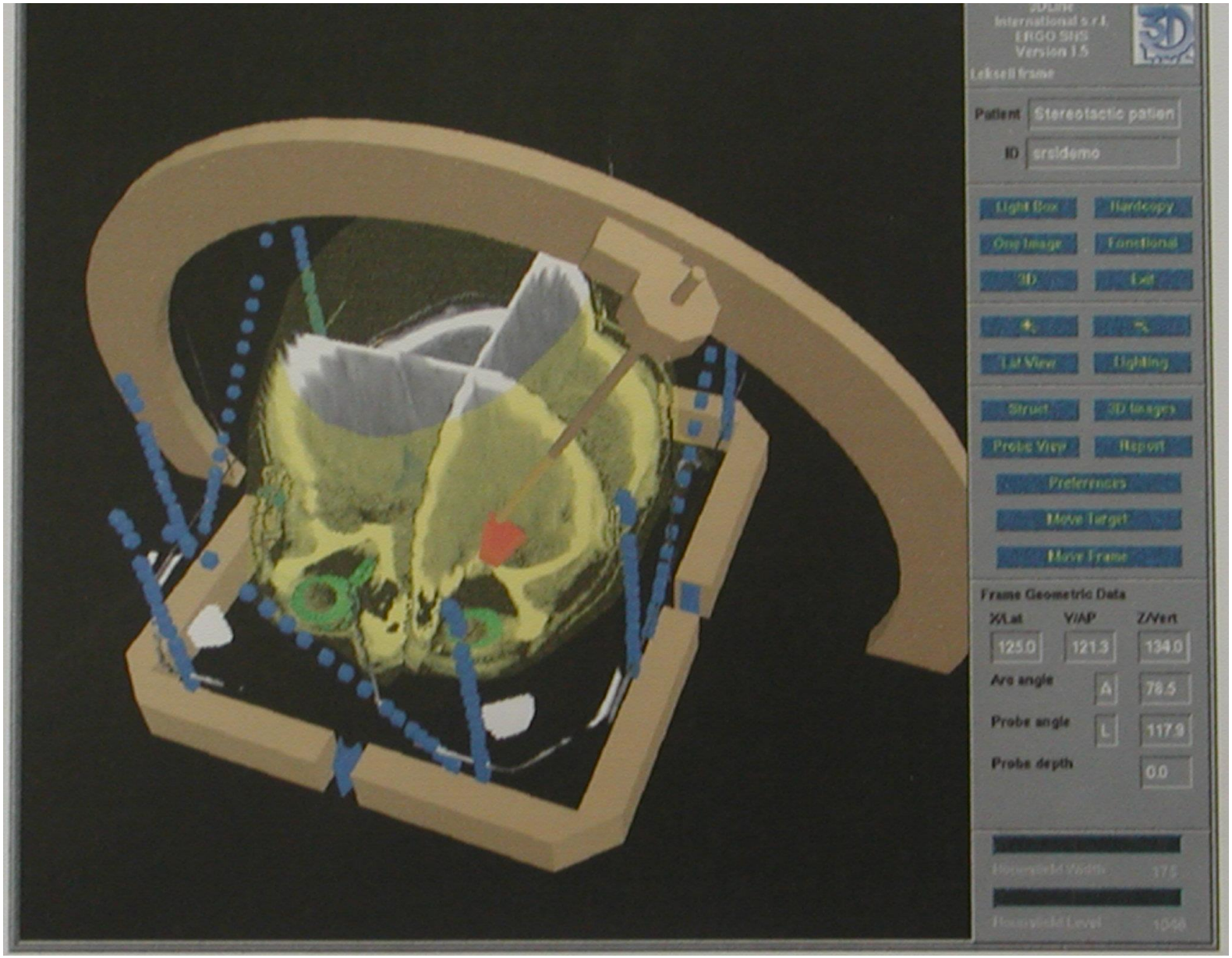

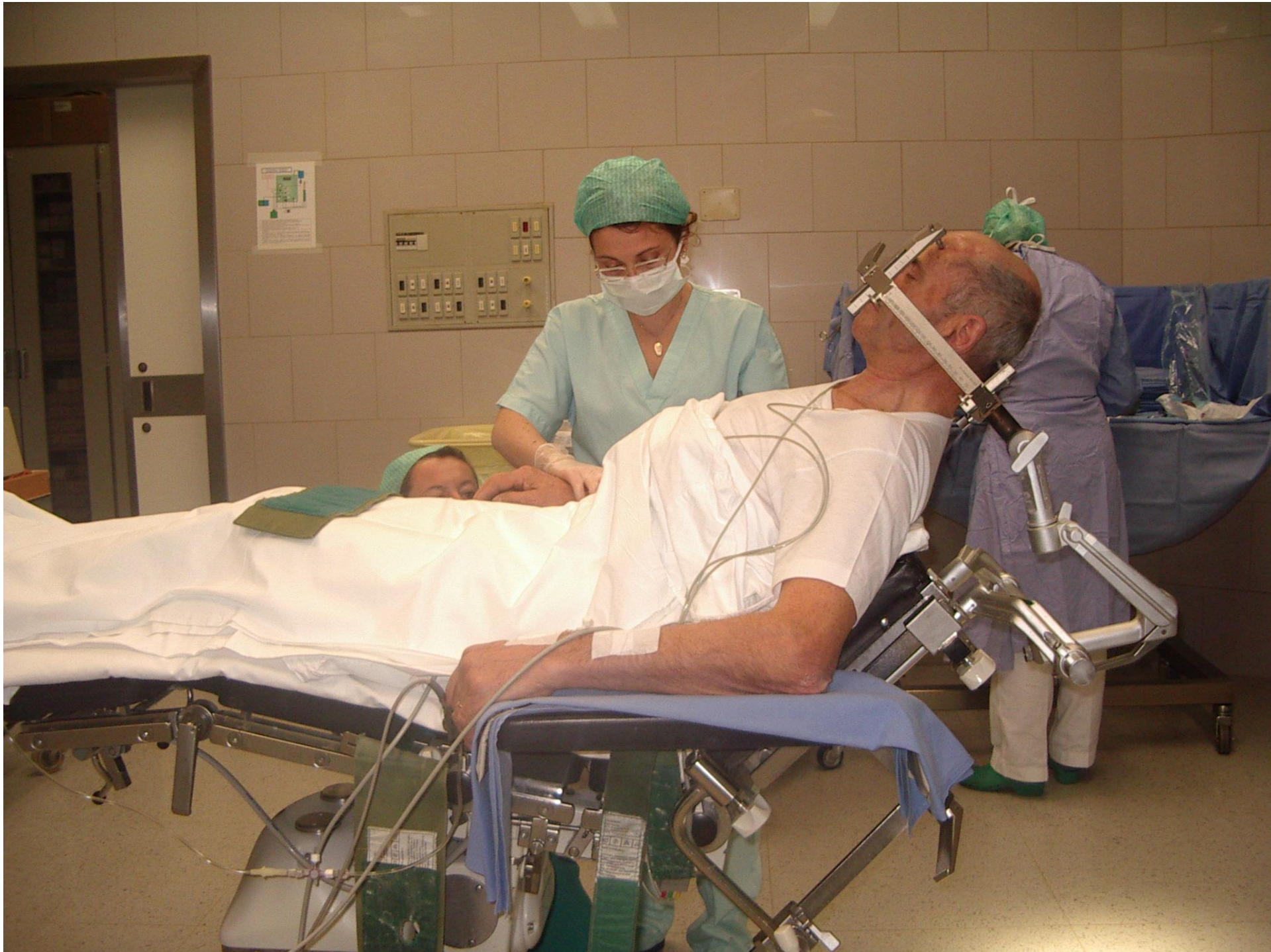

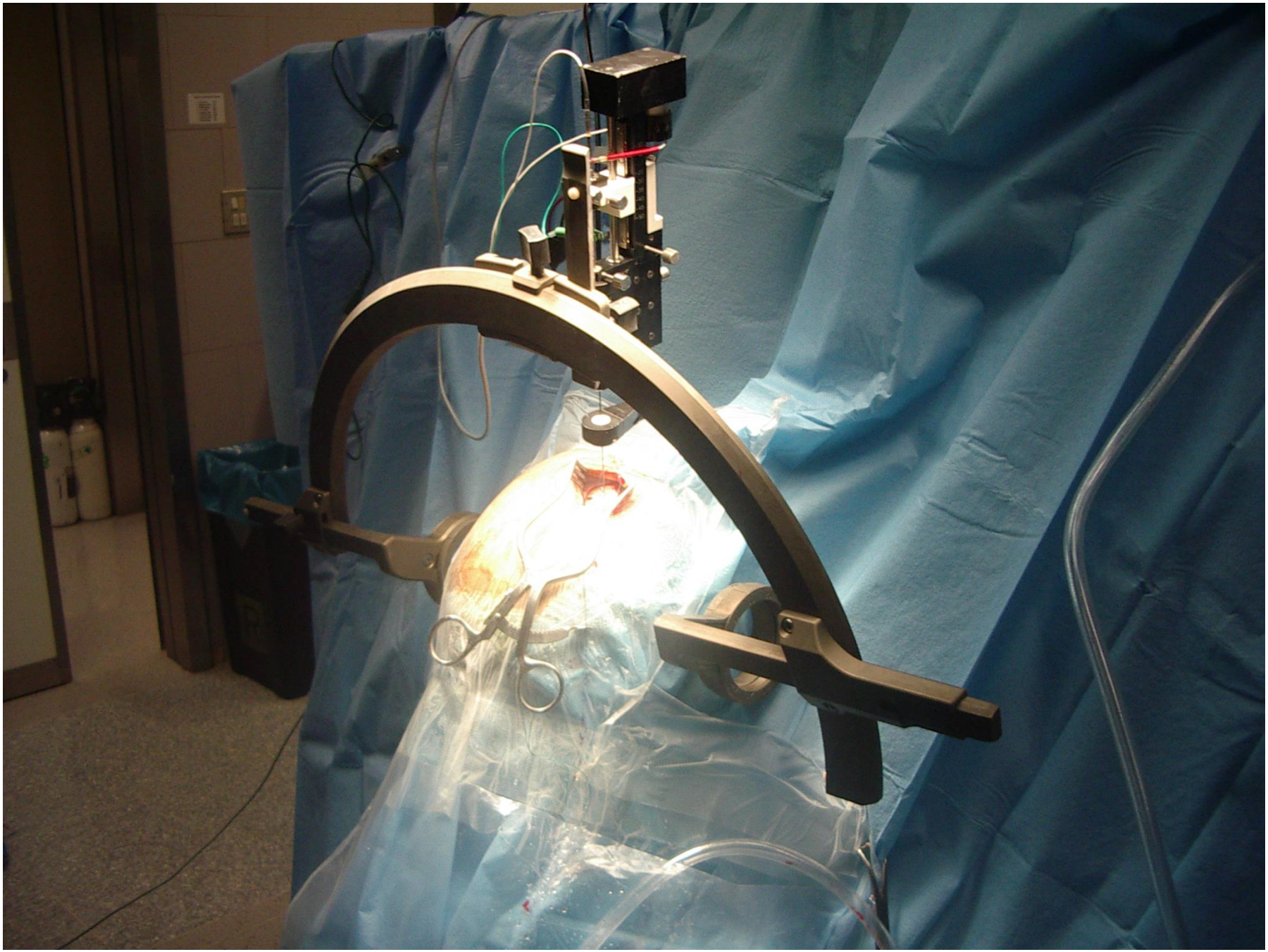

# IOM

- Semi-microregistrazione
- Semi-micro stimolazione
- Macrostimolazione

- Awake / asleep

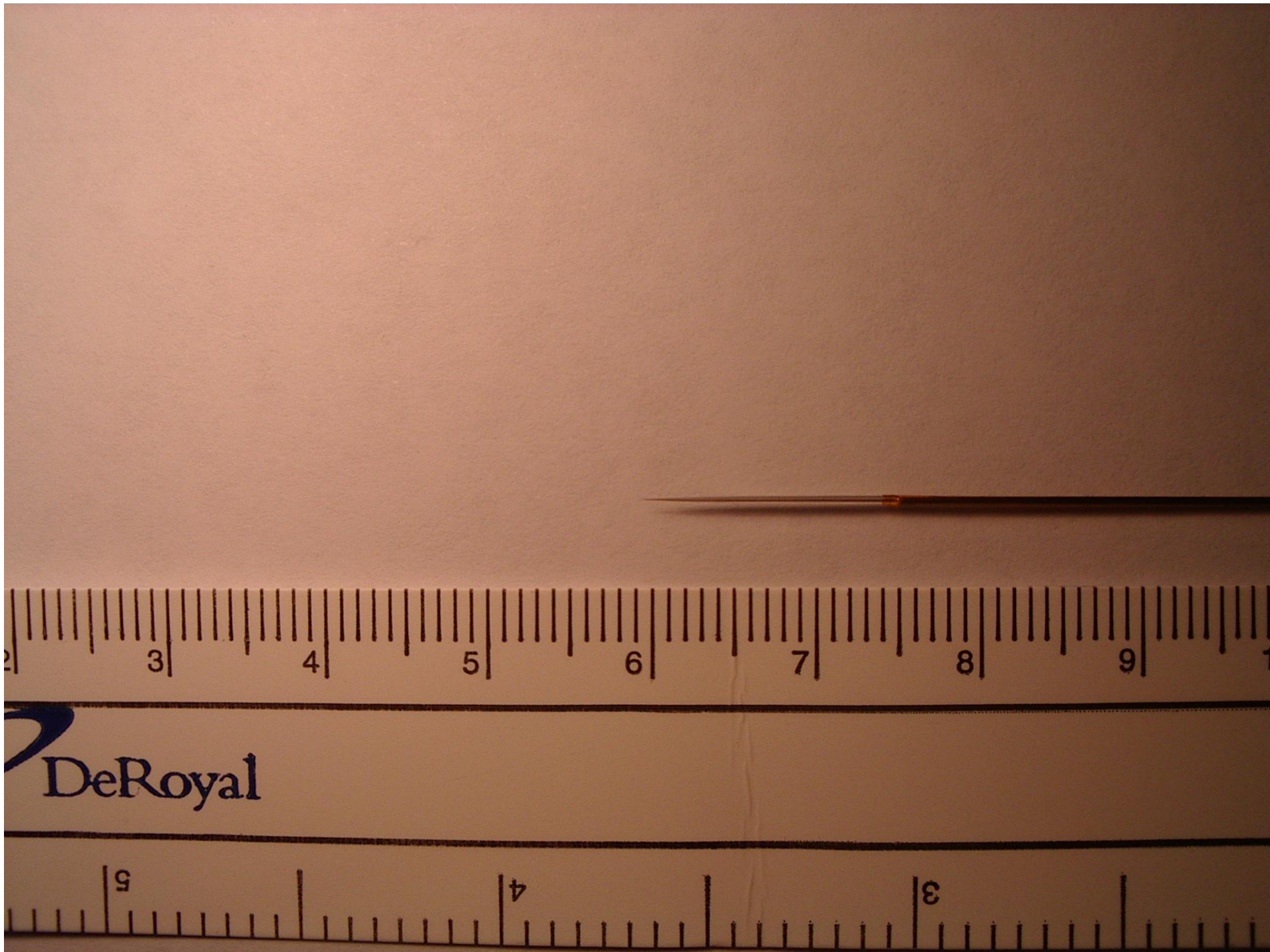
3
4
5
6
7
8
9
DeRoyal
5
4
3

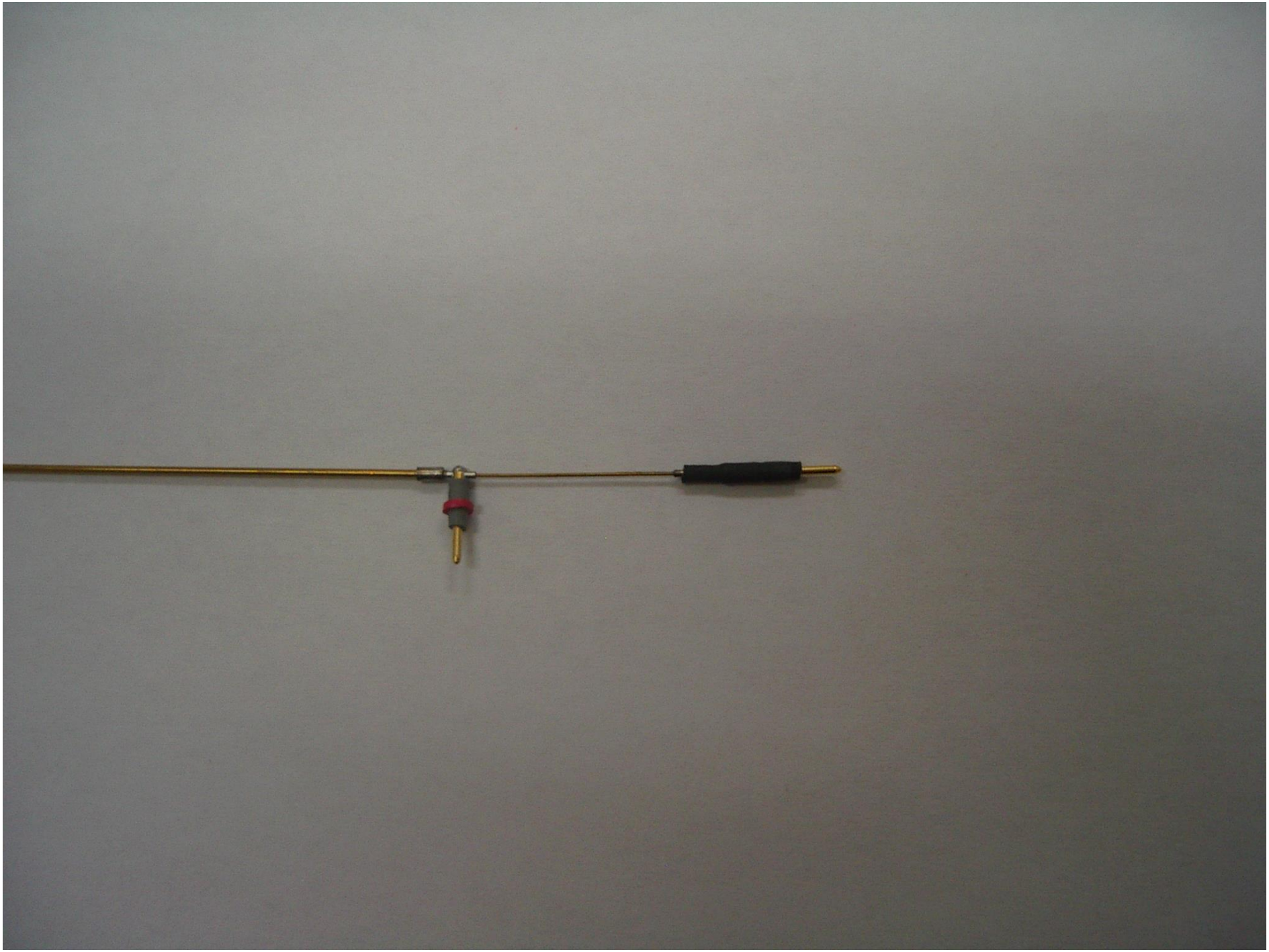

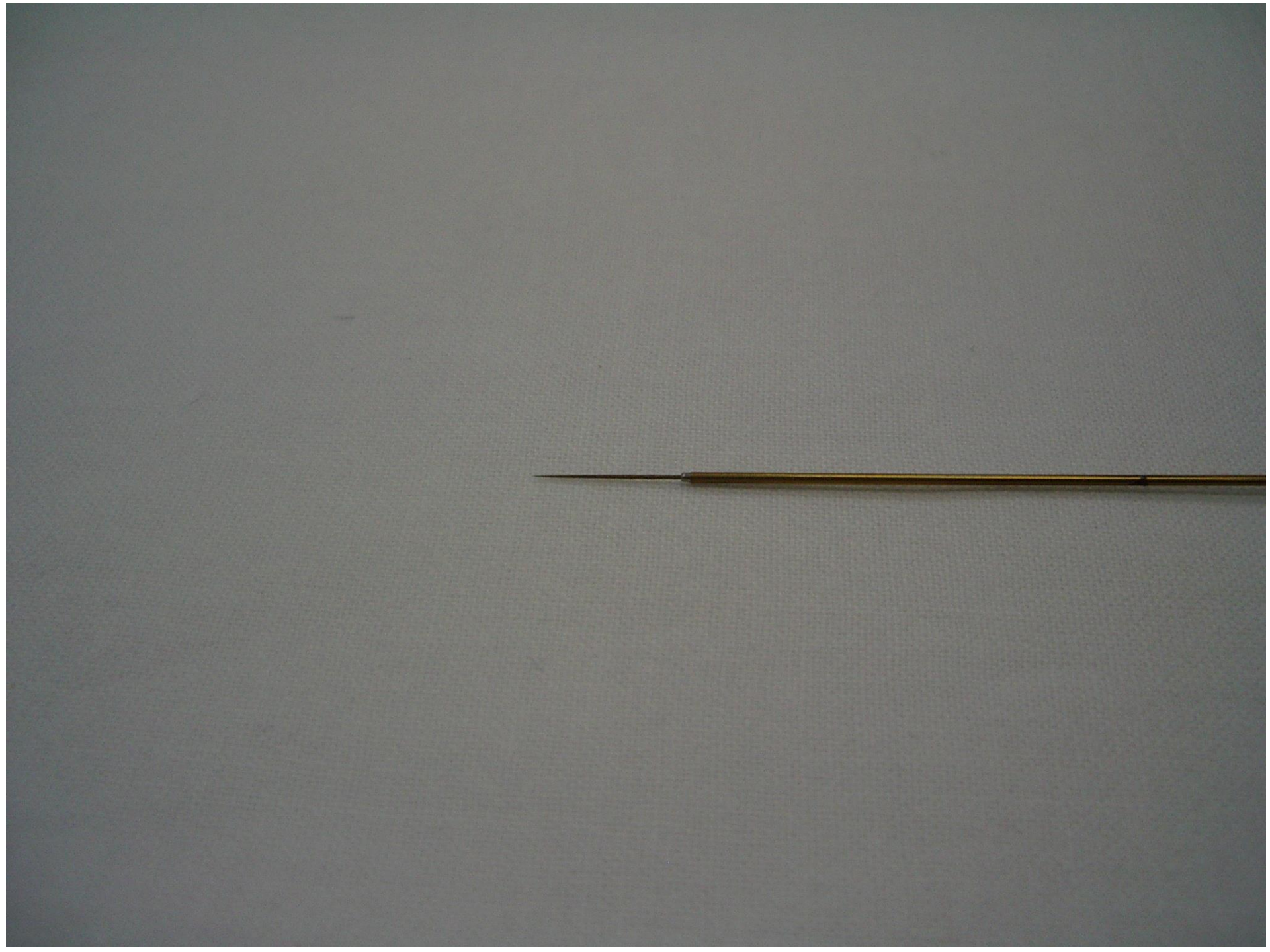

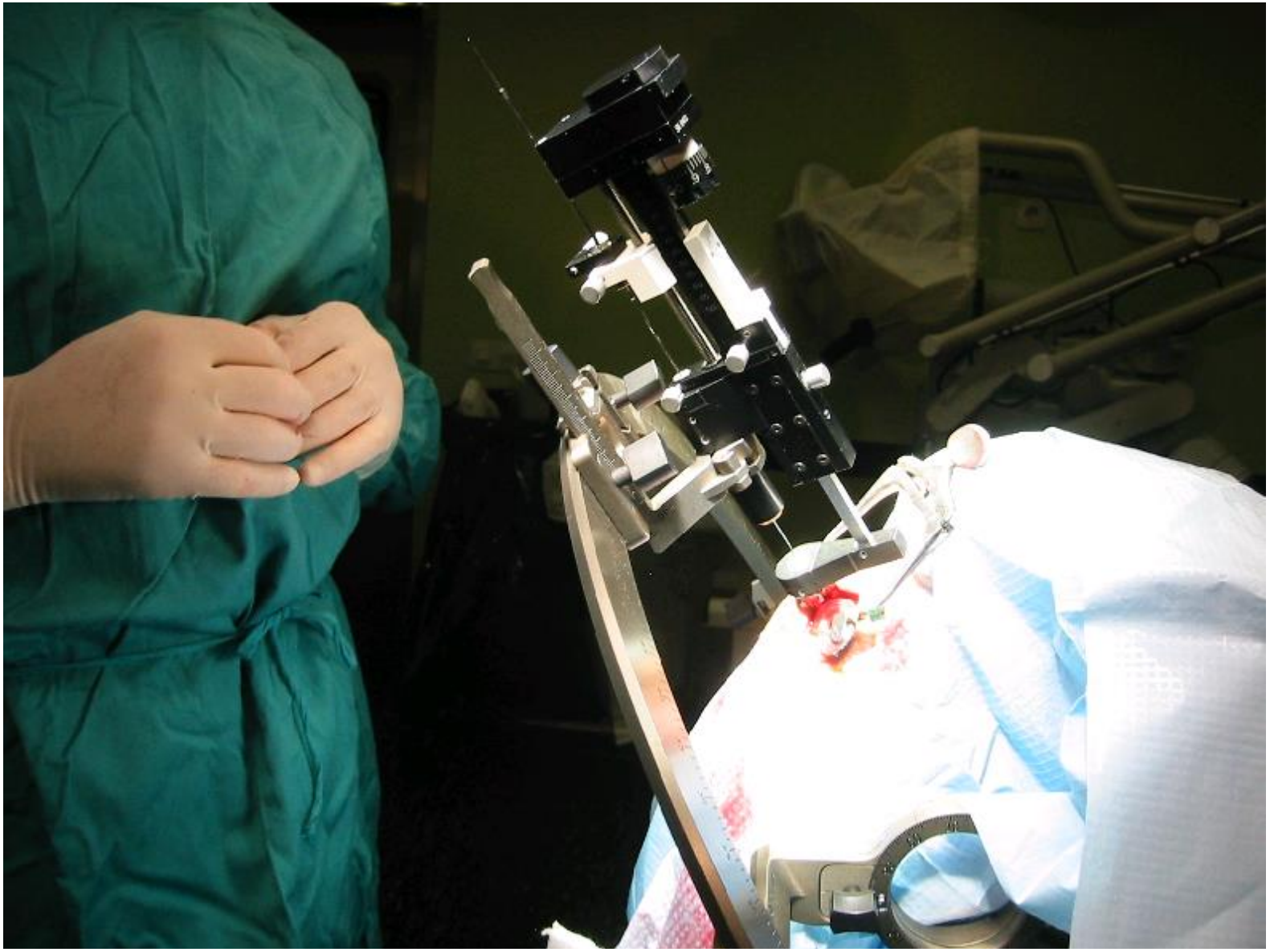

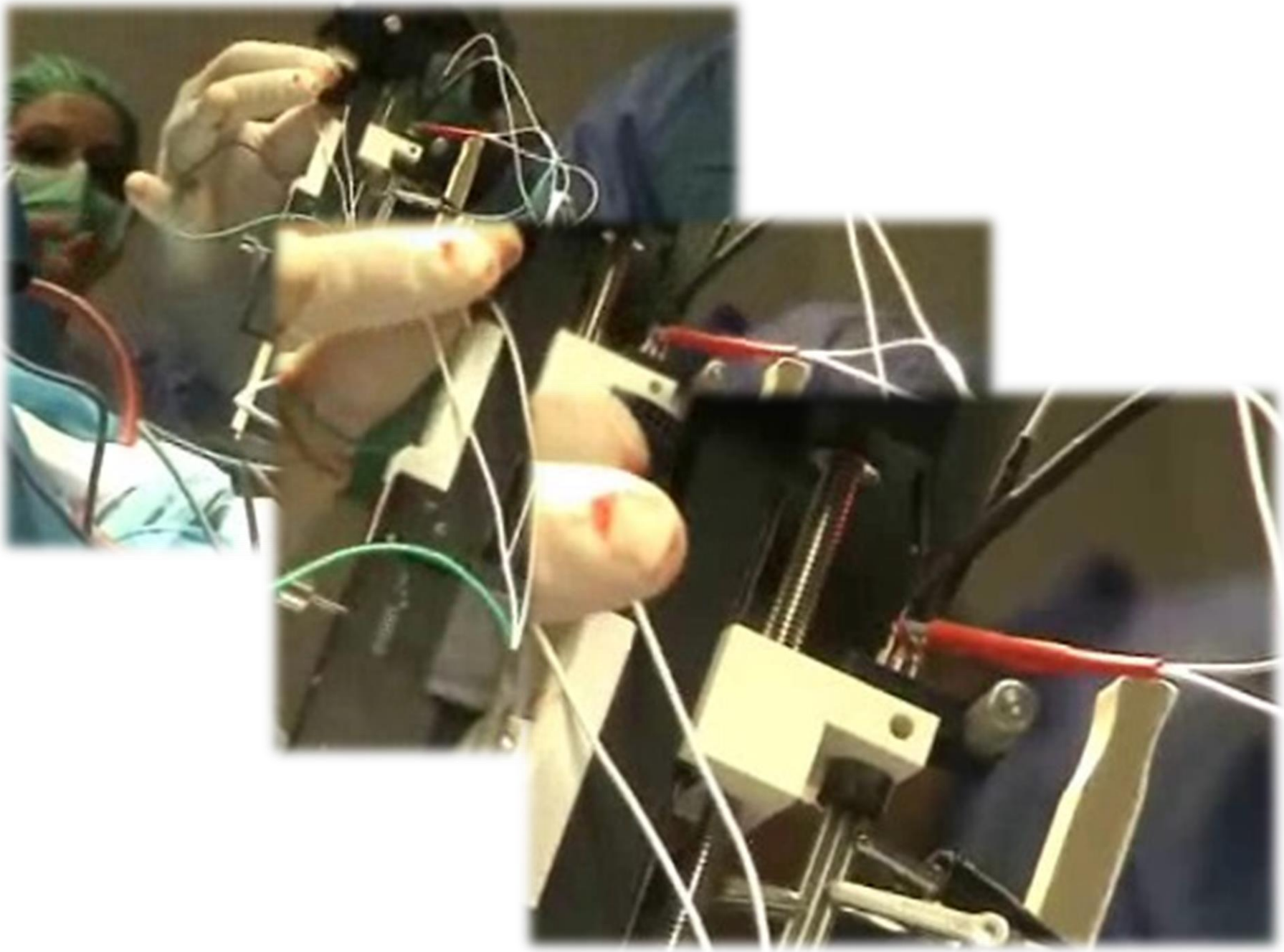

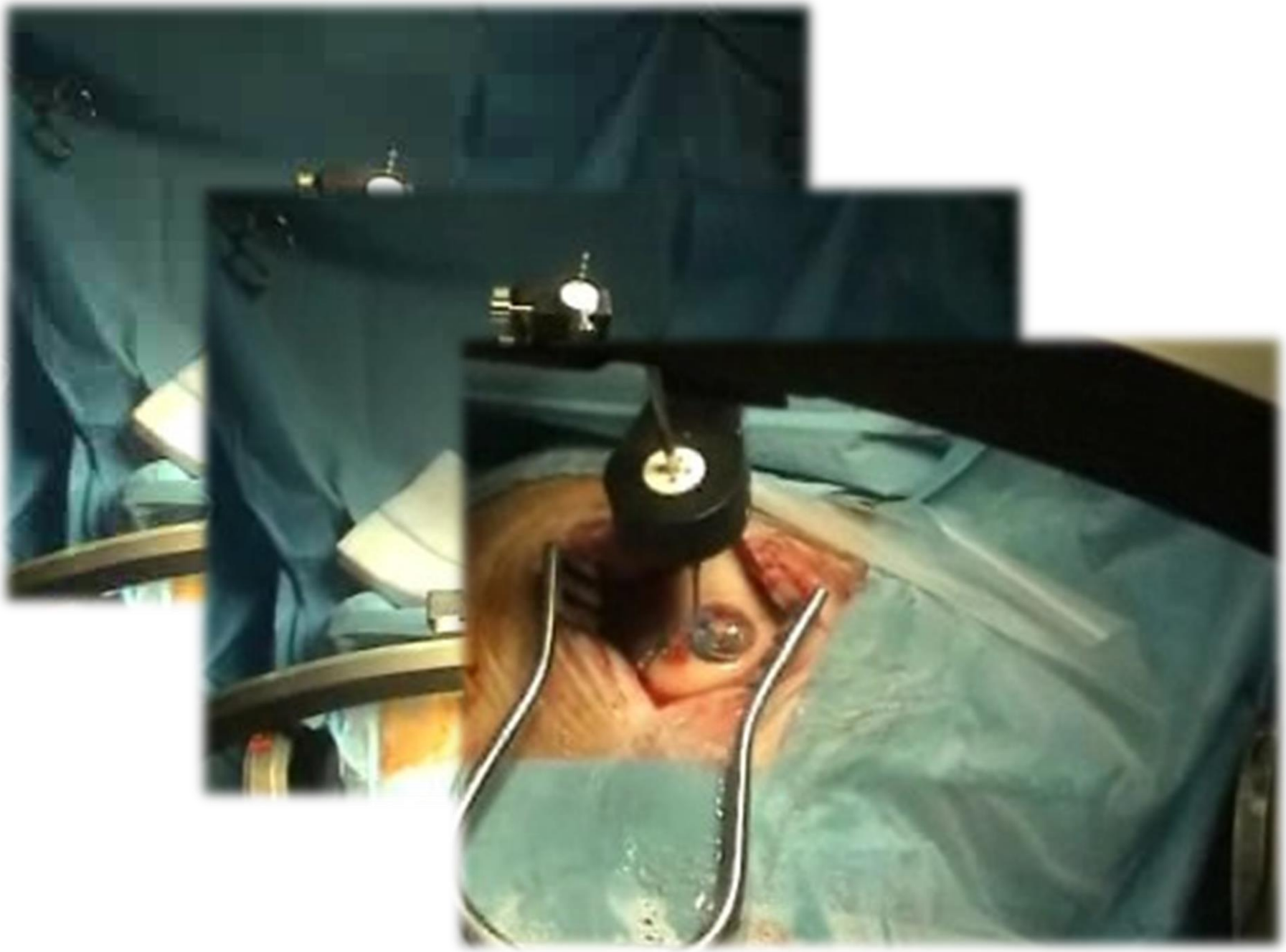

# Monitoring intraoperatorio

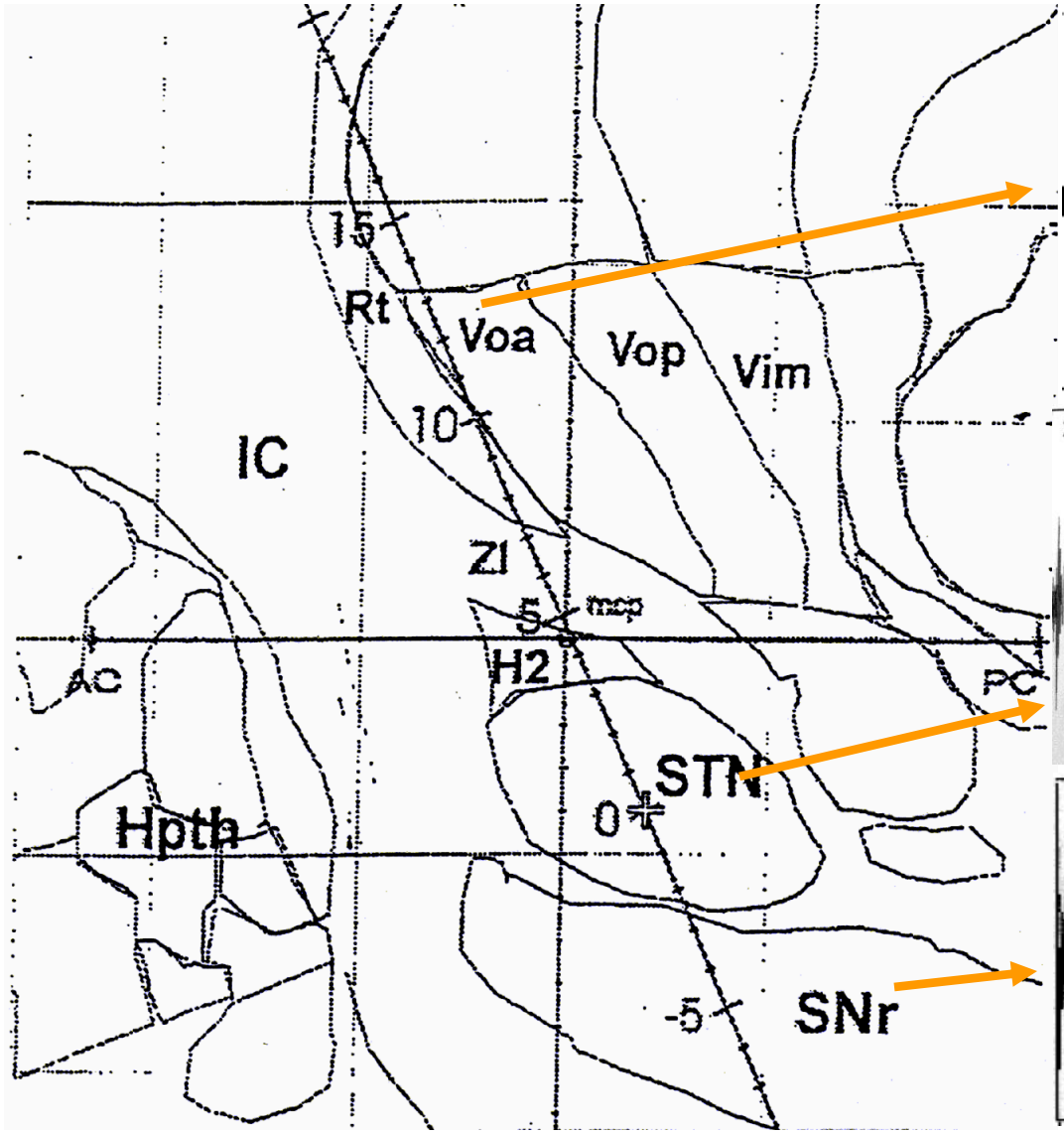


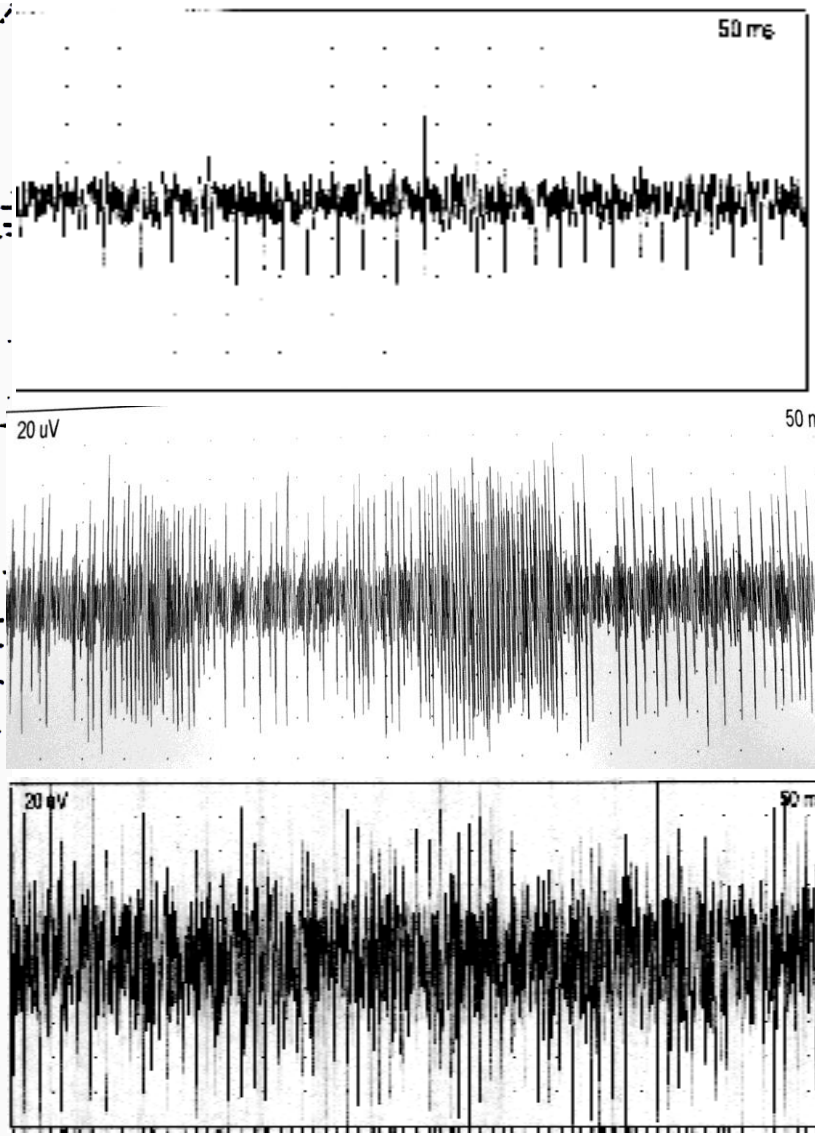

# Stimolazione intra-operatoria
# Effetti collaterali

- Ipofonia, disartria: fibre corticobulbari adiacenti al bordo anteriore del NST
- Contratture: fibre corticospinali adiacenti al bordo laterale del NST
- Movimenti occhio ipsilaterale: fibre del nucleo oculomotore localizzate in posizione mediale rispetto al NST

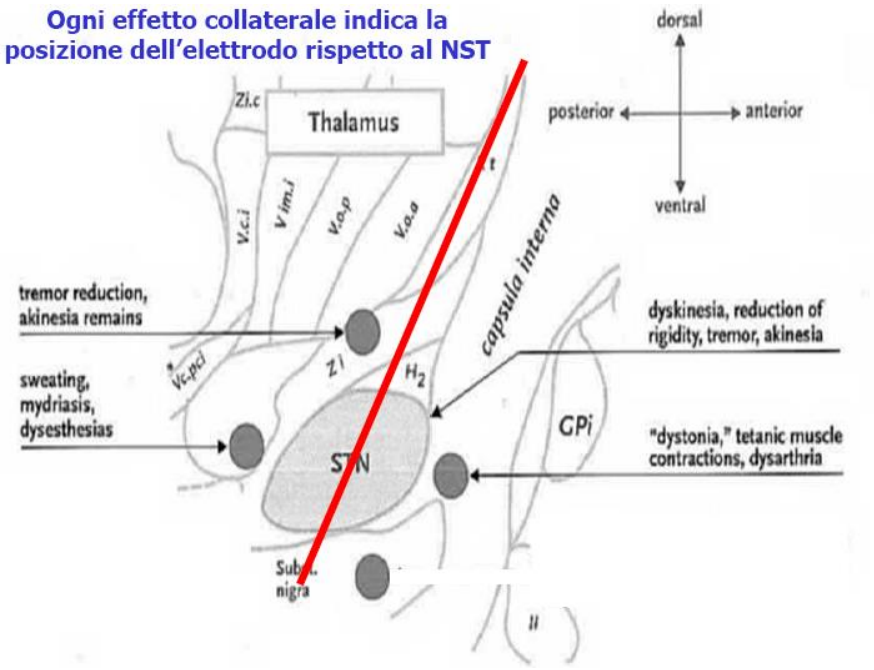

# Stimolazione intra-operatoria
# Effetti collaterali

- **Parestesie: lemnisco mediale localizzato posteriormente al NST**
- **Effetti neurovegetativi (sensazione di calore uni- o bilaterale, sudorazione, midriasi): NST, zona incerta**

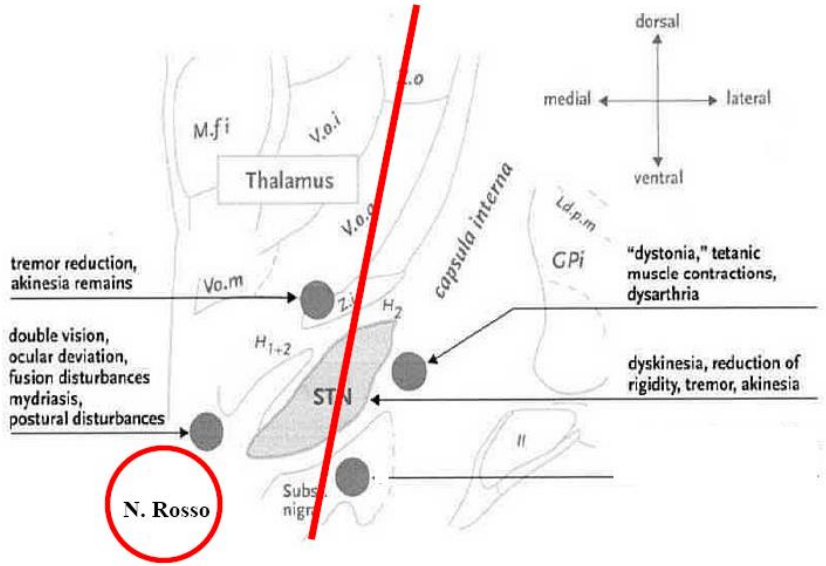

# Nuove acquisizioni neurofisiologiche sull'attività dei nuclei della base

- **Pathological subthalamic nucleus oscillations in PD: Can they be the cause of bradykinesia and akinesia?**

  Moran Weinberger a, William D. Hutchison a,b, Jonathan O. Dostrovsky
  Department of Physiology, University of Toronto, Toronto, ON, Canada b Toronto Western Research Institute, Toronto, ON, Canada

  **Experimental Neurology 219 (2009) 58–61**

## Medtronic®

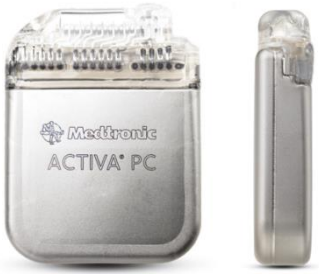







## Boston®

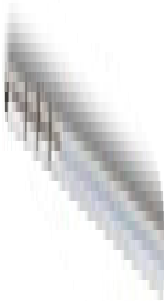


## St. Jude®

World Neurosurg. 2011 Jul-Aug;76(1-2):164-72; discussion 69-73. doi: 10.1016/j.wneu.2011.02.029.

**Clinical safety of brain magnetic resonance imaging with implanted deep brain stimulation hardware: large case series and review of the literature.**

Zrinzo L1, Yoshida F, Hariz MI, Thornton J, Foltynie T, Yousry TA, Limousin P.14

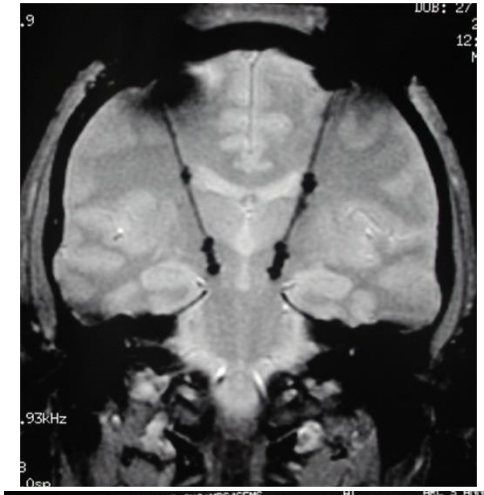

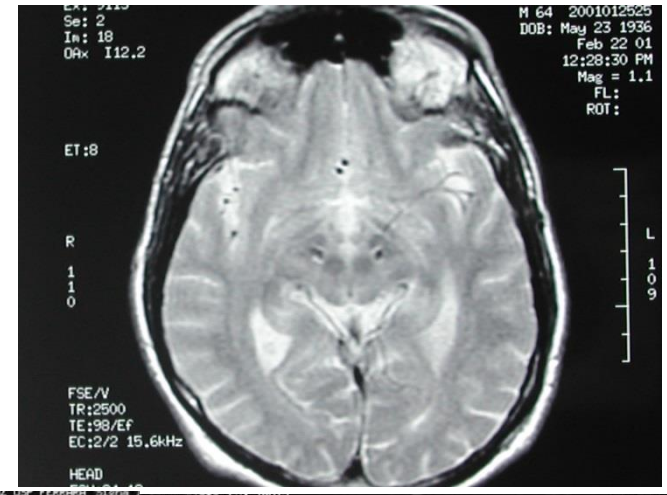


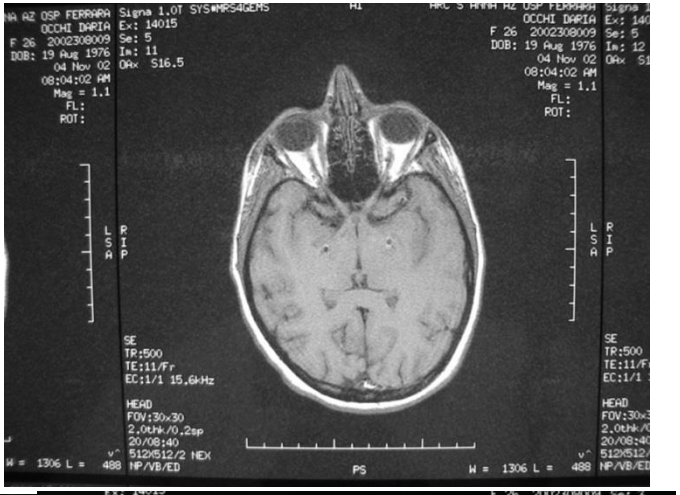


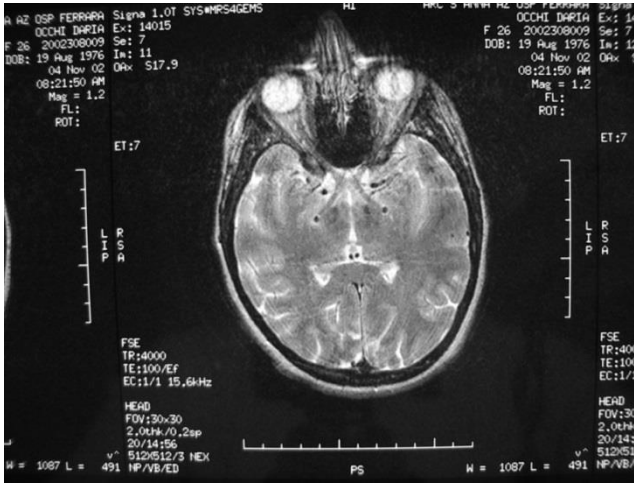


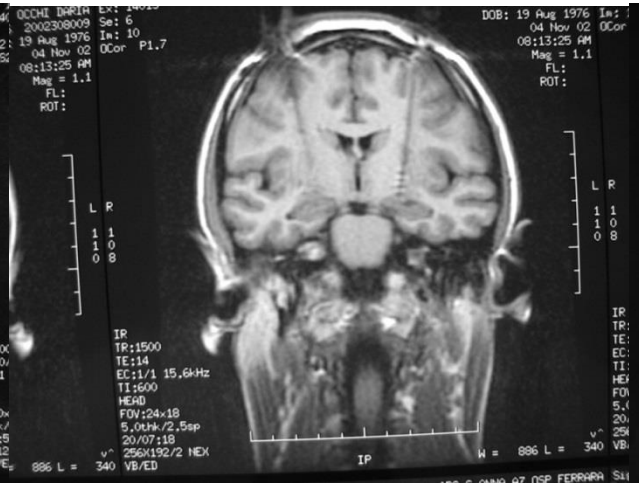


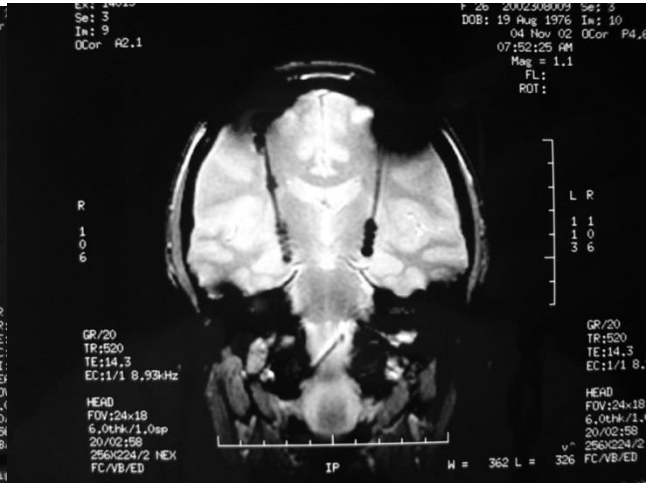

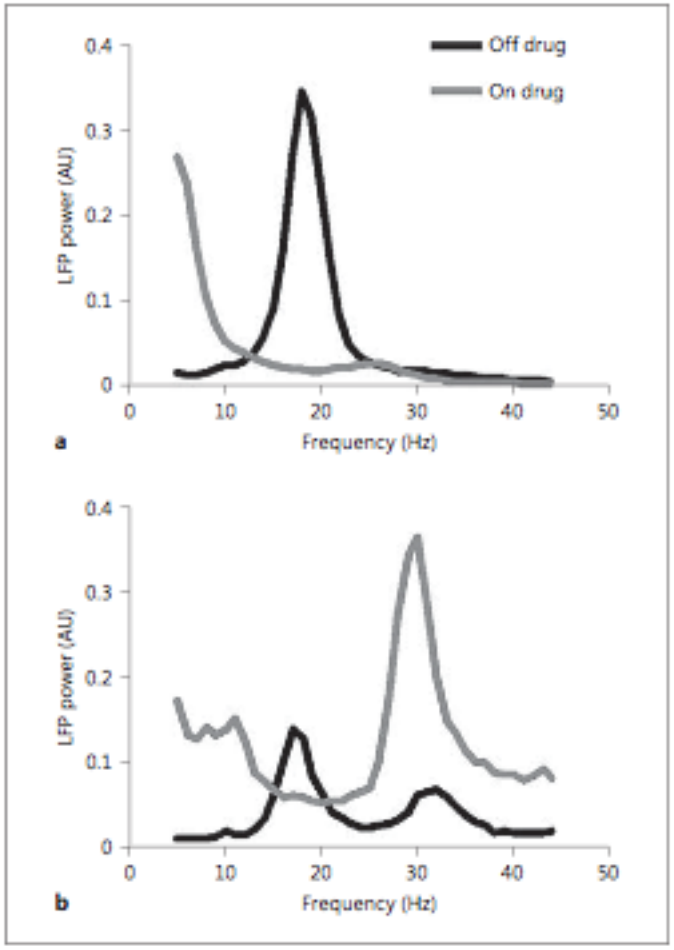


**Fig. 1.** LFP power spectra recorded from 2 patients with implanted STN electrodes for the treatment of PD. **a** The power of beta-frequency oscillations is severely diminished by dopaminergic medication in this patient. **b** A decrease in low beta oscillations (approx. 17 Hz) is coupled with an increase in high beta oscillations (approx. 30 Hz) in this patient. Taken with permission from Ray et al. [20].

# Clinical Implications of Local Field Potentials for Understanding and Treating Movement Disorders

John A. Thompson[a] David Lanctin[b] Nuri Firat Ince[c] Aviva Abosch[a]

[a]Department of Neurosurgery, University of Colorado School of Medicine, Aurora, Colo., [b]Department of Neurosurgery, Division of Epidemiology, School of Public Health, University of Minnesota, Minneapolis, Minn., and [c]Department of Biomedical Engineering, University of Houston, Houston, Tex., USA

Stereotact Funct Neurosurg 2014;92:251–263

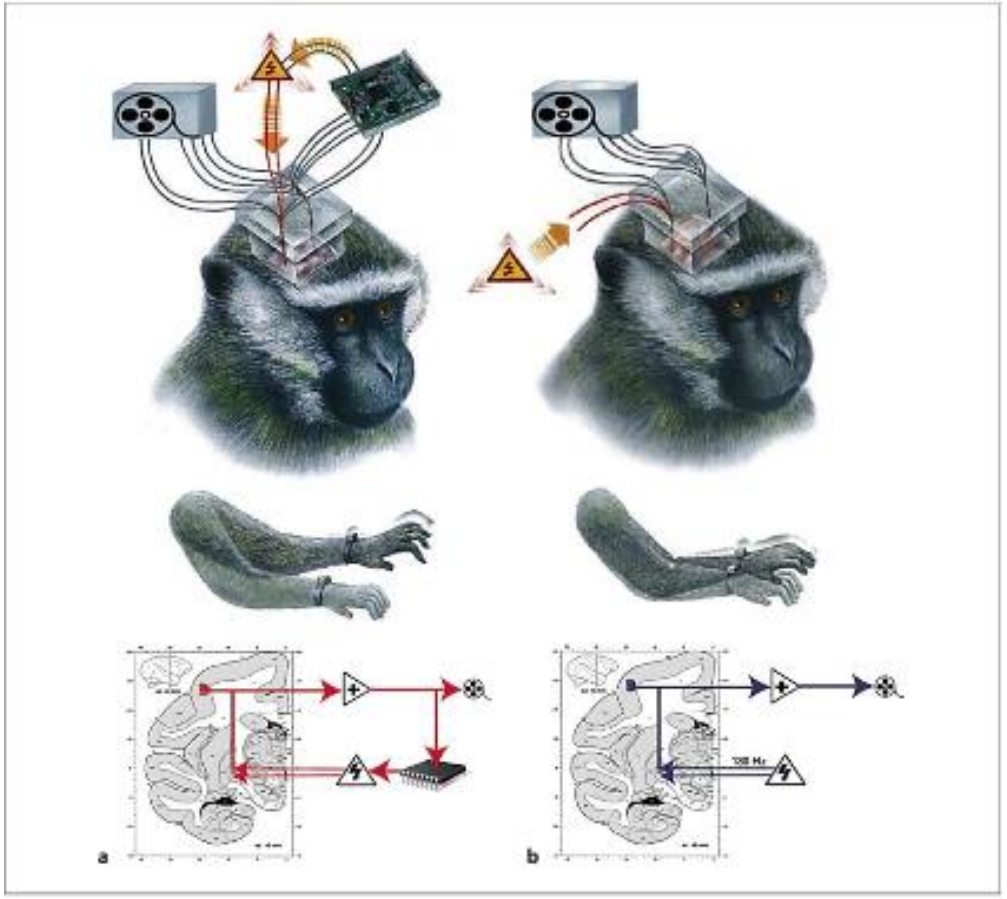


**Fig. 4. a** Schematic depiction of the African green monkey closed-loop stimulation paradigm in Rosin et al. [89]. Single-unit recordings were detected from 6 electrodes (2 GPi, 4 M1) by a data acquisition system and digital signal-processing chip. Detection of a neuronal spike triggered a short-train stimulus. **b** Schematic depiction of an open-loop stimulation paradigm in an African green monkey.

# Adaptive closed loop stimulation

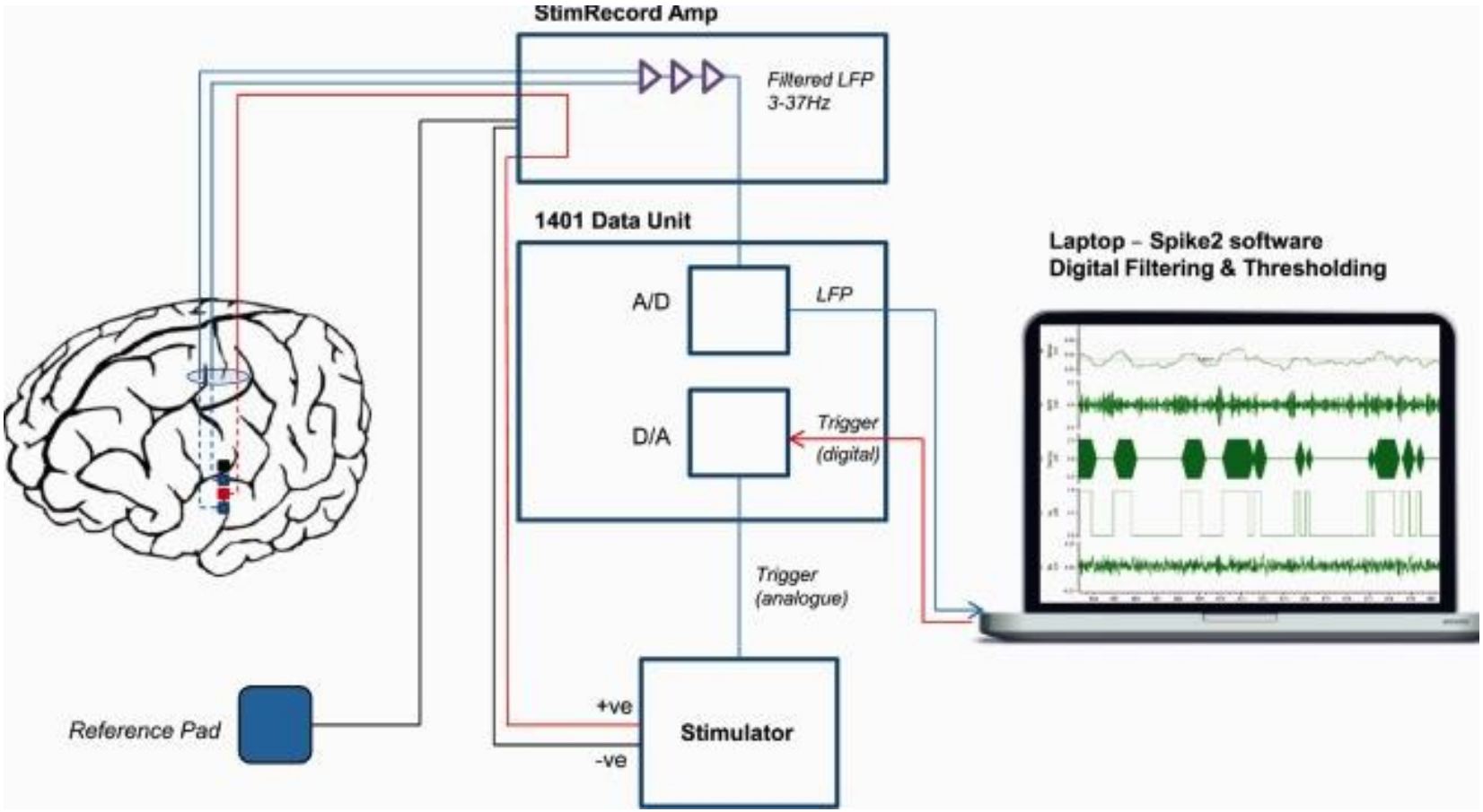


Ann Neurol. 2013 Sep;74(3):449-57. **Adaptive deep brain stimulation in advanced Parkinson disease.** Little S, Pogosyan A, Neal S, Zavala B, Zrinzo L, Hariz M, Foltynie T, Limousin P, Ashkan K, FitzGerald J, Green AL, Aziz TZ, Brown P.

**Controlling Parkinson's Disease With Adaptive Deep Brain Stimulation**

Simon Little, 1 Alek Pogosyan, 1 Spencer Neal, 2 Ludvic Zrinzo, 2 Marwan Hariz, 2 Thomas Foltynie, 2 Patricia Limousin, 2 and Peter Brown 1

# Adaptive closed loop stimulation

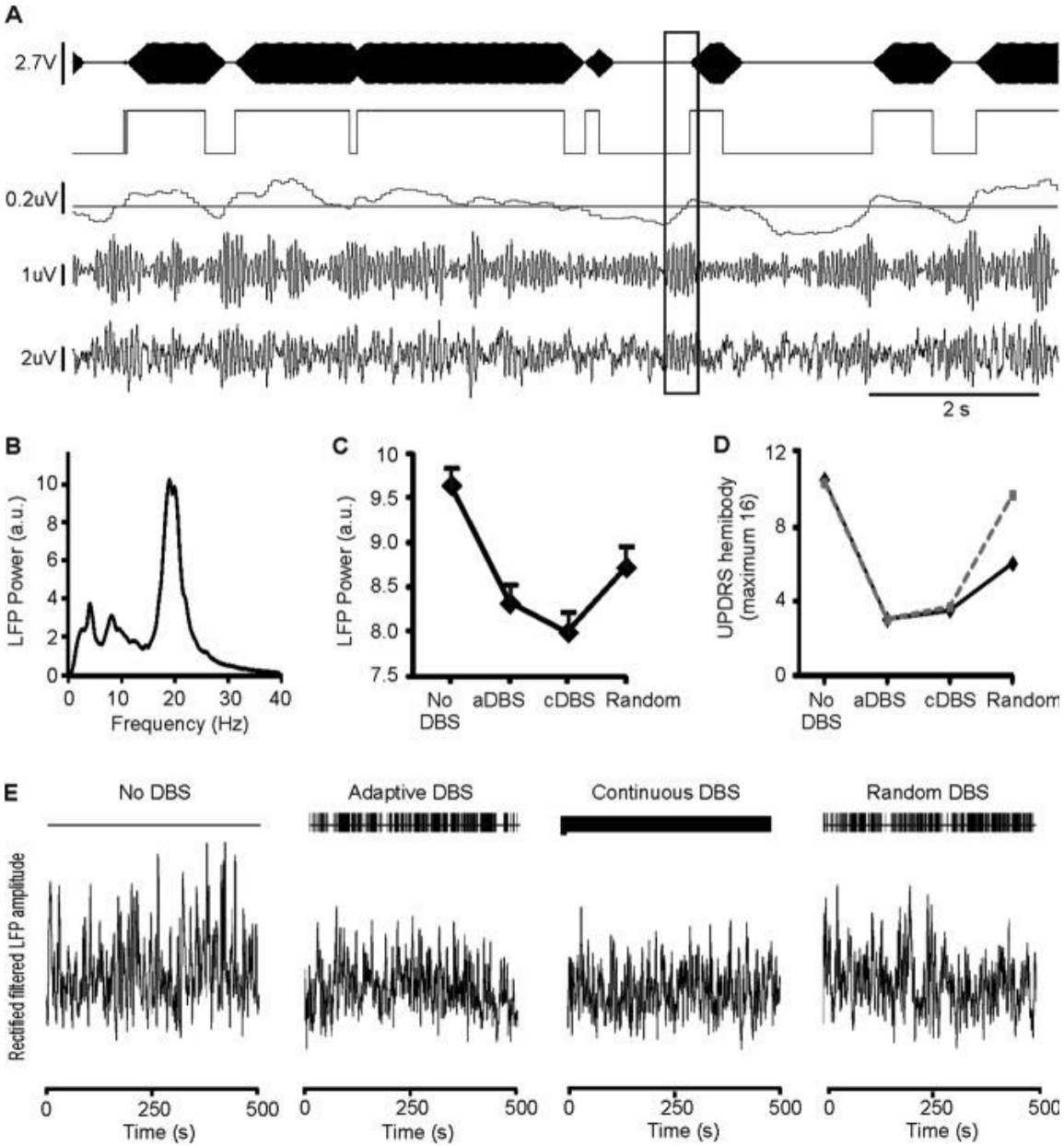


Ann Neurol. 2013 Sep;74(3):449-57. **Adaptive deep brain stimulation in advanced Parkinson disease.** Little S1, Pogosyan A, Neal S, Zavala B, Zrinzo L, Hariz M, Foltynie T, Limousin P, Ashkan K, FitzGerald J, Green AL, Aziz TZ, Brown P.

Neuromodulation. 2009 April ; 12(2): 85–103. doi:10.1111/j.1525-1403.2009.00199.x.

# Evolution of Deep Brain Stimulation: Human Electrometer and Smart Devices Supporting the Next Generation of Therapy

**Kendall H. Lee, MD, PhD**[1], **Charles D. Blaha, PhD**[2], **Paul A. Garris, PhD**[3], **Pedram Mohseni, PhD**[4], **April E. Horne, MBA**[5], **Kevin E. Bennet, MBA**[5], **Filippo Agnesi, MS**[6], **Jonathan M. Bledsoe, MD**[1], **Deranda B. Lester, MS**[2], **Chris Kimble, MS**[5], **Hoon-Ki Min, MS**[7], **Young-Bo Kim, MD, PhD**[7], and **Zang-Hee Cho, PhD**[7]

[1]Department of Neurosurgery and Physiology and Biomedical Engineering, Mayo Clinic, Rochester, Minnesota

[2]Department of Psychology, University of Memphis, Memphis, Tennessee

[3]Department of Biological Sciences, Illinois State University, Normal, Illinois

[4]Electrical Engineering and Computer Science Department, Case Western Reserve University, Cleveland, Ohio

[5]Division of Engineering, Mayo Clinic, Rochester, Minnesota

[6]Department of Physiology and Biomedical Engineering, Mayo Clinic, Rochester, Minnesota

[7]Neuroscience Research Institute, Gachon University of Medicine and Science, Incheon, South Korea

## Abstract

Deep Brain Stimulation (DBS) provides therapeutic benefit for several neuropathologies including Parkinson's disease (PD), epilepsy, chronic pain, and depression. Despite well established clinical efficacy, the mechanism(s) of DBS remains poorly understood. In this review we begin by summarizing the current understanding of the DBS mechanism. Using this knowledge as a framework, we then explore a specific hypothesis regarding DBS of the subthalamic nucleus (STN) for the treatment of PD. This hypothesis states that therapeutic benefit is provided, at least in part, by activation of surviving nigrostriatal dopaminergic neurons, subsequent striatal dopamine release, and resumption of striatal target cell control by dopamine. While highly controversial, we present preliminary data that are consistent with specific predications testing this hypothesis. We additionally propose that developing new technologies, e.g., human electrometer and closed-loop smart devices, for monitoring dopaminergic neurotransmission during STN DBS will further advance this treatment approach.

Neuromodulation. 2009 April ; 12(2): 85–103. doi:10.1111/j.1525-1403.2009.00199.x.

# Evolution of Deep Brain Stimulation: Human Electrometer and Smart Devices Supporting the Next Generation of Therapy

**Kendall H. Lee, MD, PhD**[1], **Charles D. Blaha, PhD**[2], **Paul A. Garris, PhD**[3], **Pedram Mohseni, PhD**[4], **April E. Horne, MBA**[5], **Kevin E. Bennet, MBA**[5], **Filippo Agnesi, MS**[6], **Jonathan M. Bledsoe, MD**[1], **Deranda B. Lester, MS**[2], **Chris Kimble, MS**[5], **Hoon-Ki Min, MS**[7], **Young-Bo Kim, MD, PhD**[7], and **Zang-Hee Cho, PhD**[7]

[1]Department of Neurosurgery and Physiology and Biomedical Engineering, Mayo Clinic, Rochester, Minnesota

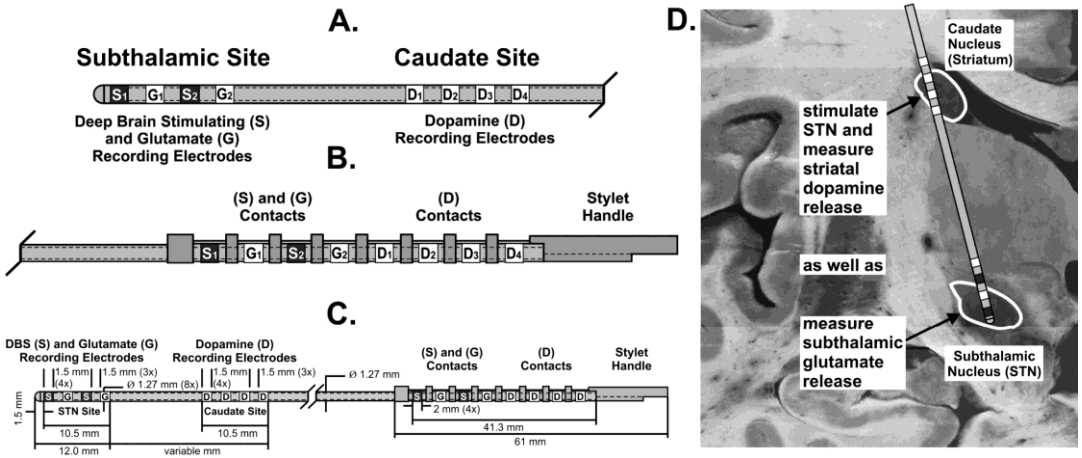




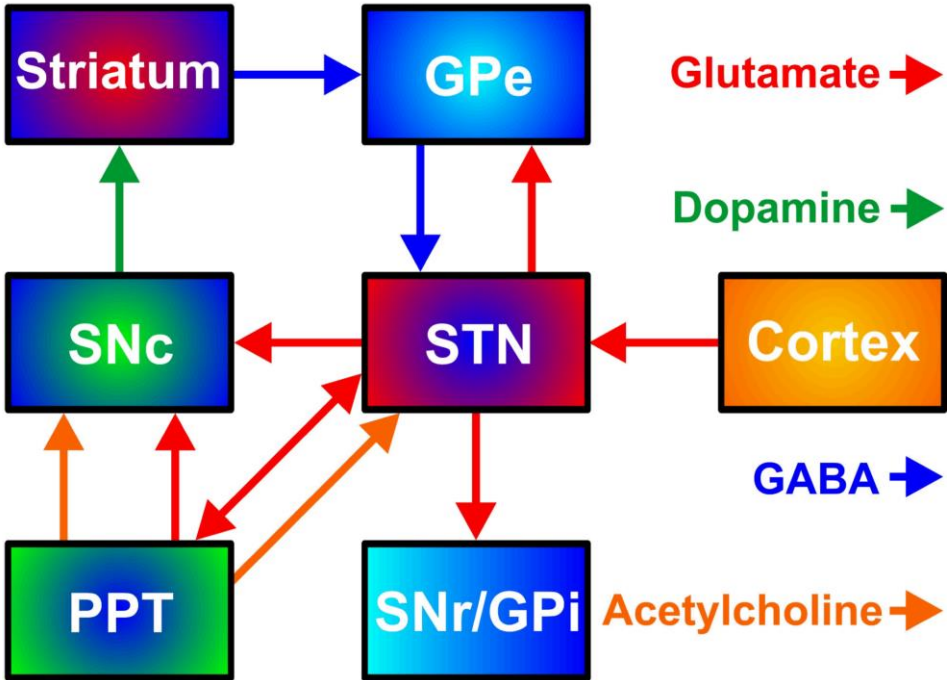


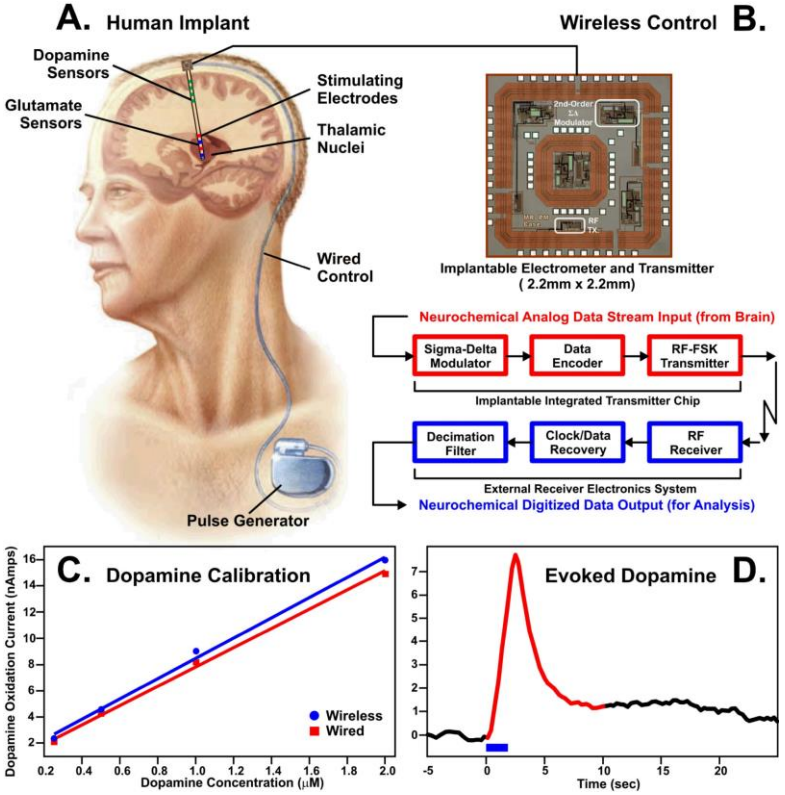

*IEEE J Solid-State Circuits*. 2013 September ; 48(9): 2203–2216. doi:10.1109/JSSC.2013.2266862.

# A Power-Efficient Wireless System With Adaptive Supply Control for Deep Brain Stimulation

**Hyung-Min Lee [Student Member, IEEE]**, **Hangue Park [Student Member, IEEE]**, and **Maysam Ghovanloo [Senior Member, IEEE]**
School of Electrical and Computer Engineering, Georgia Institute of Technology, Atlanta, GA 30308 USA.

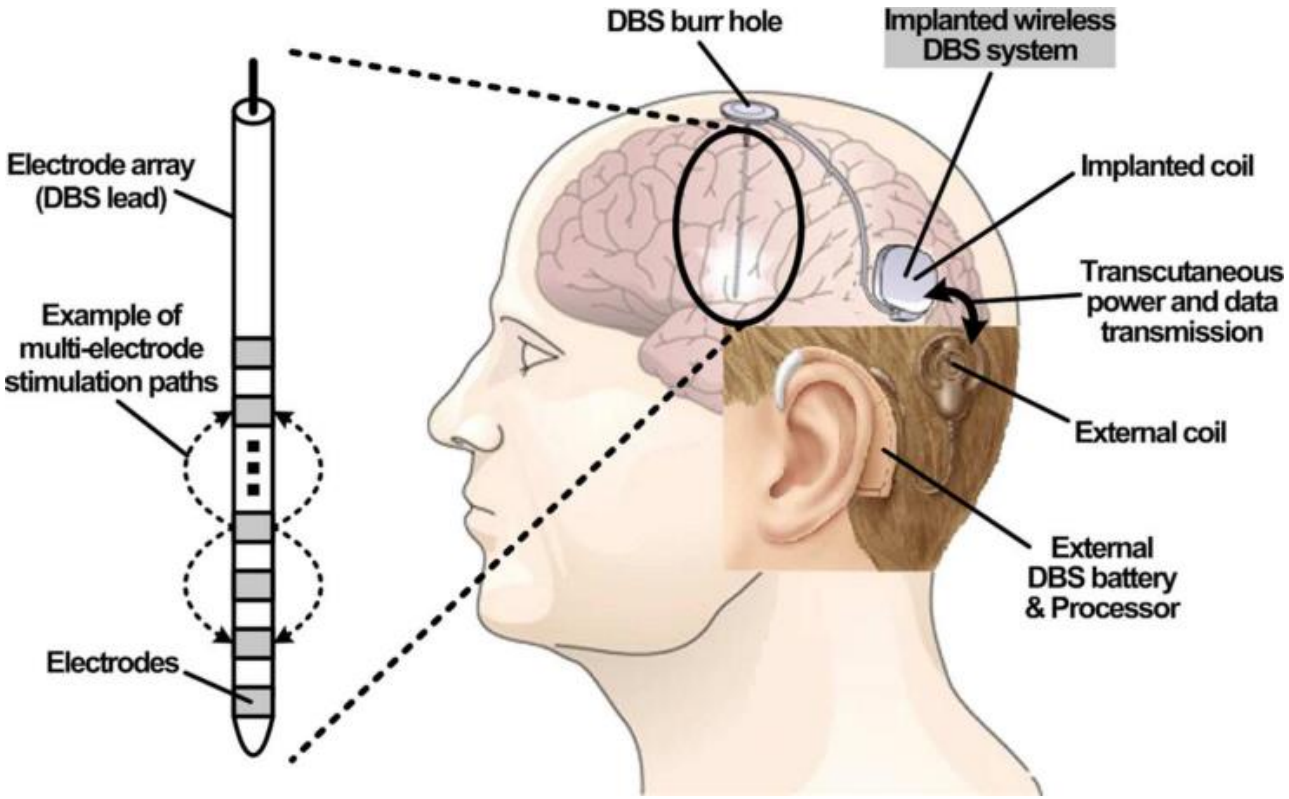


**Fig. 1.**
Conceptual configuration of a head-mounted inductively-powered DBS system in which power and data are transferred through the inductive link.

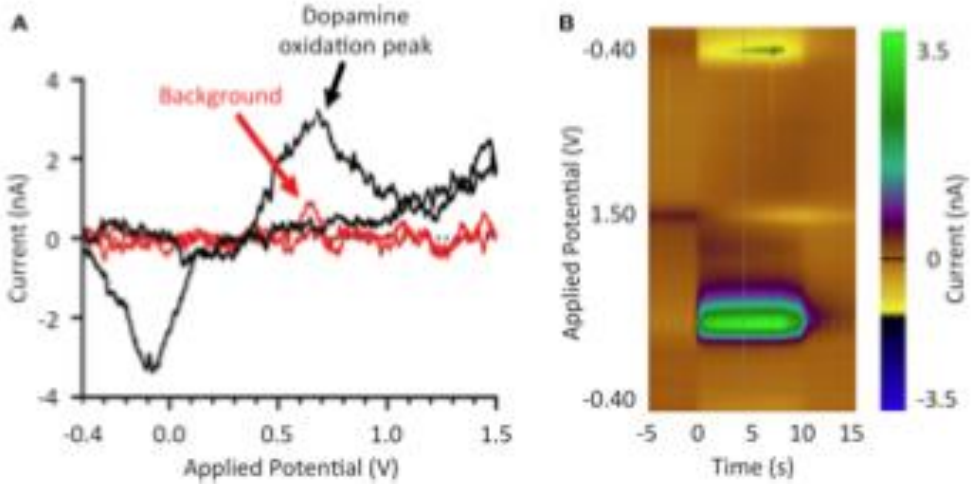


**FIGURE 1 | Stimulation-evoked dopamine responses. (A)** Dopamine redox reactions at the tip of a carbon fiber microelectrode during fast scan cyclic voltammetry. As the potential applied to the electrode increases from −0.4 to 0.0 V, extracellular dopamine is reduced (reduction peak at −3.5 nA). As the applied potential is further increased from 0.0 to 1.0 V, dopamine is oxidized (oxidation peak at 3.5 nA). Measured current background is shown in red. **(B)** Pseudo-color representation of dopamine oxidation current at +0.6 V at DBS onset (100 Hz, 2 ms, 300 μA).

frontiers in NEUROSCIENCE

**TECHNOLOGY REPORT ARTICLE**
published: 26 June 2014
doi: 10.3389/fnins.2014.00169

# A neurochemical closed-loop controller for deep brain stimulation: toward individualized smart neuromodulation therapies

***Peter J. Grahn[1], Grant W. Mallory[2], Obaid U. Khurram[1], B. Michael Berry[1], Jan T. Hachmann[2], Allan J. Bieber[2,3], Kevin E. Bennet[2,4], Hoon-Ki Min[2,5], Su-Youne Chang[2], Kendall H. Lee[2,5] and J. L. Lujan[2,5]****

[1] *Mayo Clinic College of Medicine, Mayo Clinic, Rochester, MN, USA*
[2] *Department of Neurologic Surgery, Mayo Clinic, Rochester, MN, USA*
[3] *Department of Neurology, Mayo Clinic, Rochester, MN, USA*
[4] *Division of Engineering, Mayo Clinic, Rochester, MN, USA*
[5] *Department of Physiology and Biomedical Engineering, Mayo Clinic, Rochester, MN, USA*

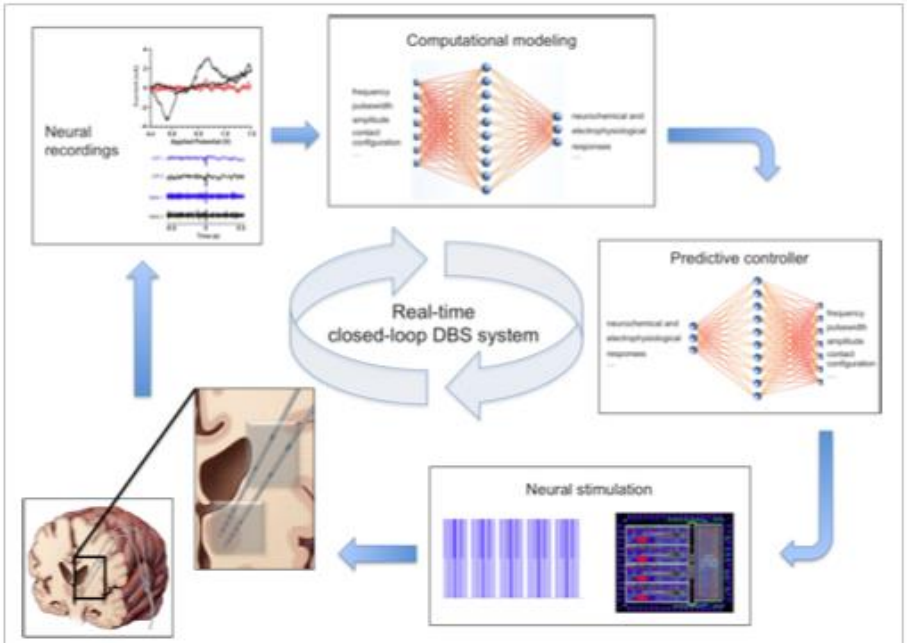


**FIGURE 2 | Real-time closed-loop deep brain stimulation system.** Clockwise from bottom left: (1) Schematic of the human brain with two electrodes (inset) for simultaneous stimulation (gray contacts) and recording of neural activity (blue contacts). (2) Example voltammogram, local field potentials, and single unit activity signals representing recorded neurochemical and electrophysiological neural activity. (3) Computational model of neurochemical and electrophysiological dynamics allows generation and optimization of data beyond the time constraints imposed by experimental conditions. (4) Smart controller uses existing neural activity to predict stimulation parameters required to achieve therapeutic neuromodulation. (5) Predicted stimulation parameters are applied to the brain using an implanted neurostimulation system.

# Current steering and field shaping electrodes

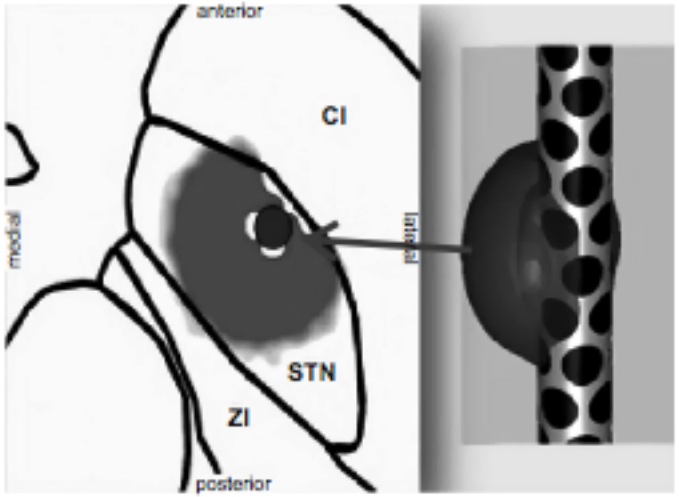


**Fig. 2.** Schematic view of the multipolar Sapiens lead called "SureStim"and a directional electric field allowing the electric field to be restricted into the target structure without spilling over laterally. STN, subthalamic nucleus; ZI, zona incerta; CI, capsula interna. (Reproduced with permission from Sapiens, Eindhoven, The Netherlands.)

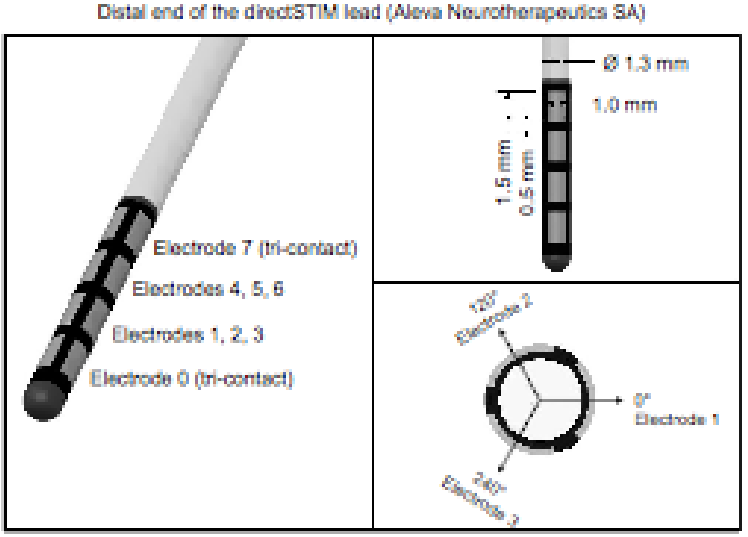


**Fig. 1.** Design of a quadripolar DBS lead called "directSTIM" where each electrode pole is divided into three independent compartments that can deliver directionally the electric current in a given direction, so called current-steering. (Reproduced with permission from Aleva Neurotherapeutics SA, Lausanne, Switzerland.)

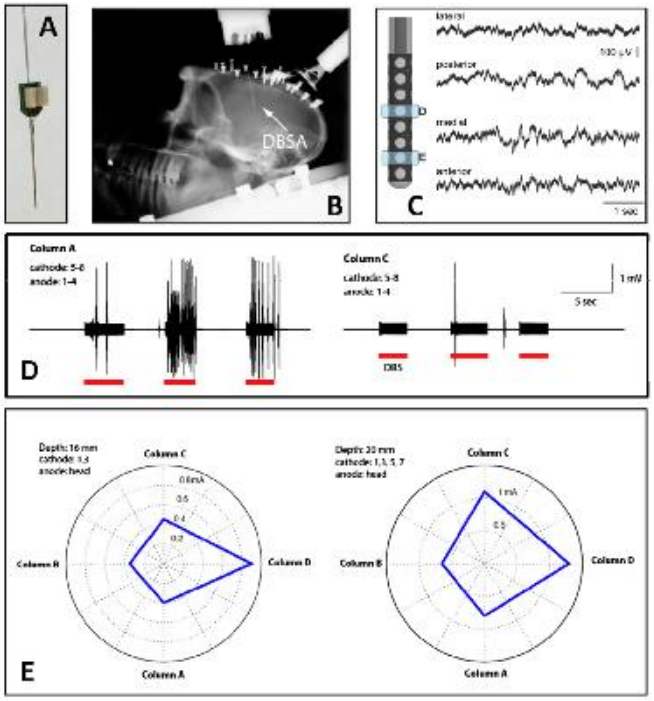


Fig. 2. Non-human primate experiment. (A) Photograph of the acute research version of the DBS-array. (B) The DBS-array was implanted acutely in the left hemisphere along a 20° anterior–posterior angle with the intended target being the globus pallidus. (C) Two sets of four radial electrodes (blue) were examined in terms of local field potentials. (D) The capacity of the DBS-array to deliver directionally-selective stimulation was confirmed by comparing EMG activity during stimulation on either the medial (column A) or lateral (column C) side of the DBS-array. In this case, bipolar stimulation (0.8 mA, 300 Hz) through column A resulted in EMG responses whereas the same stimulation parameters when applied to column C did not evoke a significant EMG response. (E) Stimulation thresholds were orientation dependent and directional selectivity of motor side-effects was found at multiple depths as shown for 16 mm (left) and 20 mm (right).

Clinical Neurophysiology 122 (2011) 558–566

# Spatial steering of deep brain stimulation volumes using a novel lead design

H.C.F. Martens [a,1,*], E. Toader [a,1], M.M.J. Decré [a,1], D.J. Anderson [b,2], R. Vetter [b,2], D.R. Kipke [b,2], Kenneth B. Baker [c,d,3], Matthew D. Johnson [c,e,3], Jerrold L. Vitek [c,d,3]

[a] Philips Research, High Tech Campus 34, 5656 AE, Eindhoven, The Netherlands
[b] Neuronexus Technologies, 3985 Research Park Dr. Suite 100, Ann Arbor, MI 48108, USA
[c] Cleveland Clinic, Department of Neurosciences, NC30, 8900 Euclid Ave., Cleveland, OH 44195, USA
[d] University of Minnesota, Department of Neurology, 516 Delaware Street SE, Minneapolis, MN 55455, USA
[e] University of Minnesota, Department of Biomedical Engineering, 7-105 NHH, 312 Church Street SE, Minneapolis, MN 55455, USA

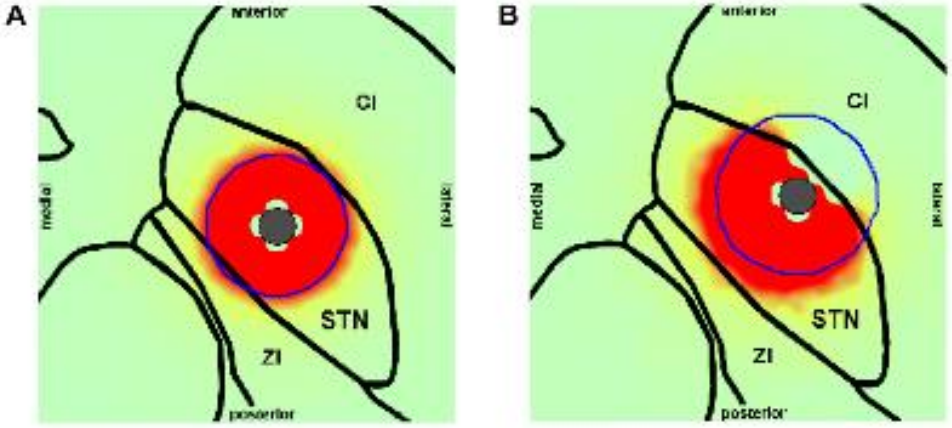


Fig. 5. Example demonstrating how DBS-array *VTA* steering can correct for small lead misplacement. *VTA* distributions are overlaid to scale on an axial slice of the STN area from the Schaltenbrand–Wahren atlas. The *VTA* in steering mode is depicted by the red regions (20 mV AF threshold). The blue line represents the 20 mV threshold value for the symmetric stimulation mode. (A) The lead is situated in the middle of the anatomical target (STN) and a symmetric configuration is optimal in this case. (B) The DBS-array is displaced 1 mm lateral and 1 mm anterior with respect to the middle of the STN. The use of *VTA* steering enabled by the DBS-array enables to optimally cover the STN while spread to adjacent structures is kept to a minimum. By contrast, a symmetric (state-of-the-art) mode of identical stimulus amplitude (blue isoline) would stimulate adjacent structures yet sub-optimally cover STN. ZI, zona incerta; CI, capsula interna.

# Directional deep brain stimulation: an intraoperative double-blind pilot study

Claudio Pollo,[1] Alain Kaelin-Lang,[2] Markus F. Oertel,[1] Lennart Stieglitz,[1] Ethan Taub,[3] Peter Fuhr,[4] Andres M. Lozano,[5] Andreas Raabe[1] and Michael Schüpbach[2]

Brain 2014: 137; 2015–2026 | 2015

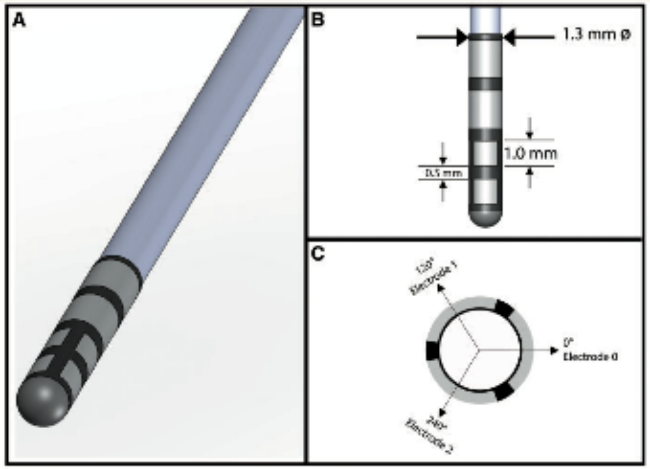


Figure 1 Distal end of the directSTNAcute lead. (A) 3D representation. (B) Longitudinal view showing the dimensions of the directional electrodes and spacing. (C) Axial view with angles of direction.

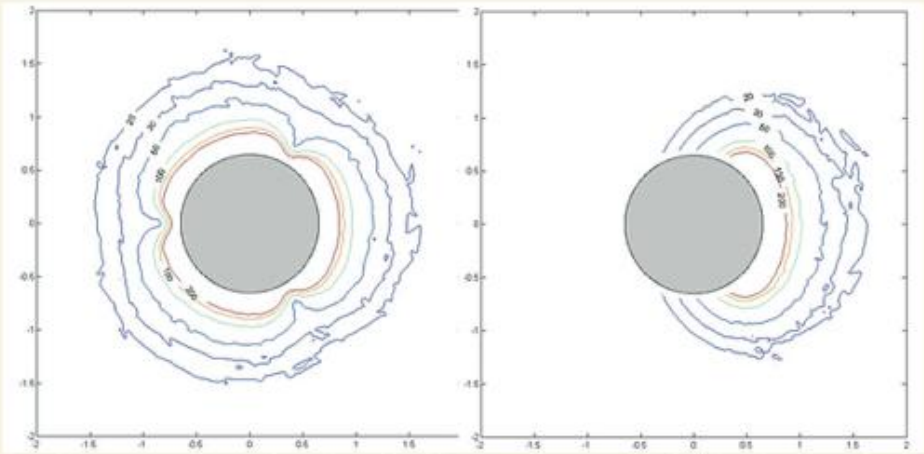

Figure 4 Transverse view of activated tissue volume isolines, when 1 -V stimulation is applied. *Left:* All three electrodes simultaneously activated. *Right:* One-directional electrode activated. The disc represents a cross-section of the lead. The *x*- and *y*-axis labels represent millimetres from the centre of the lead.

# Directional deep brain stimulation: an intraoperative double-blind pilot study

Claudio Pollo,[1] Alain Kaelin-Lang,[2] Markus F. Oertel,[1] Lennart Stieglitz,[1] Ethan Taub,[3] Peter Fuhr,[4] Andres M. Lozano,[5] Andreas Raabe[1] and Michael Schüpbach[2]

Brain 2014: 137; 2015–2026 | 2015

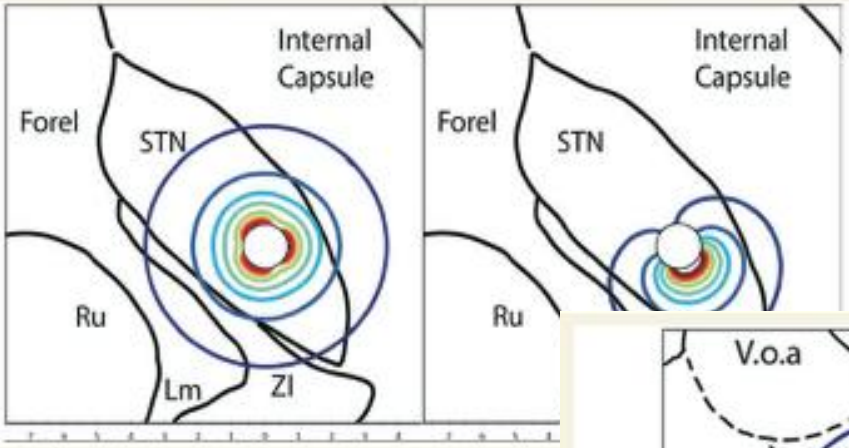


Figure 2 Axial projection of two stimulation modes using Finite Element Analysis adapted from the Schaltenbrand and Wahren atlas, Plate 54 Hv = −3.5. *Left*: All t applied current of 3 mA (1 mA per contact). *Right*: Postero-lateral directional electro the internal capsule. Horizontal scale represents the distance from the centre of th incerta; Lm = Lemniscus medialis; Ru = nucleus Ruber; Forel = Forel field.

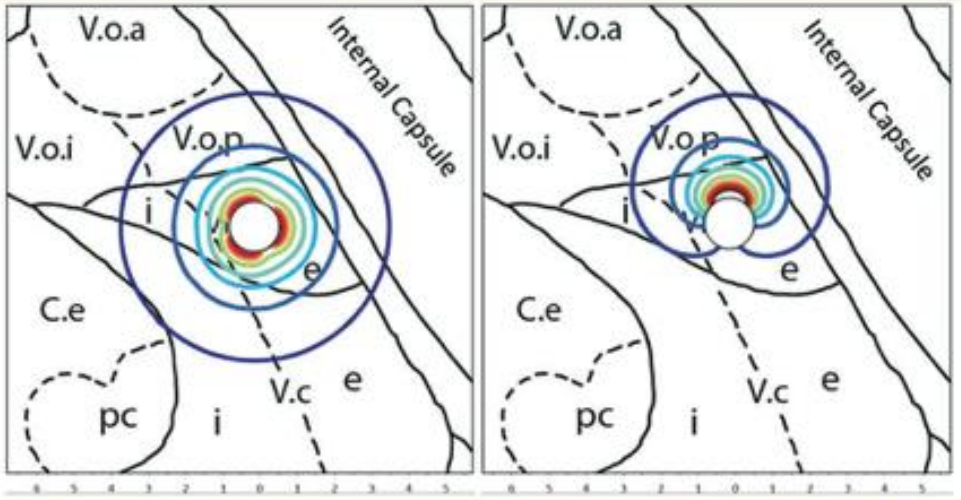


Figure 3 Anatomical representation in the axial projection of region surround the nucleus ventralis intermedus implantation site adapted from the Schaltenbrand and Wahren atlas, Plate 53 Hd = +2. *Left*: All three electrodes simultaneously activated with a total applied current of 3 mA (1 mA per contact). *Right*: Anterior directional electrode active with an applied current of 1.8 mA, avoiding the sensory thalamus. The horizontal scale represents the distance from the centre of the lead in mm. e = externus; i = internus; pc = parvocellularis; C.e = nucleus centralis externus; V.c = nucleus ventralis caudalis; V.o.p = nucleus ventralis oralis posterior; V.o.a = nucleus ventralis oralis anterior; V.o.i = nucleus ventralis oralis internus.

# Eventi Avversi DBS STN

**Mcclelland - Columbia University 2005**

| ADVERSE SIDE EFFECT | No of electrodes (82) | % |
|---|---|---|
| Parestesia | 49 | 59.8 |
| Dystonic contraction | 13 | 15.9 |
| Eyelid-opening apraxia/ocular motor effects | 8 | 9.8 |
| Dysartria | 6 | 7.3 |
| Dyskinesia | 5 | 6.1 |
| Dizzines/ataxia | 5 | 6.1 |
| Numbness | 4 | 4.9 |
| Diplopia/blurred vision | 2 | 2.4 |
| Lightheadedness | 2 | 2.4 |
| Blepharospasm | 1 | 1.2 |
| Confusion | 1 | 1.2 |
| Mutism | 1 | 1.2 |
| None | 21 | 25.6 |

# Effetti Collaterali DBS-STN

| | *Transitori* | *In corso* | *Stabili* |
|---|---|---|---|
| **DBS correlati** | | | |
| Parestesie | 5 | - | - |
| Discinesie disabilitanti | 4 | 1 | - |
| Diplopia | 1 | - | - |
| Depressione,apatia, abulia | 3 | - | - |
| Mania, aggressività | 1 | - | - |
| ↑cadute | 3 | - | - |
| ↑ ipofonia,disartria | - | - | 2 |
| Aprassia delle palpebre | 3 | - | - |
| Incremento ponderale | 7 | - | 2 |

# Effetti collaterali in corso di aggiustamento parametri DBS

| | Transitori | Stabili |
|---|---|---|
| **DBS correlati** | | |
| Parestesie | 37 | - |
| Discinesie disabilitanti | 18 | 5 |
| Diplopia | 5 | - |
| Depressione,apatia, abulia | 23 | 6 |
| Mania, aggressività | 1 | - |
| ↑cadute | 14 | - |
| ↑ ipofonia,disartria | 13 | 7 |
| Aprassia delle palpebre | 8 | - |
| Incremento ponderale | 33 | 17 |

# COMPLICANZE DBS

| Centro | Emorragie | Ematomi sottodurali | Infezioni Erosioni | Dislocazioni Rotture | Malfunz |
|---|---|---|---|---|---|
| Benabid 1996 Grenoble 177 VIM | 3.4% | | | | |
| Lang 1998 Toronto | 8% | | 11% | | |
| DBSPDSG 2001 198 STN 79 GPi | 1.5% 5.1% | | | | |
| Benabid 2001 Grenoble | 2-4% | | 6.4% | | |
| Kondziolka 2002 Pittsbourg 66 VIM | | 1.5% | 15% | 16.6% | |
| Hariz 2002 Umea - Svezia | MER aumenta fino a 5 volte il rischio di emorragia | | | 25% | |

# COMPLICANZE DBS

| Centro | Emorragie | Ematomi sottodurali | Infezioni Erosioni | Dislocazioni Rotture | Malfunz |
|---|---|---|---|---|---|
| Eltahawy 2003<br>Toronto<br>15 GPi per distonia | | | | | 6.6% |
| Terao 2003, Tokyo<br>90 PD<br>12 ET<br>8 Dys | Lesioni 15.8%<br>DBS 3.4% | | 11% | | |
| Rodriguez-Oroz2004, Pamplona<br>10 PD | | | 10% | | |
| Ford 2004<br>Columbia Univ. NY<br>30 STN | 6.6%<br>(1 stroke) | 6.6% | 10% | | |
| Lyons 2004<br>Kansas City<br>81 STN | 1.2% | | 6% | 26% | |
| Starr 2004<br>San Francisco<br>23 Dys | 4.3% | | | | |

# Complicanze DBS su 77 pazienti PD operati

| | Numero | % paziente | % traccia |
|---|---|---|---|
| **Procedura correlate** | | | |
| Emorragia intracerebrale | 1° * | 1.5 | 0.4 |
| Ematoma sottodurale cronico (ESC) | 1° | 1.5 | 0.4 |
| Infezione tasca | 1° | 1.5 | 0.4 |
| Migrazione elettrodo | 3** | 4.5 | 1.3 |
| Rottura estensioni | - | - | |
| Erosione cutanea | 3° | 4.5 | 1.3 |
| Stato confusionale transitorio | 1° | 1.5 | 0.4 |
| Crisi epilettiche | 1° * | 1.5 | 0.4 |
| TOTALE COMPLICAZIONI | 11 EVENTI | 9 PAZIENTI 13.6 % | |

* Stesso paziente ° STN ** 2 STN (di cui 1 per ESC), 1 GPi

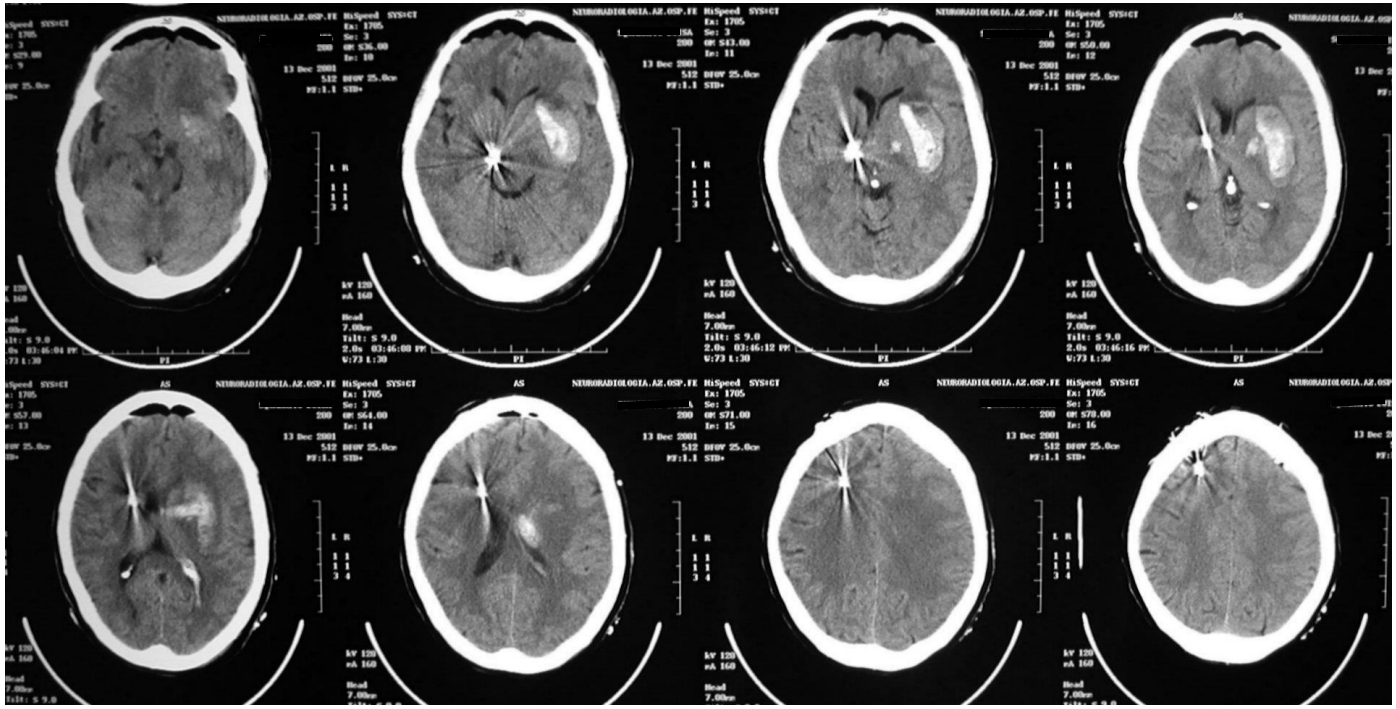
NEURORADIOLOGIA.AZ.OSP.FE HiSpeed SYS+CT
13 Dec 2001
kV 120
mA 160
Head
7.00cm
Tilt: S 9.0
2.0s
PI

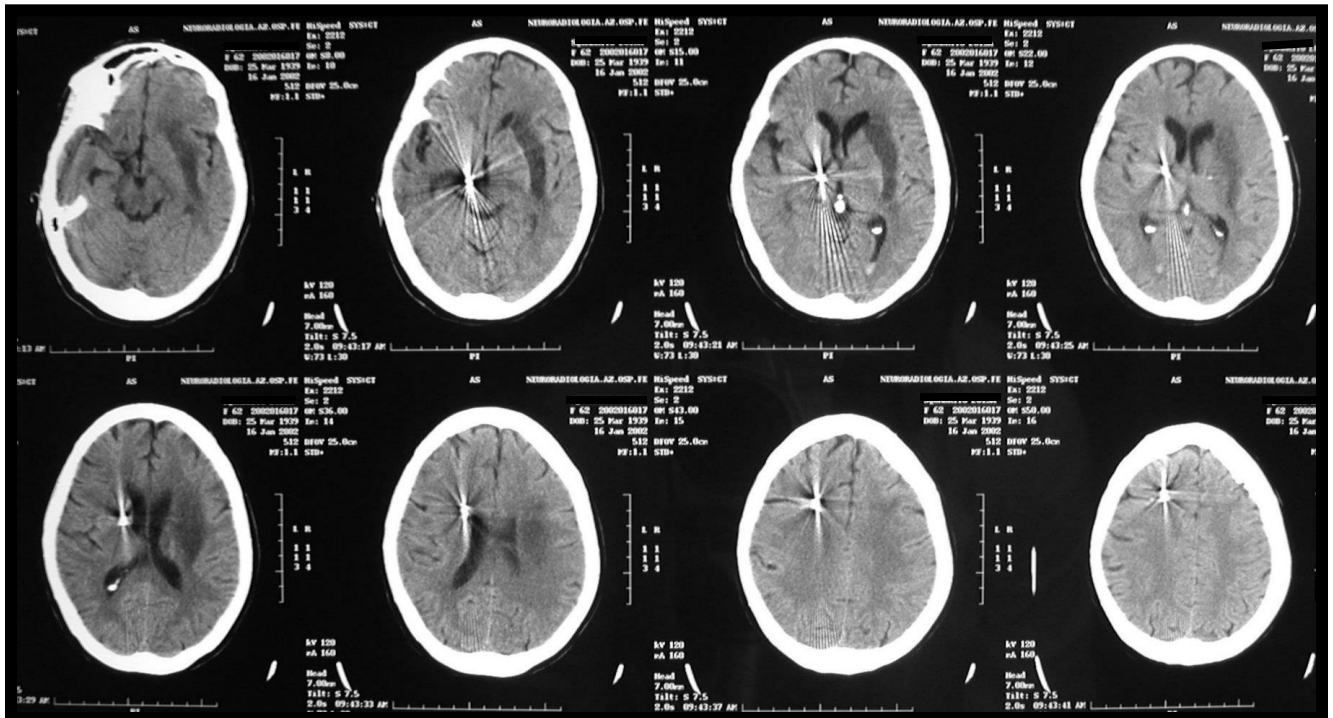
NEURORADIOLOGIA.AZ.OSP.FE HiSpeed SYS+CT
F 62 2002016017
DOB: 25 Mar 1939
16 Jan 2002
512 DFOV 25.0cm
kV 120
mA 160
Head
7.00cm
Tilt: S 7.5
2.0s
PI

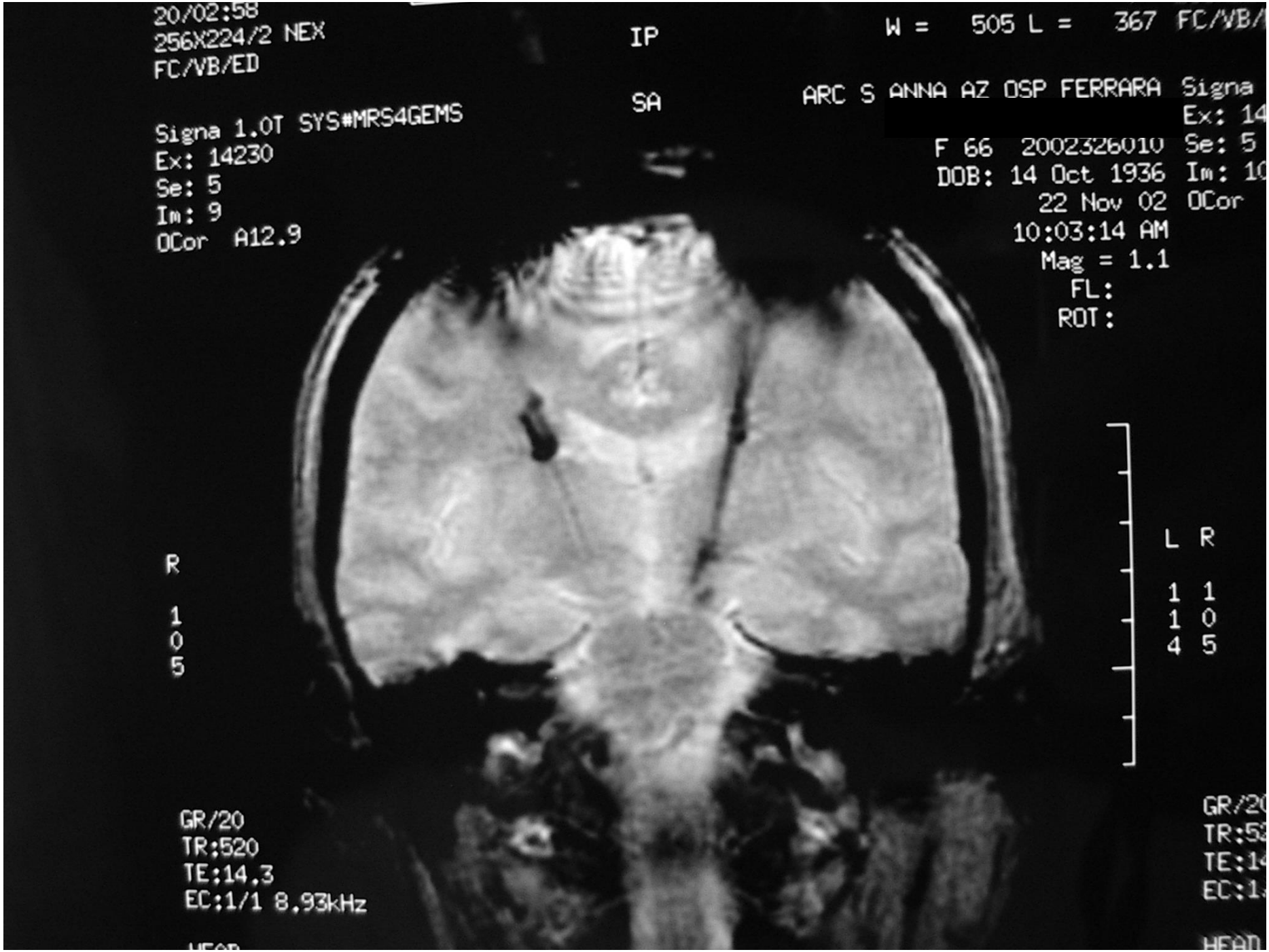
20/02:58
256X224/2 NEX
FC/VB/ED
Signa 1.0T SYS#MRS4GEMS
Ex: 14230
Se: 5
Im: 9
OCor A12.9
IP
SA
W = 505 L = 367 FC/VB/
ARC S ANNA AZ OSP FERRARA Signa
Ex: 14
Se: 5
Im: 1
OCor
F 66 2002326010
DOB: 14 Oct 1936
22 Nov 02
10:03:14 AM
Mag = 1.1
FL:
ROT:
R
1
0
5
L R
1 1
1 0
4 5
GR/20
TR:520
TE:14.3
EC:1/1 8.93kHz
GR/2
TR:5
TE:1
EC:1
HEAD